



1 **Bidirectional coupling of a long-term integrated assessment model** 2 **REMIND v3.0.0 with an hourly power sector model DIETER v1.0.2**

3 Chen Chris Gong¹, Falko Ueckerdt¹, Robert Pietzcker¹, Adrian Odenweller^{1,3}, Wolf-Peter Schill², Martin
4 Kittel², Gunnar Luderer^{1,3}

5 ¹ Potsdam Institute for Climate Impact Research (PIK), Potsdam, Germany

6 ² German Institute for Economic Research (DIW Berlin), Berlin, Germany

7 ³ Global Energy Systems Analysis, Technische Universität Berlin, Berlin, Germany

8 *Correspondence to:* Chen Chris Gong (chen.gong@pik-potsdam.de)

9

10 **Abstract.** Integrated assessment models (IAMs) are a central tool for the quantitative analysis of climate change mitigation
11 strategies. However, due to their global, cross-sectoral and centennial scope, IAMs cannot explicitly represent the temporal and
12 spatial details required to properly analyze the key role of variable renewable electricity (VRE) for decarbonizing the power
13 sector and enabling emission reductions through end-use electrification. In contrast, power sector models (PSMs) can
14 incorporate high spatio-temporal resolutions, but tend to have narrower sectoral and geographic scopes and shorter time
15 horizons. To overcome these limitations, here we present a novel methodology: an iterative and fully automated soft-coupling
16 framework that combines the strengths of a long-term IAM and a detailed PSM. The key innovation is that the framework uses
17 the market values of power generations as well as the capture prices of demand flexibilities in the PSM as price signals that
18 change the capacity and power mix of the IAM. Hence, both models make endogenous investment decisions, leading to a joint
19 solution. We apply the method to Germany in a proof-of-concept study using the IAM REMIND v3.0.0 and the PSM DIETER
20 v1.0.2, and confirm the theoretical prediction of almost-full convergence both in terms of decision variables and (shadow)
21 prices. At the end of the iterative process, the absolute model difference between the generation shares of any generator type for
22 any year is <5% for a simple configuration (no storage, no flexible demand) under a “proof-of-concept” baseline scenario, and
23 6-7% for a more realistic and detailed configuration (with storage and flexible demand). For the simple configuration, we
24 mathematically show that this coupling scheme corresponds uniquely to an iterative mapping of the Lagrangians of two power
25 sector optimization problems of different time resolutions, which can lead to a comprehensive model convergence of both
26 decision variables and (shadow) prices. The remaining differences in the two models can be explained by a slight mismatch
27 between the standing capacities in the real-world and optimal modeling solutions purely based on cost competition. Since our
28 approach is based on fundamental economic principles, it is applicable also to other IAM-PSM pairs.

29 **1 Introduction**

30 Thanks to decade-long policy support in many regions of the world and technological learning, the costs of both wind power
31 and solar photovoltaics have plummeted (IEA, 2021; Lazard, 2021). These types of variable electricity generation are now
32 highly cost competitive against other alternatives, such that their deployment is increasingly driven by market forces instead of
33 climate policies. Among the newly added renewable generations in 2020, nearly two thirds were cheaper than the cheapest new
34 fossil fuel (IRENA, 2020). Due to both cost declines and pressing concerns over climate change, investing in these clean and
35 abundant resources has become a crucial part of national and regional strategies to decarbonize the power sector (The White
36 House, 2021; Cherp et al., 2021; National long-term strategies, 2022; Rechsteiner, 2021; ICCSD Tsinghua University, 2022).



37 Given this dramatic development in the power sector over the past two decades, a universal consensus has emerged among
38 energy transition scholars and policy makers: emissions in the power sector are relatively “easy-to-abate” (Luderer et al., 2018;
39 Azevedo et al., 2021; Clarke et al., 2022). Compared with other primarily non-electrified end-use sectors such as buildings,
40 transport and industry, the technologies required to transform the power sector are low-cost, mature and readily available. This
41 trend has in recent years led to a second emerging consensus: the power sector will be the fundamental basis of a future low-
42 cost, efficient and climate-neutral energy system (Brown et al., 2018b; Ram et al., 2018; Ramsebner et al., 2021; Luderer et al.,
43 2022a). In addition to direct electrification, which requires end-use transformations of currently non-electrified demand,
44 emerging technological developments in hydrogen and e-fuels produced from renewable electricity have also contributed to the
45 broadening of potential technology portfolios for the “hard-to-abate” sectors, such as high temperature heat and chemical
46 productions (Parra et al., 2019; Bhaskar et al., 2020; Griffiths et al., 2021). Together, direct and indirect electrification support a
47 broad concept of “sector coupling”, which facilitates decarbonization by powering end-use demand with variable renewable
48 energy sources (Ramsebner et al., 2021).

49 Due to the pivotal role of electrification and sector coupling in mitigation scenarios, there is an increasing demand on the scope
50 and level of detail of energy-economy models used to guide the energy transition and climate policies. The models would
51 ideally encompass a global, multi-decadal and multi-sectoral scope, such that the scenarios are relevant for international and
52 regional climate policies, while simultaneously incorporating a high level of spatio-temporal detail. The latter is important to
53 account for the specifics of variable renewable electricity generation as well as its physical and economic interplay with the
54 electrification of energy demand (Li and Pye, 2018; Brunner et al., 2020; Prol and Schill, 2020; Böttger and Härtel, 2022;
55 Ruhnau, 2022). This need for improved modeling methods or frameworks, which has to overcome the trade-off between scope
56 and detail, is a substantial methodological challenge. It entails realizing two main objectives:

57 Objective 1) Accurately model the power sector transformation over long time horizons in terms of investment and dispatch,
58 especially at high shares of variable renewable energy (VRE) sources. Long-term pathways for the following power
59 sector quantities and prices should accurately incorporate short-term hourly details:

- 60 a) capacity and generation mix of the power sector,
- 61 b) market values (annual average revenues per power generation unit) for variable and dispatchable plants,
- 62 c) capacity factors of the dispatchable plants and the curtailment rates of variable renewables,
- 63 d) storage capacity and dispatch.

64 Objective 2) Accurately model direct electrification of end-use sectors as well as indirect electrification technologies such as
65 green hydrogen production, where existing and emerging sources of power demand can be in-part flexibilized.

66 **1.1 Current modeling approaches and limitations**

67 Current energy system models broadly fall into two distinct categories, carried out by two research communities with little
68 institutional overlap: integrated assessment models (IAMs) and power sector models (PSMs), each with its own strengths and
69 weaknesses. IAMs are comprehensive models of global scale and span multiple decades, linking macroeconomics, energy
70 systems, land-use and environmental impacts (Stehfest et al., 2014; Calvin et al., 2017; Huppmann et al., 2019; Baumstark et al.,
71 2021; Keppo et al., 2021; Guivarch et al., 2022), therefore providing an “integrated assessment” of multiple factors (Rotmans
72 and van Asselt, 2001). IAMs substantially shape the IPCC assessments on long-term climate mitigation scenarios, and play an
73 important role in policy making (Rogelj et al., 2018; UNEP, 2019; NGFS, 2020; P.R. Shukla et al., 2022). In comparison to
74 IAMs, PSMs typically have narrower spatial and sectoral scopes and shorter time horizons, but provide higher resolutions and
75 increased technological detail (Palzer and Henning, 2014; Zerrahn and Schill, 2017; Brown et al., 2018a; Ram et al., 2018;



76 Sepulveda et al., 2018; Blanford and Weissbart, 2019; Böttger and Härtel, 2022). This allow PSMs to more accurately model the
77 power sector under high VRE shares (Bistline, 2021; Chang et al., 2021). Note that we use the term “power sector model” here
78 to represent all general smaller-scope models than IAMs (usually by geographical or time horizon measures), even though many
79 of them have sector-coupling aspects and do not only contain the traditional power sector.

80

81 IAMs and PSMs are therefore limited by a lack of spatio-temporal detail and a lack of scope, respectively. IAMs usually have a
82 temporal resolution no shorter than a year (Keppo et al., 2021) and therefore include simplified representations of hourly power
83 sector variability, which mimic the real-world dynamics to varying degrees of success (Pietzcker et al., 2017). In general, a lack
84 of high temporal resolutions can lead to difficulties when estimating the optimal level of variable renewable generation, often
85 either over- or underestimating the market value of solar or wind generation, the challenges of variable renewable integration,
86 the peak hourly residual demand, and the need for energy storage and baseload (Pina et al., 2011; Haydt et al., 2011; Ludig et
87 al., 2011; Kannan and Turton, 2013; Welsch et al., 2014; Luderer et al., 2017; Pietzcker et al., 2017; Bistline, 2021). While
88 approximate methods such as parameterization via residual load duration curves (RLDCs) are able to capture the supply-side
89 dynamics of VREs, they remain methodologically limited for representing the flexible demand-side dynamics (Ueckerdt et al.,
90 2015; Creutzig et al., 2017). Besides limited temporal resolutions, IAMs also usually have coarse spatial resolutions, which can
91 lead to an under- or overestimation of transmission grid bottlenecks, geographical variability of wind and solar resources, and of
92 the flexibility requirements to balance supply and demand (Aryanpur et al., 2021; Frysztacki et al., 2021; Martínez-Gordón et
93 al., 2021). PSMs, on the other hand, usually lack the global and sectoral scope required for addressing global climate mitigation,
94 in part because of limited availability of detailed data, and due to computational challenges. Furthermore, PSMs with a short-
95 term horizon may lack the vintage tracking of standing capacities, capacity evolution over time, as well as long-term perfect
96 foresight, which can help policy makers and companies to look ahead beyond the short-term business cycles, to invest early and
97 to actively drive technical progress. In contrast, in IAMs such as REMIND, proactive early investment is a built-in feature,
98 because the optimization is done from a long-term social planner’s perspective. In IAMs, investing early in the technological
99 learning phase results in lower costs of energy expenditure later, avoiding the severity of punishment to economic growth later
100 in time in the form of lower consumption, which raises the welfare which the model optimizes.

101 **1.2 Iterative coupling for full model convergence**

102 IAMs and PSMs differ in scope and resolution across three main modeling dimensions: temporal, spatial and technological. A
103 soft-coupling approach can tap into these complementarities and combine their strengths, at potentially only a moderate increase
104 in computational cost. The main challenge of the soft-coupling approach is to show that the two models can converge under
105 coupling, which leads to a joint equilibrium that maximizes regional interannual intertemporal welfare in the IAM and
106 minimizes total power system costs in the PSM. Ideally, the converged model offers the “best of both worlds”: it has both the
107 broad scope required to assess global long-term energy transitions, as well as the technical resolution required to capture the
108 interplay between VREs, storage and newly electrified demand on a much shorter time scale.

109 Approaches aiming to bridge the “temporal resolution gap” between long-term energy system models and hourly PSMs have
110 been proposed in the past (Deane et al., 2012; Sullivan et al., 2013; Alimou et al., 2020; Brinkerink, 2020; Seljom et al., 2020).

111 While these achieved some aspects of Objective (1) with adequate results, none attempted to incorporate and achieve Objective
112 (2). In addition, there is a methodological gap in the previous attempts to a full harmonization of the multiscale models. By a
113 full harmonization, we mean a comprehensive coupling of the power sector dynamics, and an eventual model convergence in
114 capacities, generation, and prices. In none of the previous studies, price information has been fed back into the long-term models



115 from the short-term models for the complete set of generation technologies, only partial price information has been exchanged
116 in one of the studies (Seljom et al., 2020). Without a feedback mechanism through prices, the investment in the coupled model
117 will very likely be sub-optimal due to two effects: 1) because of the misalignment in prices in the two models, there is a
118 mismatch in investment incentives, resulting in a mismatch for optimal capacities if both models are completely endogenous; 2)
119 in all previous studies, the capacities are fixed in the PSM and only the long-term model is allowed to invest in new capacities.
120 This implementation can further propagate and sustain the price mismatch due to (1) via nontrivial shadow prices from these
121 capacity bounds, and create in turn price distortions in the PSM that can be passed on to the IAM. Therefore, the methodological
122 gap in previous work prevented a comprehensive convergence of the coupled models of both quantities and prices. As we show
123 later in this study, without a comprehensive coupling of price information, no system-wide convergence can be achieved.
124 However, with price coupling as our method proposes, we could achieve all aspects of Objective (1), as well as Objective (2) for
125 one type of flexible demand with adequate numerical results, and therefore represents a first step to bridge the previous
126 methodological gap.
127 Compared to previous studies, our approach features three main innovations: 1), the coupling is achieved by linking market
128 values, and not hard fixing quantities, allowing both models to invest “as endogenously as possible”; 2), the market values of all
129 power sector technologies are coupled, not just the electricity price of the system or the market value of a particular technology,
130 allowing models to achieve close to full convergence; 3) under idealized coupling assumptions and for a simplified “proof-of-
131 concept” model without storage, we can mathematically derive the necessary conditions under which comprehensive model
132 convergence can be reached, which puts multiscale coupling on firm theoretical footing. Our coupling approach is bi-
133 directional, iterative and fully automated.
134 To showcase such a framework and its ability to achieve iterative convergence, we couple the PSM DIETER, which has an
135 hourly resolution (8760 hours in a year) and the IAM REMIND for a single-region Germany. Germany is a well-suited case
136 study for exploring high VRE shares in the power sector. The country is expected to meet stringent climate targets despite the
137 country’s high level of residential and industrial power demand, relatively small geographical size and lack of solar endowment
138 during winter seasons. Nevertheless, the German government has set very ambitious targets for the expansion and use of
139 variable renewable energy sources (DIW Berlin, 2022). A viable zero-carbon power mix in Germany must include an adequate
140 amount of storage and transmission for the renewable generation, as well as “clean firm generation” such as geothermal,
141 biomass or gas with carbon capture and storage (CCS) (Sepulveda et al., 2018).

142 **2 Models**

143 The models used in this study are well-documented open source models (REMIND is an open source model but requires
144 proprietary input data to run). A side-by-side comparison of the scope, resolution and other specifications of the two models can
145 be found in Appendix A. The coupling scope can be found in Appendix B. Details on model input data can be found in
146 Supplemental Material S-1.

147 **2.1 IAM: REMIND**

148 REMIND (REgional Model of INvestments and Development) is a process-based IAM, which describes complex global energy-
149 economy-climate interactions (Baumstark et al., 2021). REMIND has been frequently used in long-term planning of
150 decarbonization scenarios, most notably in the IPCC (IPCC, 2014; Rogelj et al., 2018; P.R. Shukla et al., 2022). The REMIND
151 model links different modules, which describe the global economy, the energy, land and climate systems, with a relatively
152 detailed representation of the energy sector compared to non-process-based IAMs. The model is formulated as an interannual



153 intertemporal optimization problem. Due to the computational complexity of nonlinear optimization, the model simulates a time
154 span from 2005 to 2100 with a temporal resolution of either 5 years (between 2005 to 2060) or 10 years (between 2070 to 2100).
155 The years in REMIND are representative years of the surrounding 5 or 10-year period, e.g. year “2030” represents the 5-year
156 period 2028 to 2032. Spatially, the model represents the world composed of aggregated global regions (Fig. B1). For each
157 region, using a nested constant elasticity of substitution (CES) production function, the model maximizes interannual
158 intertemporal welfare as a function of labor, capital, and energy use (Baumstark et al., 2021). The macro-economic projections
159 of REMIND come from various established global socio-economic scenarios jointly used by social scientists and economists –
160 the so-called Shared Socioeconomic Pathways (SSPs) (Bauer et al., 2017).
161 By default, REMIND runs in a regionally decentralized iterative “Nash mode”, where all regions are run in parallel and the
162 interannual intertemporal welfare is maximized for each region for each internal “Nash” iteration. Trade flows between the
163 regions are determined between the Nash iterations. During the Nash algorithm, REMIND regions share partial information
164 between each other, which are trade variables in primary energy products and goods. The Nash algorithm is said to converge,
165 when all markets are cleared and no region has the incentive to change their behavior regarding their trade decisions, i.e. no
166 resources can be reallocated to make one region better off without making at least one region worse off. A successfully
167 converged run of stand-alone REMIND under “Nash mode” usually consists of 30 to 70 iterations of single-region models in
168 parallel. Each parallel single-region model usually takes 3–6 minutes to solve. A typical REMIND run in the Nash mode lasts
169 2.5–6 hours depending on the level of sectoral details included. The latest version REMIND (v3.0.0) is published as an open-
170 source version on github (Release REMIND v3.0.0 · remindmodel/remind, 2022). REMIND is implemented as a nonlinear
171 programming (NLP) mathematical optimization problem. In REMIND, the nonlinearity consists of the welfare function, the
172 CES production functions, adjustment costs, technological learning, the extraction cost functions, the bioenergy supply function
173 and nonlinear constraints, among others.

174 **2.2 PSM: DIETER**

175 DIETER (Dispatch and Investment Evaluation Tool with Endogenous Renewables) is an open-source power sector model
176 developed for Germany and Europe. In a long-run equilibrium setting (i.e. a competitive benchmark), the model minimizes
177 overall system costs of the power sector for one year. DIETER determines the least-cost investment and hourly dispatch of
178 various power generation, storage, and demand-side flexibility technologies. In previous literature, different versions of the
179 model have been used to explore scenarios with high VRE shares, where storage (Zerrahn et al., 2018; Zerrahn and Schill, 2017;
180 Schill and Zerrahn, 2018), hydrogen (Stöckl et al., 2021), power-to-heat (Schill and Zerrahn, 2020), or solar prosumage (Say et
181 al., 2020; Günther et al., 2021) are evaluated with a high degree of technological detail. DIETER recently also contributed to
182 model comparison exercises that focused on power sector flexibility for VRE integration and sector coupling (Gils et al., 2022b,
183 a; van Ouwkerk et al., 2022).
184 As a first step to building a model coupling infrastructure, we implemented an earlier and simpler version of DIETER (v1.0.2),
185 which is purely based on the General Algebraic Modeling System (GAMS). It has limited features on ramping constraints,
186 flexible demand, and storage. The model minimizes total investment and dispatch cost of a power system for a single region,
187 considering all consecutive hours of one full year. The technology portfolio contains conventional generators such as coal and
188 gas power plants, nuclear power, as well as renewable sources such as hydroelectric power, solar PV and wind turbines.
189 Endogenous storage investment and dispatch, as well as demand flexibilizations are offered as additional features that can be
190 turned on or off. DIETER, like many PSMs, is a linear program (LP). A typical stand-alone run (with essential features) lasts



191 from several seconds to several minutes for a single region. See Zerrahn and Schill, 2017 for a detailed documentation of the
192 initial model, which was implemented purely in GAMS.

193 **3 A novel coupling approach**

194 It is central to our approach that the price-based variables, such as the market values of electricity generation, are exchanged
195 between the models. This approach ensures full convergence – including both quantity convergence as well as price
196 convergence in the market equilibrium. Here, we first introduce the intuition behind this approach, then conduct a deep dive into
197 the economic theory behind energy system modeling.

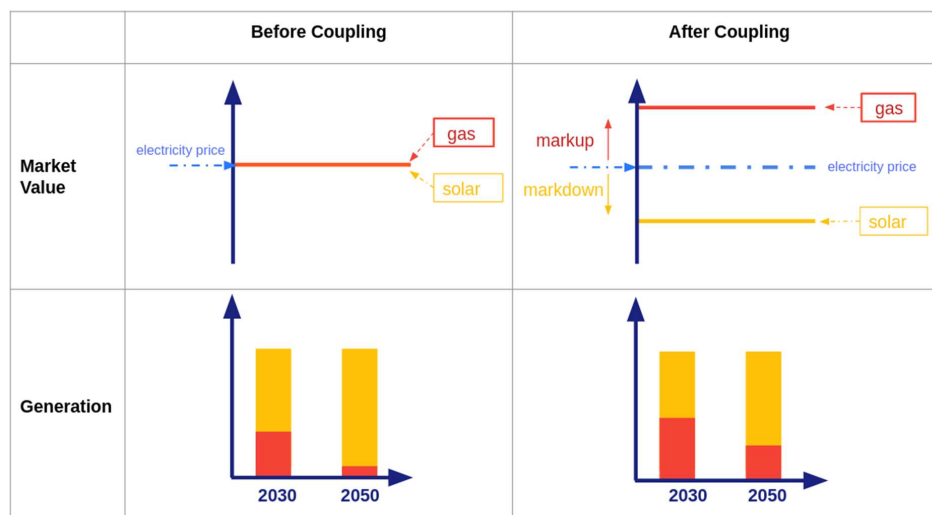
198 Economic concepts such as market values or capture prices (Böttger and Härtel, 2022), as key variables in our coupling,
199 translate the physical characteristics of variable power generation or flexible consumption into economic ones. For example,
200 generation technologies differ with respect to physical features and constraints – solar and wind generation depends on current
201 weather conditions as well as diurnal and seasonal patterns, whereas this is less the case for dispatchable power plants such as
202 coal, gas, biomass, nuclear or storage (López Prol and Schill, 2021). One consequence of this is that, for example, prices in
203 hours where PV does not produce will be essentially set by other, and usually more expensive forms of generation. In cost-
204 minimizing PSMs, the shadow prices of the energy balance are interpreted as wholesale market prices (Brown and Reichenberg,
205 2021; López Prol and Schill, 2021). Therefore in general, hourly-resolution PSMs are well equipped to translate such physical
206 constraints of generation into (wholesale) power market price time series. By providing such prices generated by PSMs (among
207 other variables of the power sector dynamics) to IAMs, the latter can be indirectly informed about power market dynamics
208 happening on much shorter time scales, even if they lack hourly resolutions. Over iterations, the prices from PSMs act as “price
209 signals” to induce investment decision changes in IAMs, which can in turn provide feedback to the PSMs until the two models
210 converge.

211 One innovation of our method is that the prices used for the model coupling can be symmetrically applied on the power supply
212 side as well as the demand side. On the supply side, the coupling method mainly utilizes the concept of market value (i.e. annual
213 average revenue per energy unit of a generator) in a competitive market at equilibrium. Generally speaking, market values of
214 generation usually convey the degree of variability intrinsic to a given source of power supply, and reflect the generator’s ability
215 to meet an inflexible hourly demand, especially given lower cost of variable generation compared to dispatchable technologies.
216 Mirroring the concept of the market value, on the demand side, there is the concept of the “capture price” of electricity demand,
217 which conveys the degree of demand-side flexibility. Note that there may be multiple terminologies for demand-side electricity
218 prices, we use “capture price” to be consistent with one of the literatures on this topic. The capture price is the average
219 electricity price that a flexible demand technology pays over a year. For example, flexible demand technologies such as heat
220 pumps, electrolyzers or electric vehicles (EVs) can take advantage of electricity at hours when the generation is cheap to obtain
221 a lower “capture price”, whereas inflexible demand has to pay a higher price on average. Price information given from a PSM to
222 an IAM from both the supply and demand sides can change the IAM’s inherent investment and dispatch decisions of power
223 generation as well as inflexible and flexible demand-side technologies.

224 For an intuitive understanding of our innovative coupling scheme, we take the supply-side as an example, and use a toy model
225 to visualize the approach of coupling via market values. The market values of electricity generating technologies have been
226 studied in depth (Sensfuß, 2007; Sensfuß et al., 2008; Hirth, 2013; Mills and Wisser, 2015; Hildmann et al., 2015; Koutstaal and
227 va. Hout, 2017; Figueiredo and Silva, 2018; Hirth, 2018; Brown and Reichenberg, 2021). The general idea of the coupling is
228 illustrated in Fig. 1 for a simplified case of only two types of generators – dispatchable gas turbines and solar photovoltaics with
229 variable output. Note that we assume the system is at a solar share of > 50% and no storage, such that the solar market value is



230 below average electricity price, and that of gas generation is above. Before the coupling, for a general IAM with coarse temporal
 231 resolution and without any VRE integration cost parameterizations, there is no differentiation between the market values of gas
 232 and solar generators – they are both equal to the electricity price. Thus, there is no differentiated revenue for one MWh
 233 generated by variable sources and dispatchable sources. The lack of market value differentiation is a direct consequence of the
 234 limited temporal resolution in IAMs, which cannot represent hourly dynamics. However, through a market-value-based
 235 coupling, the IAM can be informed by the PSM via a price “markup”. The annual price markup is defined as the difference
 236 between the market value of a specific technology and the annual average revenue that all generators together earn for one unit
 237 of generation (i.e. the annual average electricity price that a user pays). Under our soft-coupling approach, the markups from the
 238 PSM act as price-signals that change the composition of the energy mix in the next iteration of the IAM. Since in this simple
 239 example with a lot of PV and no storage, the gas generator is “more valuable” to the system, as it can generate electricity in
 240 times of scarcity (night), and thus it will receive a positive markup. When this positive price incentive is transferred from the
 241 PSM to the IAM, it increases the optimal level of investment into gas generation in the next IAM iteration. At the same time,
 242 solar generation receives a negative price incentive, reducing the optimal level of investments in the next iteration. Ultimately,
 243 the higher market value of gas turbines is due to: 1) its higher cost compared to solar (when gas is at <50% market share), 2) its
 244 ability to set prices in hours of low solar output and inflexible electricity demand. As we later show through mathematical
 245 theory of model convergence, other information besides markups also needs to be transferred such as capacity factors (annual
 246 average utilization rates of the generators).



247
 248 **Figure 1: Schematic illustration of the coupling approach for a simple power system in an IAM with coarse temporal**
 249 **resolution, consisting of only gas and solar generators (no storage). Left column: before coupling; right column: after**
 250 **coupling. Top row: endogenous prices (electricity price, market values of solar and gas generators); bottom row:**
 251 **endogenous quantities (generation mix). The markups (as part of a larger set of interfaced variables) are the differences**
 252 **between market values and electricity prices, and are given by the PSM of high temporal resolution as price signals to**
 253 **the IAM. Usually, it is called a “markup” when the market value is higher than the annual average electricity price, and**
 254 **“markdown” if it is the other way around. For simplicity, in the rest of the text we only refer to “markup” and**



255 **“markdown” collectively as “markup”, regardless of whether the market value is higher or lower than the average**
256 **electricity price.**

257

258 There are several advantages to this new coupling approach centered on linking prices. First, instead of simply prescribing
259 quantities such as yearly generation and capacities, the approach allows endogenous investment decisions to be made by both
260 models as they converge towards a joint solution. This gives maximal freedom to the coupled models, while minimizing
261 unnecessary distortions from one model to the other when some necessary quantities are being prescribed. Second, our coupling
262 scheme provides an elegant treatment of both supply- and demand-side technologies using the concept of “market values” on the
263 one hand and “capture prices” on the other. Third, from a theoretical point of view, transferring the market values of all the
264 generation types in a system alongside mappings of other relevant system parameters can lead to a convergence of the solutions
265 of the two models under idealized coupling circumstances. It can be rigorously shown that our method contains an exhaustive
266 list of interfacing parameters and variables for full model convergence of both quantities and prices. To the authors’ best
267 knowledge, the last point has not been explored or shown in any previous work.

268 In certain IAMs, VRE integration cost parameterization has been implemented to mimic the economic consequences of
269 variability of VRE, especially when the models have lower temporal resolution. Such VRE integration costs are contained in the
270 uncoupled default REMIND power sector modeling. However, the exact parameterization always depends on a particular set of
271 technological costs and parameters which might be subject to changes (Pietzcker et al., 2017), and the parametrization often
272 needs to be carried out anew under new assumptions and scenarios. In contrast, the model coupling approach is more general,
273 and no such bespoke parametrization is needed.

274 Inspired by the theoretical framework based on the Karush–Kuhn–Tucker (KKT) conditions for power sector optimization
275 problems (Brown and Reichenberg, 2021), we develop the theoretical basis for the coupling method in this section, which we
276 use for validating convergence in numerical coupling in later sections. In Section 3.1, we analytically formulate the fundamental
277 economic theory of the coupling approach. We first introduce the power sector formulations in the two uncoupled models (Sect.
278 3.1). Then we carry out a derivation of the convergence conditions and criteria, where we map the Lagrangians of the two
279 power-sector problems at different time resolutions, and derive the equilibrium condition for the coupled models (Sect. 3.2). In
280 Sect. 3.3, we introduce the iterative coupling interface which contains all the previously derived convergence conditions. For
281 REMIND information being passed on to DIETER (Sect. 3.3.1), and DIETER information being passed on to REMIND (Sect.
282 3.3.2), we list and define the variables and parameters being exchanged at the interface, as well as additional constraints and
283 implementations which serve to improve the coupling.

284 A complete list of mathematical symbols and list of abbreviations can be found in the appendices.

285 In the following sections, we first formulate the two uncoupled models, then move onto discussing coupled models. The
286 theoretical tools we develop here are the foundation to the numerical implementation of coupling, and serve to validate and
287 assess the model convergence in the result sections.

288 **3.1 Descriptions of uncoupled models**

289 REMIND and DIETER are both optimization models. REMIND maximizes interannual global welfare from 2005 to 2150,
290 whereas DIETER minimizes the power sector system cost for a single year and a single region. For a given REMIND “Nash”
291 iteration (see Sect. 2.1), the single-region economy is in long-term equilibrium after the optimization problem is solved. Since
292 given fixed national income, lower energy system costs mean higher consumption which leads to increased welfare (see
293 Appendix C for details), maximizing welfare can be assumed to correspond to minimizing energy system costs, a part of which



294 is power sector costs. Therefore, to reduce the complexity of our analysis, we formulate an uncoupled REMIND model based
 295 solely on the power sector cost minimization and not the total welfare maximization. For stand-alone REMIND, the multi-year
 296 power system cost for a single region equals the sum of all variable and fixed costs of generation,

$$297 \quad Z = \sum_{y,s} (c_{y,s}P_{y,s} + o_{y,s}G_{y,s}), \quad (1)$$

298 where c represents the fixed cost for capacity, o represents the variable cost of running power generation, P denotes endogenous
 299 capacity, and G denotes endogenous generation (defined as including curtailment in REMIND). P and G are the decision
 300 variables of the problem. The sum in the objective function is over time index y and power generating technology type s . The
 301 REMIND time index y stands for one representative year, which represents 5 or 10 years centered around it. So even though the
 302 time step is 5 to 10 years, the time resolution is one year. For example, “ $y=2020$ ” represents the years 2018-2022. Capital letters
 303 (both Latin and Greek) denote independent decision variables of the optimization problem. We classify an endogenous decision
 304 variable as independent if it is not uniquely determined by one or more other decision variables, and has no binding constraints
 305 applied to itself that is not already accounted for by the constraints on the decision variable(s) it depends on. Note that for
 306 simplicity, we treat all costs in REMIND in this formulation as if they are exogenous. In reality, REMIND has endogenous fixed
 307 costs due to technological learning as well as endogenous interest rate. Some types of variable costs such as fuel costs are also
 308 endogenous, which are determined based on primary energy balance equations for oil, gas and biomass. CO2 prices can also be
 309 endogenous under emission constraints.

310 Under the simplifying assumptions made for the derivation in this paper, the only independent decision variables are capacities,
 311 generations and curtailments. Small letters denote either exogenously given parameters or endogenous shadow prices.

312 For stand-alone DIETER which has a year-long time horizon, the power system cost is:

$$313 \quad \underline{Z} = \sum_s c_s P_s + \sum_h [\underline{q}_s (\underline{G}_{h,s} + \underline{I}_{h,vre})], \quad (2)$$

314 where $\underline{G}_{h,s}$ is the endogenous hourly power generation (excluding curtailment, note that this is different from the generation
 315 variable definition in REMIND), h is the hourly index in a year from 1 to 8760, s is the index for the power generating
 316 technology in DIETER. \underline{I} is hourly curtailment, only applicable in the case of variable renewables vre ($vre \subset s$). Technology
 317 type s can be subdivided into two subsets: vre and dis (“dispatchables”). For simplicity, we abbreviate the index subscript from
 318 $s|s = vre$ to vre and $s|s = dis$ to dis . Here in order to differentiate from REMIND notations, we use underscore $\underline{}$ to denote
 319 DIETER parameters and variables. Note that for simplicity, in the derivation we treat the technology types in both models as
 320 being identical, although in fact the technologies in the two models are not one-to-one mapped (Fig. B2). During the coupling
 321 all interface parameters and optimal decision variables need to be upscaled or downscaled when transferred from one model to
 322 the other.

323 The cost minimization of total power sector cost Z and \underline{Z} under constraints yields the optimal values of the decision variables,
 324 denoted as $(P_{y,s}^*, G_{y,s}^*)$, and $(\underline{P}_s^*, \underline{G}_{h,s}^*, \underline{I}_{h,s}^*)$.

325 Without coupling and under a baseline scenario, there are several constraints for each model. In the following equations we
 326 denote the shadow price (i.e. the Lagrangian multiplier) of a constraint by the symbol following \perp . We use small greek letters to
 327 denote endogenous shadow prices, and small Latin and Greek letters to denote exogenous parameters. The major constraints are
 328 as follows (“c” stands for “constraint”):

329 c1) Constraint on generation for meeting demand, a.k.a. “supply-demand balance equation”, or “balance equation” in short:

$$330 \quad \text{REMIND (annual):} \quad d_y = \sum_s G_{y,s} (1 - \alpha_{y,s}) \quad \perp \lambda_y,$$

$$331 \quad \text{DIETER (hourly):} \quad \underline{d}_h = \sum_s \underline{G}_{h,s} \quad \perp \underline{\lambda}_h,$$



332 where d_y denotes annual REMIND power demand, and \underline{d}_h denotes DIETER hourly demand. The shadow prices (Lagrange
 333 multipliers) λ_y and λ_h represent the annual and hourly electricity prices in REMIND and DIETER, respectively, and are
 334 equal to the marginal cost of one additional unit of electricity generation. $\alpha_{y,s}$ is the annual VRE curtailment ratio in
 335 REMIND. Note that technically speaking, REMIND electricity demand d_y is determined endogenously, partially via
 336 competition with other energy carriers at the final energy consumption level, such as the competition between electricity and
 337 gaseous carriers such as natural gas or hydrogen in household heating. But because here we have reduced REMIND to only
 338 intra-power sector dynamics for the purpose of mathematical analysis, we treat demand as exogenous.

339 c2) Constraint on maximum capacity by the available annual potential ψ_s in a region:

340 REMIND: $P_{y,s} \leq \psi_s \perp \omega_{y,s}$,

341 DIETER: $\underline{P}_s \leq \underline{\psi}_s \perp \underline{\omega}_s$.

342 Note that the resource constraint in REMIND is only relevant for wind, solar and hydro, and is assumed to be constant over
 343 the model horizon. Biomass availability is not modeled via a regional potential constraint. Instead the availability of biomass
 344 is priced in through the soft-coupling to the land-use model MAgPIE via a supply curve.

345 c3) Constraint on generation being non-negative:

346 REMIND: $-G_{y,s} \leq 0 \perp \xi_{y,s}$,

347 DIETER: $-\underline{G}_{h,s} \leq 0 \perp \underline{\xi}_{h,s}$.

348 Note that there are several other similar constraints on other positive variables such as capacities and curtailment. In practice,
 349 during the derivation they behave similarly to this positive generation constraint, therefore for simplicity, we do not include
 350 them in the derivation.

351 c4) Constraint on maximum generation from capacity:

352 REMIND: $G_{y,s} = \phi_{y,s} P_{y,s} * 8760 \perp \mu_{y,s}$,

353 DIETER: (variable renewables) $\underline{G}_{h,vre} + \underline{G}_{h,vre} = \underline{\phi}_{h,vre} \underline{P}_{vre} \perp \underline{\mu}_{h,vre}$

354 (dispatchables) $\underline{G}_{h,dis} \leq \underline{P}_{dis} \perp \underline{\mu}_{h,dis}$,

355 where $\phi_{y,s}$ is the exogenous annual average capacity factor of the power plant s in REMIND in year y , and $\underline{\phi}_{h,vre}$ is the
 356 exogenously given hourly theoretical capacity factor (i.e. before curtailment) of VRE in DIETER. Note that strictly
 357 speaking, curtailments in the uncoupled REMIND and DIETER are endogenous decision variables but are not independent
 358 variables. However, here we use capital letter to denote hourly curtailment in DIETER as an independent decision variable to
 359 account for curtailment costs and other curtailment constraints that can arise from a more general formulation of the model.

360 c5) “Historical” constraints on capacities in REMIND. This makes REMIND a so-called “brown-field model”, i.e. a model
 361 accounting for the standing capacities in the real-world. Past capacities ($y < 2020$) are hard-fixed, i.e. the variable capacities
 362 are fixed to certain numeric values. Current capacities ($y = 2020$) are “soft-fixed”, i.e. the variable capacities are fixed to a
 363 corridor around certain standing numeric values: the lower bounds guarantee the already planned capacities, and the upper
 364 bounds reflect the finite physical capabilities of scaling up, defined by 5% above the 2020 real-world data. For simplicity,
 365 we use only one constraint for both past and current capacities,

366 $P_{y,s} \geq p_{y,s} \perp \sigma_{y,s}$ for $y \leq 2020$,

367 where $p_{y,s}$ represents the standing capacities of technology s at time y in REMIND in the past and present years.

368 c6) Near-term upscaling constraint on VRE capacity expansion, represented by an upper bound on near-term capacity addition
 369 in model period $(y - \Delta y, y)$, $\Delta P_{y,s} := P_{y,s} - P_{y-\Delta y,s}$, where Δy is the REMIND model time step:



370 $\Delta P_{y,s} \leq q_{y,s} \perp \gamma_{y,s}$ for $y = 2025$,
371 where $q_{y,s}$ is equal to twice the added capacity during the 2010-2020 period (only applied to Germany in default REMIND).
372 Note that constraints (c5) and (c6) introduce interannual intertemporality into the power sector of REMIND. This additional
373 interannual intertemporality determines that the model equilibrium can only be strictly satisfied across the sum of all model
374 periods and not for a single period. Another source of intertemporality in REMIND is due to the adjustment cost, which we
375 ignore in the main text of this study since it introduces non-linearity in the power sector and also plays a relatively small role in
376 the overall dynamics.
377 Note that regarding the simplification of REMIND above, to the authors' best knowledge, there is no theoretical or empirical
378 concept that addresses the validity of drawing equivalence between welfare maximization and energy system cost minimization
379 in IAMs. Naively, given GDP is unchanged, decreasing energy system cost raises consumption and therefore welfare. However,
380 this is only valid under the assumption that energy is a substitute (and not a complement) to capital and labor, i.e. one usually
381 cannot raise economic output (GDP) simply by spending more on higher energy expenditure (while satisfying the same level of
382 energy demand). Nevertheless, this is likely a necessary condition and not a sufficient one for proving the equivalence. More
383 theoretical research will be needed to draw a precise and rigorous equivalence. However, in practice, we see that during our
384 numerical calculation the model is well behaved according to this reduced theory, which means that the parameters in the
385 models are in a regime where such an assumption is valid, at least in the case of IAM REMIND.

386 **3.2 Economic theory of model convergence**

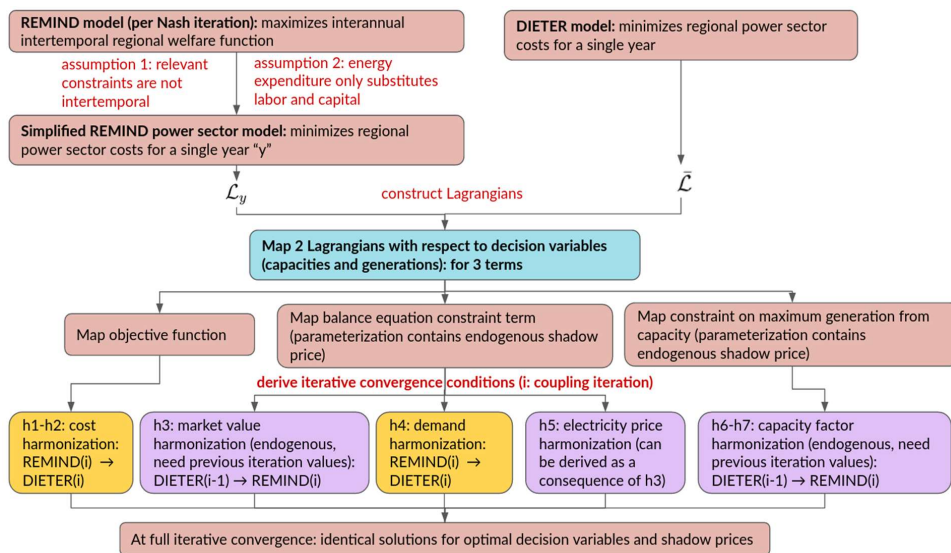
387 In the last section we have discussed the stand-alone uncoupled power sector formulations in REMIND and DIETER. In this
388 section we discuss the coupled models and its convergence. Under simplified assumptions, we first derive the mapping between
389 the models which are necessary for a convergence (Sect. 3.2.1-2), then we derive theoretical relations which are later used to
390 validate the numerical results of the coupled run (Sect. 3.2.3).

391 **3.2.1 Derivation of convergence conditions**

392 Our aim is to develop a method under which comprehensive convergence can be reached for soft-coupled multiscale models.
393 We achieve this by deriving a mapping of the two problems, such that their decision variables have identical optimal solutions
394 and the endogenous shadow prices are also equal across the models. The convergence conditions of the coupled REMIND-
395 DIETER model for the power sector are the result of such a mapping. Below, we first define what is meant by a “comprehensive
396 model convergence”, and then sketch the workflow of the derivation of a coupling framework which would result in a
397 comprehensive model convergence of both decision variables and shadow prices. The detailed derivation is in Appendix D.
398 Here, we derive the conditions under which the endogenous decision variables are identical at each model's optimum, i.e. $P_{y,s}^* =$
399 $P_{y,s}^*$, and $G_{y,s}^*(1 - \alpha_{y,s}^*) = \sum_h \underline{G}_{y,h,s}^*$ (or equivalently pre-curtailment generation $G_{y,s}^*$ and $\sum_h (\underline{G}_{y,h,s}^* + \Gamma_{y,h,s}^*)$). A convergence of
400 the solutions of these two sets of annual decision variables for each technology s and for each year y , along with the
401 convergence of shadow prices gives rise to “comprehensive model convergence”. We show below that this can only be achieved
402 if there is a harmonization at the level of the KKT Lagrangians of the two problems, following the methods first developed by
403 Karush, Kuhn and Tucker (Karush, 1939; Kuhn and Tucker, 1951).
404 Our coupling approach fundamentally relies on mapping the parameterization of the Lagrangians for both optimization
405 problems. It is trivial to show that as long as the KKT Lagrangians are identical with respect to the decision variables, the
406 solutions of the problem are identical. For example, if an optimization problem A has Lagrangian $L_1 = a_1 x + b_1 y$ and



407 another problem B has Lagrangian $L_2 = a_2 * x + b_2 * y$, where x and y are decision variables of the optimization problems.
 408 Then if we let $a_1 = a_2$, $b_1 = b_2$, the two problems are identical, and they must have identical optimal solutions for the
 409 decision variables x^* and y^* . This is the basic logic behind the Lagrangian-based method. The challenge in the case of
 410 REMIND and DIETER is to show that when a decision variable representing the same physical quantity, for example, the
 411 annual power generation from a technology is defined with low resolution in one problem, and is defined with high resolution in
 412 another, that there is nevertheless a viable mapping between the two Lagrangians. In this case, the parameterization of the
 413 Lagrangian is not only limited to exogenous parameters of the model, but also includes endogenous shadow prices and
 414 endogenous decision variables from the other model. Due to the endogenous nature of the latter two, the parametrization in the
 415 current-iteration model A must come from the solved results from the last iteration from model B, and vice versa. Fig. 2
 416 illustrates the workflow of the analytical derivation of the convergence conditions.



417
 418 **Figure 2: The schematics of the Lagrangian-based derivation procedure for a simplified version of REMIND-DIETER**
 419 **iterative convergence. After simplifying assumptions, we can construct the Lagrangians of the reduced REMIND model**
 420 **and the full DIETER model for a single year (Eqs. (3)-(4)). Comparing and mapping terms in the Lagrangians (a key**
 421 **step in bold), we discover that iterative exchange of a broad range of information is needed for a fully harmonized**
 422 **parameterization of the Lagrangians. Under the harmonization specified in the seven convergence conditions (color**
 423 **coded for directions of information flow), the coupled models can give rise to identical optimal solutions of the models'**
 424 **respective (annual aggregated) decision variables, and hence a full quantity convergence. The necessary shadow price**
 425 **convergence is shown in the detailed derivation of the harmonization conditions (h1-h7) in Appendix D.**
 426

427 The analytical derivation workflow, as shown in Fig. 2, is described in detail as follows. First, we apply simplifying assumptions
 428 to reduce the complexity of the uncoupled models (before the key step in blue in Fig. 2). Assumptions have to be made to justify
 429 reducing the scope of the REMIND model, such that for the purpose of the analysis, it is on equal footing as DIETER. We
 430 achieve this by reducing the global REMIND model to single-sector (the power sector), single-year, and single-region. To
 431 reduce the REMIND model from a macroeconomic-energy model to a power-sector-only model, we make similar assumptions
 432 as before when formulating the uncoupled REMIND power sector (see Sect. 3.1). To reduce the REMIND model further to a



433 single year, we assume that the models only contain constraints in the power sector that are not intertemporal, i.e. ignoring the
 434 brown-field and near-term constraints for now. Since for each iteration of the REMIND model under “Nash mode”, inter-
 435 regional trading happens between the iterations, the single-iteration optimization model is already for a single region, and
 436 therefore does not require simplification. After these simplifying steps, in this part of the derivation, we can treat REMIND’s
 437 power sector as “separate” from the rest of the model, and treat the dynamics of a single year in REMIND as independent from
 438 the dynamics of other years. Later, the numerical results of the convergence can confirm to a large degree the validity of these
 439 assumptions, especially in the green-field temporal ranges, i.e. where the intertemporal brown-field constraints have little
 440 influence on the dynamics. Note that with the inclusion of these intertemporal constraints in the derivation, the mapping
 441 becomes more complicated, especially for the near-term range, i.e. before 2035. So in practice, this derivation of the coupling
 442 interface is only an approximation to what is needed for a full convergence of DIETER and REMIND, since it deliberately
 443 ignores such constraints. See also Sec. 6.1.

444 After the necessary simplification assumptions, we construct the Lagrangians for the simplified model REMIND and for
 445 DIETER (after the blue block in Fig. 2) (Gan et al., 2013). For a single-year reduced REMIND power sector model, the
 446 Lagrangian is:

$$447 \quad \mathcal{L}_y = \underbrace{\sum_s (c_{y,s} P_{y,s} + o_{y,s} G_{y,s})}_{\text{REMIND objective function}} + \underbrace{\lambda_y \left[d_y - \sum_s G_{y,s} (1 - \alpha_{y,s}) \right]}_{\text{annual electricity balance equation constraint}} + \underbrace{\sum_s \mu_{y,s} (G_{y,s} - 8760 * \phi_{y,s} P_{y,s})}_{\text{maximum generation from capacity constraint}} . \quad (3)$$

448 We would like to map it to the single-year DIETER Lagrangian $\underline{\mathcal{L}}$:

$$449 \quad \underline{\mathcal{L}} = \underbrace{\sum_s [c_s P_s + o_s \sum_h (G_{h,s} + \Gamma_{h,vre})]}_{\text{DIETER objective function}} + \underbrace{\sum_h \lambda_h \left(d_h - \sum_s G_{h,s} \right)}_{\text{hourly electricity balance equation constraint}} + \underbrace{\sum_{h,dis} \mu_{h,dis} (G_{h,dis} - P_{dis})}_{\text{maximum dispatchable generation from capacity constraint}} \\ 450 \quad + \underbrace{\sum_{h,vre} \mu_{h,vre} (G_{h,vre} + \Gamma_{h,vre} - \phi_{h,vre} P_{vre})}_{\text{maximum renewable generation from capacity and weather constraint}} . \quad (4)$$

451 The algebraic derivation of mapping the two Lagrangians term-by-term is presented in Appendix D. From this algebraic
 452 mapping, we can derive seven harmonization conditions (h1-h7) required for a full convergence. Conditions (h1-h7) are the
 453 subsequent basis for most of the information exchanged at the coupling interface. Among them, conditions (h3, h5-7) (purple
 454 blocks in Fig. 2) indicate conditions which contain endogenous information that must come from the previous iteration of
 455 DIETER that is passed on to REMIND, such as markup and capacity factors. Conditions (h1-2, h4) (yellow blocks) indicate
 456 conditions which contain information that come from the previous iteration of REMIND and are passed on to DIETER. For
 457 schematics of the coupled iterations, see Appendix E.

458 This Lagrangian-mapping-based derivation can theoretically show that our approach (in its most simple form) necessarily leads
 459 to model convergence, and has the advantage of being mathematically straight-forward and rigorous. The necessary information
 460 from the power sector dynamics is all contained in the list of conditions derived from such a mapping. If the coupling contains
 461 less information, a convergence is not possible; at the same time, for a model convergence, one does not need to pass on any
 462 additional information beyond what is contained in this list of conditions. The list of information derived here is therefore
 463 complete and exhaustive for a coupled convergence.

464 3.2.2 List of convergence conditions

465 The convergence conditions (h1-h7), which are derived in detail in Appendix D following the procedure in Sect. 3.2.1, are
 466 summarized here:

467 **h1)** annual fixed costs are harmonized: $c_{y,s} = \underline{c}_{y,s}$,



468 **h2)** annual variable costs are harmonized: $o_{y,s} = \underline{o}_{y,s}$.

469 **h3)** annual average market values for each generation type s are harmonized via markups from DIETER. We let $\eta_{y,s}(i-1)$

470 denote the markup for technology s in year y in the last iteration DIETER, i.e. the difference between market value and
 471 annual average price of electricity:

$$472 \quad \eta_{y,s} = \frac{\sum_s \lambda_{y,h} \underline{G}_{y,h,s}}{\sum_h \underline{G}_{y,h,s}} - \frac{\sum_h \lambda_{y,h} \underline{d}_{y,h}}{\sum_h \underline{d}_{y,h}} . \quad (5)$$

Market values_s
Annual average electricity price_s

473 This is the heart of our coupling approach, using markups as the “price signals”. Intuitively, the markups represent the
 474 market value differences between REMIND and DIETER. The harmonization of market values is implemented by
 475 iteratively adjusting the market value for each generator type in REMIND to be the same as that in DIETER. As long as
 476 the market values (or per-unit-generation revenues) and costs are harmonized, the economic structures of the power
 477 market are identical and the models can converge.

478 Using markup Eq. (5), we modify the original objective function Z in the coupled version of REMIND by subtracting the
 479 product of markups and generations summed over all technologies and all years:

$$480 \quad Z' = Z - \sum_{y,s} \eta_{y,s}(i-1) G_{y,s}(1 - \alpha_{y,s}), \quad (6)$$

481 where Z' is the modified REMIND objective function in the coupled version, i is the iteration index of the iterative soft-
 482 coupling.

483 **h4)** annual power demands are harmonized: $\sum_h \underline{d}_{y,h} = d_y$,

484 **h5)** annual average prices of electricity are harmonized:

$$485 \quad \lambda_y = \frac{\sum_h \lambda_{y,h}(i-1) \underline{d}_{y,h}(i-1)}{\sum_h \underline{d}_{y,h}(i-1)}, \quad (7)$$

486 where $(i-1)$ indicates that the endogenous results are from the last iteration. This is shown in Appendix D to be a direct
 487 consequence of (h3) and (h4).

488 **h6)** annual average capacity factor for each generation type s are harmonized:

$$489 \quad \phi_{y,s} = \sum_h \phi_{y,h,s}(i-1) / 8760, \quad (8)$$

490 where $\phi_{y,h,s}(i-1) = \frac{G_{y,h,s}(i-1)}{P_{y,s}(i-1)}$ is the hourly capacity factor in DIETER, determined by endogenous hourly generation
 491 and annual capacities in the last iteration.

492 **h7)** annual curtailment are harmonized:

$$493 \quad G_{y,vre} \alpha_{y,vre} = \sum_h G_{y,h,vre}(i-1). \quad (9)$$

494 In mapping the Lagrangians (Eqs. (3-4)), except the objective function, the rest of the parametrization contains endogenous
 495 shadow prices and endogenous quantities. Since endogenous values can only be known ex post, this imposes a strict requirement
 496 on the coupling that it must be iterative, with the endogenous part of the parameterization coming from previous iteration
 497 optimization results – usually from the other model. The mapping of the endogenous information requires careful argument in
 498 each case (i.e. the derivation of (h3)-(h7)). In the case of the balance equation constraint Lagrangian term (corresponding to
 499 (c1)), the shadow prices of the constraint in current-iteration REMIND model are exogenously corrected by a set of technology-
 500 specific “markups” (see Sect. 3.1 introduction), such that the new “corrected” market value in REMIND is manipulated to
 501 match the market value of the previous iteration of DIETER. This is the heart of our coupling approach, using markups as the
 502 “price signals”. In the case of the constraint on maximum generation from capacity (corresponding to (c4)), the endogenous



503 shadow prices in the current iteration REMIND can be shown to be automatically mapped to the those in the previous iteration
504 of DIETER, given that the annual average capacity factors in the constraints are harmonized (h6-h7).
505 In actual implementation, most of the above mappings are modified for numerical stability (Sect. 3.3.2, Appendix H).

506 **3.2.3 Theoretical tools for validating convergence**

507 Here we first state the convergence criteria, which are mathematical relations which are being satisfied under model
508 convergence. Then we also discuss equilibrium conditions of the coupled models which alongside the convergence criteria can
509 be used to check numeric results to validate and assess the convergence outcome.

510 Under a theoretical full convergence of the coupled model,

511 v1) annual average electricity prices,

512 v2) capacities,

513 v3) (post- or pre-curtailment) generations,

514 all should be identical at the end of the coupling in both models. These are the most important criteria by which we validate full
515 model convergence. Technically, electricity price convergence (v1) (i.e. convergence condition (h5)) can be derived from (h3)-
516 (h4). Nevertheless, we check this ex post, together with quantity convergence (v2-v3). In actual coupled model runs, following
517 only the convergence conditions (h1-h7), the convergence criteria (v1-v3) might not be exactly fulfilled. Therefore in practice,
518 in order to validate the degree of numerical convergence, the alignment between REMIND and DIETER generation shares is set
519 to be within a few percentage points before coupled runs terminate.

520 Besides using convergence criteria (v1-v3), we also use a type of equilibrium condition – the so-called “zero-profit rules”
521 (ZPRs) to validate the numerical model convergence. ZPRs are mathematical relations which state that under market
522 equilibrium, prices are equal to the costs for electricity. This is not always the case, especially in the situation where there are
523 extra constraints in the model which distort this equality. ZPRs contain model parameters and decision variables at market
524 equilibrium, and they can be derived from the KKT conditions of the model (Appendix F). ZPRs are therefore reliable tools in
525 ascertaining the sources of market values or the price of electricity of the power sector, because according to the ZPRs, one can
526 always decompose the prices into the cost components, i.e. so-called levelized costs of electricity (LCOE). The decomposition
527 of prices into cost components is important, because the prices of electricity in the power market are overdetermined by the
528 energy mix, so it is possible that two different power mixes correspond to the same electricity price. In numerical results, a
529 slight mismatch of energy mix at the end of the coupling is unavoidable, so alongside comparing the prices, it is often helpful to
530 compare the makeup of the LCOE across the models, such that they also appear harmonized at the end of the iterative
531 convergence. Overall, ZPRs is a helpful tool for visualizing and understanding the power market dynamics, both from the point
532 of view of each generator type as well as from the point of view of the entire electricity system. It is worth noting, that the zero-
533 profit rules, which are mathematical conditions derived from an idealized modeling of the power sector as fully competitive, are
534 only an approximation to the real-world markets, where firm profits exist. ZPRs in its technical definition simply means that at
535 model equilibrium, cost equals revenue. Given that the profits are defined as the difference between revenue and cost, the profits
536 are zero in this situation. The name “zero-profit rule” therefore should not be overinterpreted beyond their technical contents,
537 and one should be aware of their theoretical origin and assumptions under which they are valid.

538 The ZPRs of the coupled model can be derived based on: 1), the uncoupled models; 2), the modification made to the model due
539 to the coupling interface (h1-h7); 3), any additional modifications made to the model during our numerical implementation. In
540 the last category, for a complete numerical implementation of the coupling, we add one additional capacity constraint (c7) and
541 (c8) for each model. The first capacity constraint (c7) is created in REMIND to circumvent the issue of extremely high markup



542 from peaker gas plants in the scarcity hour of the year in the DIETER model, which otherwise causes instability during the
 543 iterative coupling. The second constraint (c8) is a simple brown-field constraint implemented in DIETER to address the fact that
 544 DIETER is a green-field model, which is otherwise ignorant about standing-capacities in the real world. For simplicity, (c7) and
 545 (c8) are not included in the convergence condition derivations in Sect. 3.2.1. The derivation of the ZPRs outlined by the above
 546 three steps have been carried out in: Appendix F (uncoupled models), Appendix G (coupled REMIND only including coupling
 547 interface, coupled DIETER including constraint (c8)), and Appendix H (coupled REMIND, including constraint (c7)).
 548 In summary, the ZPRs for both coupled models are as follows:

549 a) Coupled REMIND:

550 i) Technology-specific ZPR:

$$\begin{aligned}
 551 \quad & \frac{\sum_y (c_{y,s} P_{y,s} + o_{y,s} G_{y,s})}{\sum_y G_{y,s}} + \frac{\sum_y (c_{y,s} P_{y,s} + o_{y,s} G_{y,s}) \alpha_{y,s}}{\sum_y G_{y,s} (1 - \alpha_{y,s})} \\
 552 \quad & = - \frac{\sum_y (\omega_{y,s} - \sigma_{y,s} + \gamma_{y,s} + \nu_{y,s}) P_{y,s}}{\sum_y G_{y,s} (1 - \alpha_{y,s})} + \frac{\sum_y (\lambda_y + \eta'_{y,s}) G_{y,s} (1 - \alpha_{y,s})}{\sum_y G_{y,s} (1 - \alpha_{y,s})} \quad (10)
 \end{aligned}$$

553 ii) System ZPR:

$$\begin{aligned}
 554 \quad & \frac{\sum_{y,s} (c_{y,s} P_{y,s} + o_{y,s} G_{y,s})}{\sum_{y,s} G_{y,s}} + \frac{\sum_{y,s} (c_{y,s} P_{y,s} + o_{y,s} G_{y,s}) \alpha_{y,s}}{\sum_{y,s} G_{y,s} (1 - \alpha_{y,s})} \\
 555 \quad & = - \frac{\sum_{y,s} (\omega_{y,s} - \sigma_{y,s} + \gamma_{y,s} + \nu_{y,s}) P_{y,s}}{\sum_{y,s} G_{y,s} (1 - \alpha_{y,s})} + \frac{\sum_{y,s} (\lambda_y + \eta'_{y,s}) G_{y,s} (1 - \alpha_{y,s})}{\sum_{y,s} G_{y,s} (1 - \alpha_{y,s})} \quad (11)
 \end{aligned}$$

556 b) Coupled DIETER:

557 i) Technology-specific ZPR:

$$558 \quad \frac{c_s P_s + o_s \sum_h (G_{h,s} + \Gamma_{h,vre})}{\sum_h G_{h,s}} = - \frac{(\omega_s + \zeta_s) P_s}{\sum_h G_{h,s}} + \frac{\sum_h \lambda_h G_{h,s}}{\sum_h G_{h,s}} \quad (12)$$

559 ii) System ZPR:

$$560 \quad \frac{\sum_s [c_s P_s + o_s \sum_h (G_{h,s} + \Gamma_{h,vre})]}{\sum_{h,s} G_{h,s}} = - \frac{\sum_s (\omega_s + \zeta_s) P_s}{\sum_{h,s} G_{h,s}} + \frac{\sum_h \lambda_h d_h}{\sum_h d_h} \quad (13)$$

561 “Prime” sign indicates the term has been modified from the uncoupled versions due to implementation in the coupling. ν and ζ
 562 are capacity shadow prices introduced from the additional constraints (c7-c8) (Appendix G-H). It is worth noting that constraints
 563 (c7-c8) introduced due to coupling can impact the Lagrangians of the two models which we used to derive convergence
 564 conditions and criteria. However, in actual coupled runs, evidently there is only a moderate distortion due to these extra
 565 constraints. Condition (c8) even helps with convergence, because it puts most of the brown-field and near-term constraints
 566 which REMIND sees also into DIETER (see Sect. 6.1).

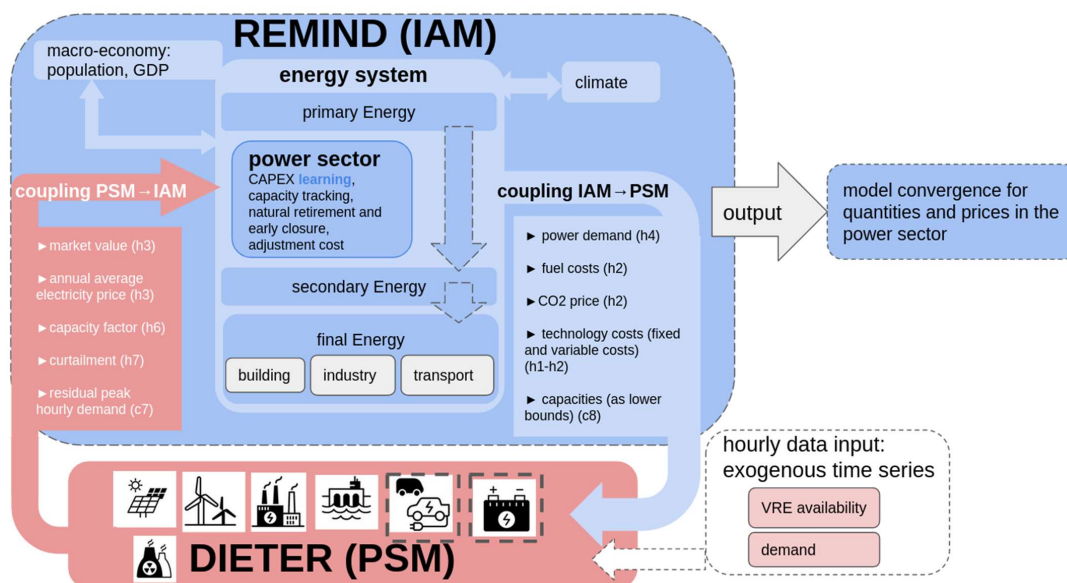
567 Due to the fact that several sources of shadow prices cannot be incorporated during the derivation for convergence (Sect. 3.2.1),
 568 in numerical experiments of coupled run it is appropriate to compare the following two types of prices across the two models for
 569 price convergence:



570 1) Electricity price convergence, not including any capacity shadow prices;
 571 2) Sum of electricity prices and all respective capacity shadow prices converge.
 572 Under the simplified analysis of convergence (discounting brown-field constraints, scarcity prices, etc), price convergence in 1)
 573 is predicted by theory (see also convergence condition (h5)). However, it is only under the most idealized situation.
 574 Convergence in 2) on the other hand includes all the prices, which should match if LCOEs match across the system. We use the
 575 first type to check price convergence over iteration, and use the second type only in the context of checking the system ZPRs
 576 across the models because of the theoretical relations between full prices and LCOEs.

577 3.3 Implementation via interface: exchange of variables

578 In this section we list parameters and endogenous variables that are exchanged between REMIND and DIETER. This already
 579 satisfies most convergence conditions, while the remaining condition (h5) is checked in Sect. 4 as part of the convergence
 580 criteria (v1-v3). An overview of the model coupling and the flow of information under convergence conditions is shown in Fig.
 581 3.



582
 583 **Figure 3: The schematics of the REMIND-DIETER iterative soft-coupling. The power sector module of IAM REMIND,**
 584 **which is between the layer of primary to secondary energy transformation, is hard-coupled with other modules inside**
 585 **REMIND such as macro-economy, industry and transport. In PSM DIETER, the power market with generators of**
 586 **various types is modeled with hourly resolution, with options for storage and flexible demand. The information**
 587 **exchanged between the models (block arrows) are determined via the convergence conditions (h1-h7) derived before**
 588 **(Sect. 3.2.1). In order to improve performance and facilitate convergence, additional constraints (c7) and (c8) are**
 589 **included in the coupling interface. The coupling interface for REMIND → DIETER is programmed as a part of modified**
 590 **DIETER code, and vice versa. Both interfaces are written in GAMS. For a single-region, the scheduling of coupled**
 591 **iterations is illustrated in Fig. E1 in Appendix E. 16 DIETER optimization problems are solved for each representative**



592 **year of REMIND in parallel, scheduled after each internal REMIND “Nash” iteration (see Sect. 2.1 for a description of**
593 **the iterative “Nash” algorithm).**

594

595 During the coupling, the following exchanges of parameters and variables take place iteratively in both directions via the
596 interface.

597 **3.3.1 REMIND to DIETER**

598 The following information flow from REMIND to DIETER.

599 1. Technology fixed costs (convergence condition (h1)):

- 600 a. Annualized capital investment cost: It is calculated from endogenously determined overnight investment cost, plant
601 lifetime, and the endogenously determined interest rate. The overnight investment cost is determined from floor cost,
602 learning rate and the endogenous global accumulated deployment. Note that investment costs decrease according to
603 endogenous learning rate. Interest rate is about 5% on average but is endogenous and time dependent in REMIND;
604 b. Annualized operation and maintenance (O&M) fixed costs (OMF): They are a fixed share of the capital costs;
605 c. Adjustment cost: It is technology-specific and is proportional to the capital investment cost. See Appendix I for its
606 implementation.

607 2. Technology variable costs (convergence condition (h2)):

- 608 a. Primary energy fuel costs: They are endogenously determined as the shadow prices of the primary fuel balance
609 equations in REMIND. Import prices, domestic prices of extraction, amount of regional reserve, and the amount of fuel
610 demand can all influence the fuel cost. The relevant fuel costs include coal, gas, biomass and uranium. The fuel costs
611 can have interannual intertemporal oscillatory components which can cause instability during iteration if coupled
612 directly. We mitigate this by conducting a linear fit to the time series before passing them to DIETER;
613 b. Conversion efficiency of each generation technology;
614 c. O&M variable costs (OMV);
615 d. CO₂ emission cost: Exogenous or endogenous CO₂ price from REMIND multiplied by the carbon content of a type of
616 fossil fuel and divided by the conversion efficiency of a generation technology gives the CO₂ cost of 1MWh of
617 generation. Note that in REMIND, biomass is considered to contain zero carbon emission when combusted.;
618 e. Grid cost: In REMIND the stylized grid capacity equation is proportional to the amount of pre-curtailment VRE
619 generation. So effectively the grid cost is a variable cost. Note that in future work, grid costs can be modeled in more
620 detail either in DIETER or in another PSM. Here, we use the parameterized grid costs which are implemented in
621 default REMIND as an approximation to the necessary grid cost.

622 3. Power demand (convergence condition (h4)). REMIND informs DIETER of the total power demand d_y of a representative
623 year y . In the next iteration of DIETER, the exogenous time series for the hourly demand from a historical year (2019) is
624 scaled up to demand of the last iteration REMIND, $d_y(i-1)$, such that the annual total power demand in DIETER is equal
625 to that of REMIND for each coupled year: $\underline{d}_h = \underline{d}_{2019,h} * \frac{d_y(i-1)}{\sum_h \underline{d}_{2019,h}}$.

626 4. Pre-investment capacities $P_{y-\Delta y/2,s}/(1-ER)$ as an additional brown-field constraint (see constraint (c8) in Appendix G).
627 ER is the endogenous early retirement rate in REMIND.

628 5. Total regional renewable resources for wind, solar and hydro (constraint (c2)), such that DIETER capacities are constrained
629 by the same total available resources as in REMIND.



630 6. Annual average theoretical capacity factors of VREs and hydroelectric in REMIND (convergence condition (h6)). We note
 631 the pre-curtailment utilization rates of VRE capacity as “theoretical capacity factors”, as these can be achieved in theory if
 632 there is no curtailment. They are usually determined by meteorological factors such as wind and solar potential, as well as
 633 the efficiency of the turbines or solar photovoltaic modules. In contrast, the post-curtailment utilization rate of VRE are “real
 634 capacity factors”, as these are the real utilization rates after optimal endogenous dispatch. The time series of theoretical
 635 utilization rate of VRE generations of one historical year in DIETER are scaled up such that the annual average theoretical
 636 capacity factors in DIETER equals the exogenous parameters in REMIND:

$$637 \quad \phi_{h,vre}(y) = \min \left(0.99, \phi_{h,vre}(y = 2019) * \frac{\phi_{vre}}{\sum_h \phi_{h,vre}(y=2019)} \right).$$

638 In DIETER, to be realistic, the rescaled hourly capacity factor for solar and wind has an upper bound at 99%. The slight
 639 mismatch of the capacity factors due to this additional upper bound is negligible

640 3.3.2 DIETER to REMIND

641 The following information is passed from last-iteration DIETER to REMIND:

- 642 1. Market values $MV'_{y,s}$ and the annual average electricity price J'_y (convergence condition (h3)), where $MV'_{y,s}$ is the annual
 643 average market value without the surplus scarcity hour price, and J'_y is the annual average electricity price without the
 644 surplus scarcity hour price.
- 645 2. Peak hourly residual power demand $\underline{d}_{residual}$ as a fraction of total annual demand $\sum_h \underline{d}_h$ (constraint (c7)). This produces the
 646 peak residual demand in REMIND $d_{residual,y}$ that is proportional to the last-iteration DIETER peak to total demand ratio
 647 $\frac{\underline{d}_{residual}(y,i-1)}{\sum_h \underline{d}_h(y,i-1)}$, and the in-iteration total annual demand $d_y(i)$:
 648 $d_{residual,y}(i) = \frac{\underline{d}_{residual}(y,i-1)}{\sum_h \underline{d}_h(y,i-1)} * d_y(i)$,
 649 where $\underline{d}_{residual}$ was defined in Appendix H (Eq. (H1)).
- 650 3. Annual capacity factors of dispatchable plants $\phi_{dis} = \frac{\sum_h \underline{g}_{h,dis}}{\underline{e}_{dis} * 8760}$ (convergence condition (h6)).
- 651 4. Annual solar and wind curtailment ratio: curtailment as a fraction to total annual post-curtailment generation $\frac{\sum_h \Gamma_{h,vre}}{\sum_h \underline{g}_{h,vre}}$
 652 (convergence condition (h7)).

653 For the information flowing from DIETER to REMIND, we use an innovative method of multiplicative “prefactors”, which can
 654 stabilize the coupling and increase the speed towards model convergence. The prefactors are automatic linear stabilizers of the
 655 current-iteration variables in REMIND. They depend on current-iteration endogenous variables in REMIND, and are multiplied
 656 usually with the last-iteration endogenous DIETER results that are exogenously passed to REMIND. This allows some degree of
 657 endogeneity in these exchanged variables, and their values can be adjusted according to the updated dynamics in the current
 658 REMIND iteration, such as interregional trading or price-demand elasticity, under which the exogenous last-iteration DIETER
 659 optimality can be used as an approximate starting point but do not necessarily hold exactly.

660 The prefactors usually depend on the differences between generation shares in the two models: e.g. the prefactor for markup is a
 661 linear function of the difference between the current-iteration REMIND endogenous generation share and last-iteration DIETER
 662 generation share. We illustrate the mechanism of prefactors using markup for solar as an example: A lower market value for
 663 solar is consistent with a higher solar share, according to the well-known self-cannibalization effect of decreasing VRE market
 664 value as the VRE share increases (Hirth, 2018). Therefore, we can introduce an automatic stabilization measure through a
 665 negative feedback loop: If the REMIND endogenous share is larger than in the last DIETER iteration, in which case the in-



666 iteration market value should be lower than the last-iteration DIETER market value, the multiplicative prefactor for market
667 value should be so constructed such that it is smaller than one. This lowers the market value for solar, and decreases the in-
668 iteration REMIND markup $\eta_{y,s}(i)$, hence preventing over-incentivizing the solar generation using the old market value based on
669 the last-iteration energy mix. Overall, this produces a stabilizing effect on the system by making the markup as a price signal
670 responsive to endogenous quantity change. We use prefactors ubiquitously when passing variables from DIETER to REMIND,
671 such that during the iteration REMIND can adjust more smoothly and easily. We discuss the implementation of these prefactors
672 in detail in Appendix H.2.

673 **4 Numerical convergence under “proof-of-concept” baseline scenario**

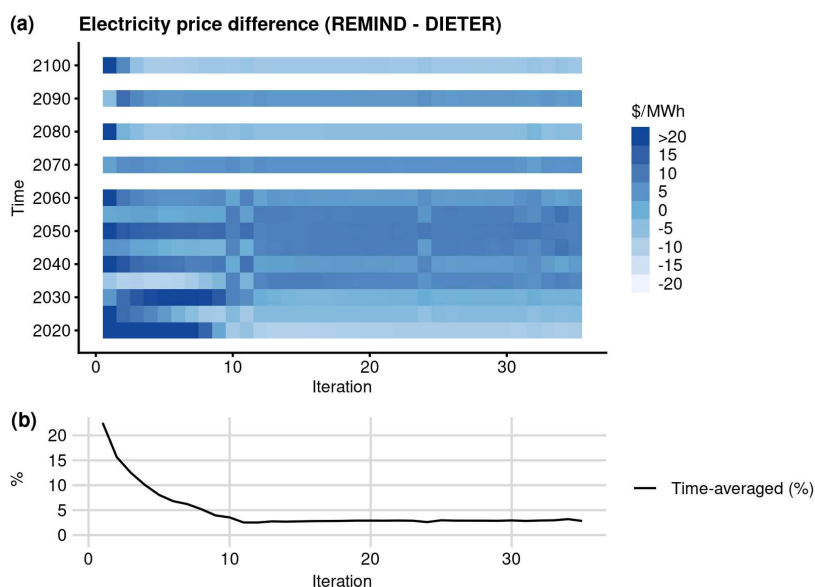
674 In this section, we check the convergence behavior for prices and quantities (capacity and generation) in coupled model runs
675 using the convergence validation criteria from the last section. Comparing the numerical results with the theoretical prediction,
676 we can validate that REMIND-DIETER soft-coupling indeed produces almost full convergence.
677 Throughout this section, we only use one scenario – a “proof-of-concept” baseline scenario. Under the “proof-of-concept”
678 scenario of the coupled run, we disable storage (i.e. batteries and hydrogen) and flexible demand (i.e. electrolyzers) in both
679 models, as this allows us to use the theoretically derived convergence criteria from Sect. 3, which would become overly
680 complex in a model with storage and flexible demand. The coupled run is under a baseline scenario, i.e. there is no additional
681 climate policy implementation. Since this is a configuration created only for comparing to the theoretical prediction, it is not
682 meant to be a policy-relevant configuration. In more policy-relevant coupled runs, we turn on storage and flexible demand (see
683 Sect. 5). For schematics and computational runtimes of the coupled iterations, see Appendix E.
684 For the coupled runs, we define a baseline scenario for single-region Germany under SSP2 assumptions, corresponding to the
685 “middle-of-the-road” scenario (for a definition of the SSPs, see Koch and Leimbach, 2022). Specifically, this means that
686 REMIND runs for all global regions in parallel, but DIETER only runs for Germany. Only information in the German power
687 sector is exchanged for the two models. We use a low CO₂ price to represent “no additional policy”, which is 30\$/tCO₂ in 2020
688 and 37\$/tCO₂ for years beyond 2020. According to the 2011 Nuclear Energy Act of Germany, remaining nuclear capacities are
689 set to early retire in REMIND within the time period until 2022. We assume hydroelectric generation in Germany to come from
690 run-of-the-river. In DIETER, we cap dispatchable generation’s annual capacity factors at 80% for non-nuclear power plants, and
691 85% for nuclear power plants, so the dispatch results are in line with real-world power sectors. This constraint only adjusts the
692 capacity factor constraint (c4), which would pose no additional distortion to our mathematical analysis.
693 Due to the particular implementation of offshore wind in REMIND, DIETER wind offshore capacities are fixed to that of
694 REMIND to avoid too much distortion. Since in our scenarios, offshore wind capacity in Germany is relatively small compared
695 to other generators, this fixing presents only a minor distortion to the coupling. Hydroelectric generation in REMIND is
696 assumed to have an average annual capacity factor of around 25%. This capacity factor is implemented as a bound in DIETER.
697 For simplicity, instead of a time series profile for hydroelectric generation, we allow the hourly capacity factor to be no higher
698 than 90%, meaning hydro is close to being dispatchable in all our scenarios. In the German context, hydro usually means run-of-
699 the-river, which has a variable output. Nevertheless, we find the 90% maximum hourly capacity factor a reasonable assumption
700 to make, since in our runs we do not yet consider pumped hydro as a technology in this study, so a more dispatchable quality of
701 hydro can be assumed. Results presented in this section belong to the same coupled run under the “proof-of-concept” scenario.



702 4.1 Electricity price convergence

703 According to theoretical convergence criteria (under simplifying assumptions, Sect. 3.2.1-3), at numerical convergence, the
704 electricity price of REMIND should be equal to the price of DIETER. However, REMIND is interannual intertemporal, whereas
705 DIETER is only year-long, so we compare the differences over time, as well as the interannual average of the price differences
706 (Fig. 4).

707



708

709 **Figure 4: Annual average electricity price convergence behavior of a coupled run for Germany under a “proof-of-**
710 **concept” baseline scenario. (a): the difference between the annual electricity price time series of REMIND and the**
711 **annual average electricity price time series in DIETER as a function of coupled iteration. (b): the interannual average of**
712 **the differences in (a) as a share of REMIND price. Due to the interannual intertemporal nature of REMIND, in (a) the**
713 **price difference can appear to have oscillatory components, obscuring the visual assessment of convergence. As a result,**
714 **we show the trend of price convergence over iterations more clearly in panel (b) by taking the temporal average of the**
715 **price differences. The REMIND price in both plots is a running average of three neighboring time periods to visually**
716 **smooth out oscillations.**

717

718 In Fig. 4a, the price difference oscillates from period to period. As the coupling starts, the REMIND price is much higher than
719 DIETER, especially in the earlier years. After around the 10th iteration, the difference in early years starts to reverse: DIETER’s
720 price becomes higher than REMIND. Around 2040-2060, REMIND has a higher average price than DIETER, due to the VRE
721 market values being higher than their LCOE. This is discussed later in Sect. 4.3.2.

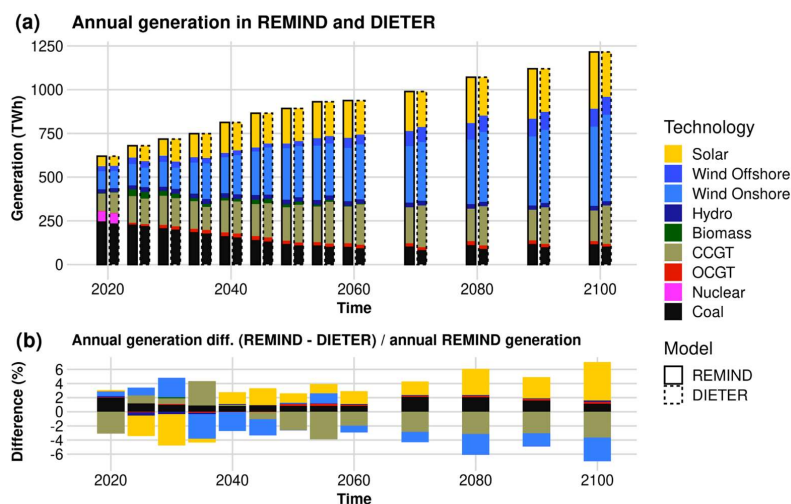
722 In Fig. 4b, we calculate the difference between two time series – the time-averaged power prices in the two models. We observe
723 the difference between them decreases over the iterations, showing a clear converging trend, and stabilizes at around 3% of the
724 REMIND price. There are two observations regarding the price convergence of the coupled run. First, the convergence happens
725 rather quickly within 10 iterations. Second, the converged value of the price difference is not exactly 0, but slightly above 0, at a



726 few percent of the full price (a few \$/MWh). Under ideal convergence conditions, according to (v1), the two prices should be
727 equal at full convergence for every coupled year. However, in practice, the average prices do not perfectly match, as there are
728 several sources of distortions from capacity shadow prices. The capacity shadow prices come from many sources in both
729 models: extra constraints such as (c7-c8) which are not part of the analysis leading to (v1), constraints that are in REMIND but
730 not in DIETER (c5-c6), and exogenous wind offshore capacity in DIETER. Some of these capacity shadow prices in both
731 models can be more or less consistent with each other (such as standing capacity constraint in DIETER and brown-field
732 constraints in REMIND), but others are not and can distort two models in different ways, causing some degrees of misalignment
733 in prices. As discussed before, prices can be overdetermined by the energy mix (Sect. 3.2.3). Therefore, some of the capacity
734 shadow prices – even though not aligned between the two models – can nevertheless cancel each other (especially averaged over
735 time), potentially causing the price differences to be moderate. To examine exactly how well the prices at the end of the
736 coupling match, we need to check the cost decomposition of prices. This is discussed later in Sect. 4.3.
737 Also note that Fig. 4b presents a time-averaged price comparison, and on average the difference between the prices in the two
738 models is small at the end of the coupling. However, when one compares the maximal deviation for any single year at the end of
739 the coupling, it can be as high as 10\$/MWh, e.g. around 2050 (Fig. 4a). This is much larger than the 3% averaged deviation in
740 Fig. 4b. However, compared to default REMIND prices (which we cannot show due to limited space), we are fairly confident
741 that the oscillation of coupled REMIND results from internal dynamics that are also visible in the default uncoupled version. So
742 a time-averaged treatment is adequate in displaying total price convergence here.

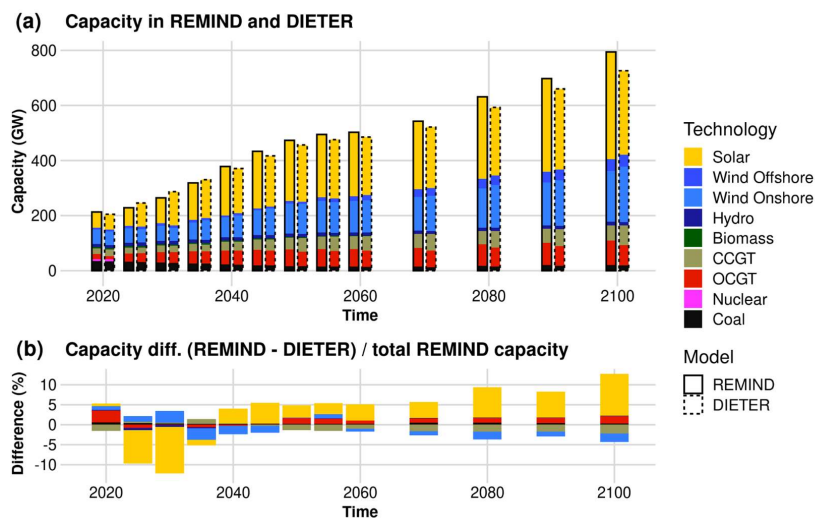
743 **4.2 Quantity convergence**

744 Besides price convergence, the capacity and generation decision variables must also converge within a certain tolerance at the
745 end of the coupling. This is reflected in the generation mix (Fig. 5) and the capacity mix (Fig. 6) at the end of the coupled run.
746 Due to the existence of several sources of mismatch between the two models already mentioned in the last section, which is
747 already manifested in the mismatch in electricity prices of the two models, a certain degree of mismatch in quantities is also
748 to be expected. Nevertheless, the agreement between the two endogenous sets of decision variables is satisfactory. For this coupled
749 run, the differences of the generation share of any single technology between the two models are smaller than 4.4% for each
750 year until 2100. Figure (5b) highlights some subtle model differences in generation. For example, after 2040, REMIND favors
751 solar and coal, whereas DIETER tends to have more combined cycle gas turbines (CCGT) and wind onshore. Due to the low
752 capacity factor of OCGT and solar compared to the capacity factors of the other generators, the capacity mix differences
753 between models are amplified for these two technologies (Fig. 6). But overall, the generation mixes and the capacity portfolios
754 at the end of coupled run are generally similar.



755

756 **Figure 5: Annual electricity generation convergence at the final iteration of a coupled run for Germany under the**
 757 **“proof-of-concept” baseline scenario. (a) Side-by-side comparison of the two generation portfolios at the end of the**
 758 **coupled run. (b) The difference between the generation mix in the two models as a share of total REMIND generation.**



759

760 **Figure 6: Capacity convergence at the final iteration of a coupled run for Germany under the “proof-of-concept”**
 761 **baseline scenario. (a) Side-by-side comparison of the two models’ capacity mix at the end of the coupled run. (b) The**
 762 **capacity difference between the two models as a share of total REMIND capacity.**

763

764 For periods that are policy relevant in the short- to medium-term (i.e. before 2070), the convergence for quantities is generally
 765 slightly worse in the near-term, i.e. in the 2020s and 2030s, likely due to the capacity bounds mismatch in the near-term (such as
 766 the capacity bounds (c5-c6) in REMIND not being completely replicated by standing capacity constraint (c8) in DIETER). If
 767 DIETER does not contain identical bounds as REMIND, then its endogenous decision will have more of a green-field rationale



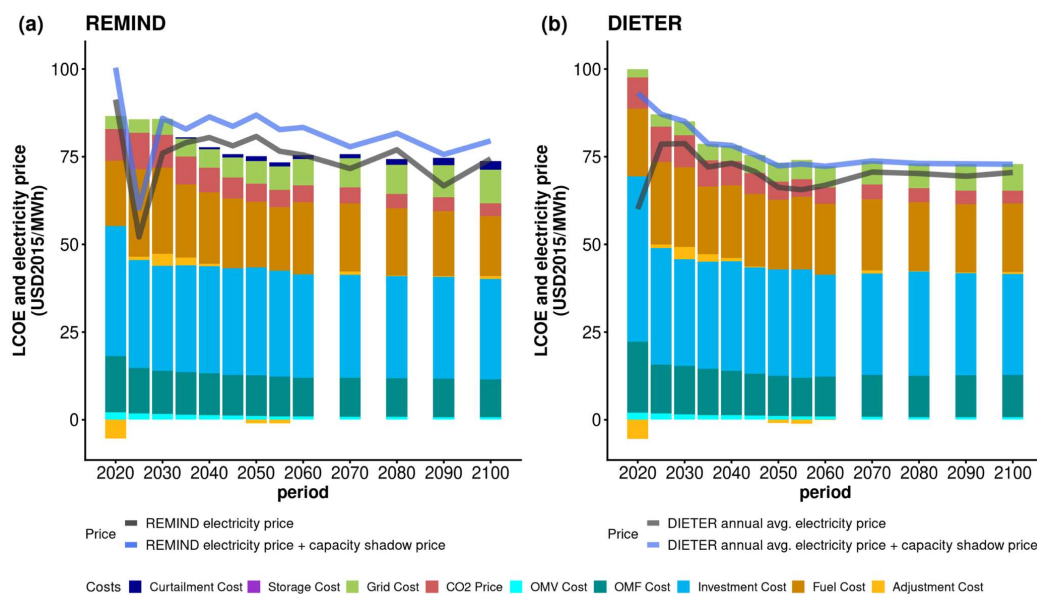
768 than REMIND does, the latter of which is more constrained in the near-term. In case an improvement of near-term convergence
769 is desired, these bounds could be implemented more carefully, and more technology-specific. Due to the limited scope, we only
770 apply a generic standing capacity constraint (c8) in DIETER to represent the basket of various constraints. The convergence of
771 quantities is also not perfect in the green-field periods, such as after 2040, where both models are less constrained by near-term
772 dynamics. The reason for this is likely due to the fact that in DIETER, hydroelectric generation is not economically competitive
773 against other cheaper forms of generation such as solar and wind. But in REMIND it is economically competitive, likely due to
774 the long life-time of the plants. Semi-exogenous wind offshore capacities in both models could also play a role. This is
775 discussed in more detail in Section 6.1.

776 **4.3 Zero-profit rules for the coupled model**

777 As our analytical discussion showed before in Sect. 3.2.3, model equilibria in the form of ZPRs are useful in validating
778 convergence in a more detailed way by decomposing prices into cost components as well as any perturbation from capacity
779 shadow prices. In this section, we first compare the system LCOE, price and capacity shadow prices of the two models for ZPRs
780 on the system level, then we show the technology-specific ZPRs. Using this validating step, we can visually ascertain that the
781 cost components and prices/market values in the two models are remarkably similar on the system level as well as on the
782 technological level, demonstrating that the underlying principle behind the coupled convergence holds to a good degree.

783 **4.3.1 System-level zero-profit rule**

784 At the convergence of the soft-coupled model, we expect ZPRs to be satisfied for the two systems individually (Eq. (11) for
785 REMIND and Eq. (13) for DIETER), i.e. each price time series also matches the LCOE time series to a good degree, barring
786 distortions from the capacity shadow prices. This is to say, under full convergence, the time series of system LCOE, and the sum
787 of the time series of the electricity prices and time series for capacity shadow prices for both models should overlap one another
788 within numerical tolerance. The costs and prices at the last iteration of the coupled run are summarized in Fig. 7. The electricity
789 prices derived from the shadow prices of the balance equations are shown in dark grey: (a), REMIND electricity price λ_y , (b)
790 DIETER annual average electricity price $J_y = \frac{\sum_h \lambda_{y,h} \underline{d}_{y,h}}{\sum_h \underline{d}_{y,h}}$. Adding all the sources of capacity shadow prices, we obtain the blue
791 lines: (a) REMIND capacity constraints (c5-c7), (b) DIETER capacity constraint (c8). All capacity shadow prices have been
792 converted to per energy unit via capacity factors. (Note: Fig. 4 shows the difference between the black lines, without considering
793 the capacity shadow prices. See Sect. 3.2.3.)
794 From Fig. 7, we can conclude that the ZPR for DIETER is satisfied to very good accuracy for every year (the blue line – the
795 sum of electricity price and capacity shadow price has exactly the same value as the sum of LCOE bars). For REMIND, the ZPR
796 is satisfied year-on-year to a lesser degree, but on average to a good degree given the interannual fluctuations. The prices in
797 coupled REMIND become very erratic for the early years (2020-2025), likely due to the interaction between the historical or
798 near-term bounds in REMIND and the exchanged information from DIETER for those years. The LCOEs component structures
799 match well across the models for most years, which serves as additional visual support on price convergence shown in Fig. 4,
800 i.e. the cost structures behind the prices are harmonized as well at the end of coupling. The origins of the differences between
801 LCOEs and prices, as well as the degree with which capacity shadow prices account for them, can be found when one examines
802 the LCOE and market values of specific technologies, which are analyzed next.
803

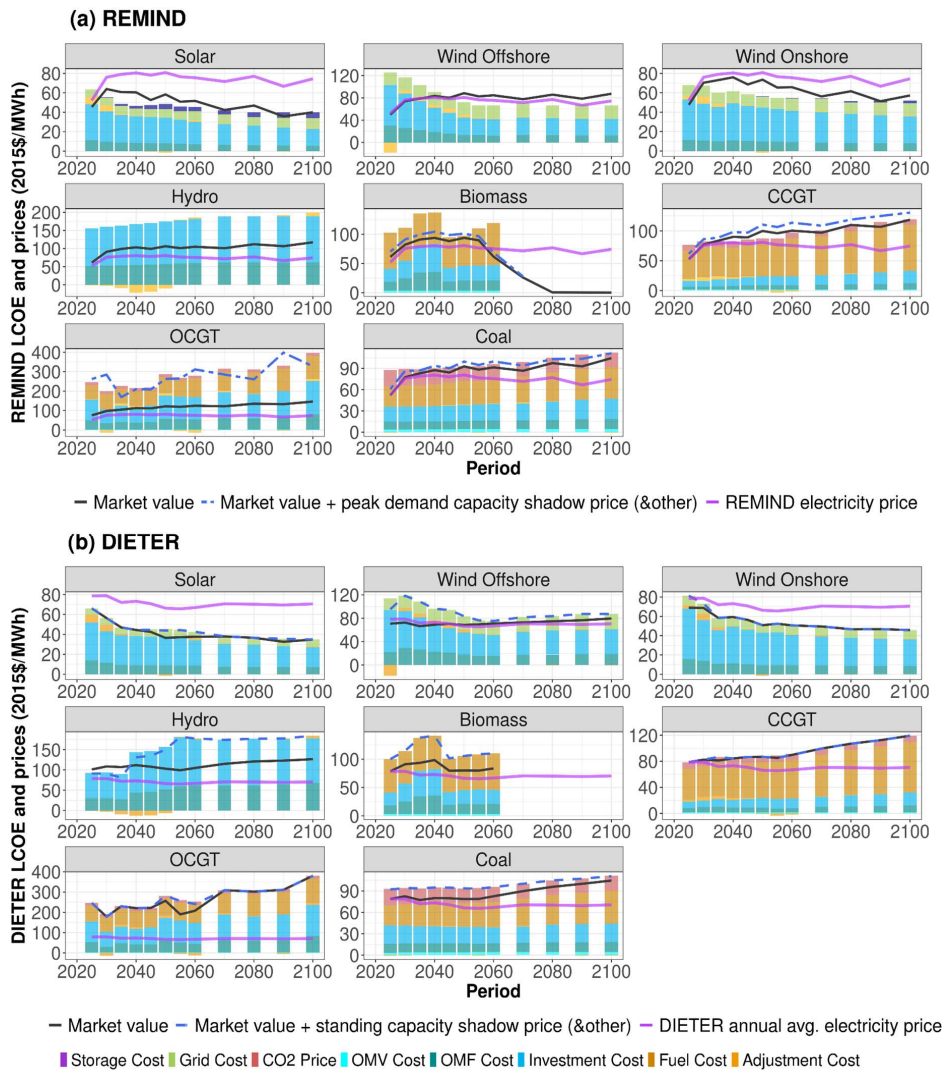


804

805 **Figure 7: Cost components of the system LCOEs (bars), electricity prices (grey lines) and the sum of electricity prices**
 806 **and capacity shadow prices for (a) REMIND and (b) DIETER under “proof-of-concept” baseline scenario. Visually the**
 807 **ZPRs for both models are satisfied within numerical tolerance. The intertemporal structure of the LCOE breakdown is**
 808 **very similar for most of the coupled periods. For DIETER, a small remaining difference exists between the price (grey**
 809 **line) and the LCOE (bars), which can be entirely explained by the capacity shadow price due to the standing capacity**
 810 **constraint. The REMIND price time series is a rolling average of 3 time periods. The large negative adjustment costs in**
 811 **2020 are due to coal and nuclear phase-out.**

812 4.3.2 Technology-specific zero-profit rule

813 After validating ZPRs on the system level, we further dive into each technology and check the ZPRs for each technology in both
 814 models at the last iteration of the coupled run (Fig. 8).



815

816 **Figure 8: Technology-specific costs and market values for (a) REMIND and (b) DIETER under “proof-of-concept”**
 817 **scenario. Cost components of the technology LCOE are plotted in stacked bars. Market values are shown in solid black**
 818 **lines. The sum of market values and all sources of capacity shadow prices are shown in dashed lines: for DIETER (two-**
 819 **dash blue lines), they contain mostly the standing capacity shadow price, and to a small extent the capacity shadow**
 820 **prices of the resource constraint; for REMIND (dashed blue lines), they contain mostly the peak demand capacity**
 821 **shadow price, and small capacity shadow prices due to brown-field and resource constraints. Electricity prices are**
 822 **shown in purple solid lines as references. Due to large positive shadow prices in 2020 due to fixings to the historical**
 823 **capacities, only periods beyond 2020 are shown. REMIND market values and capacity shadow prices are a rolling**
 824 **average of 3 time periods.**

825



826 In Fig. 8(b), DIETER LCOE and market values for the eight types of generators are shown. As expected from the ZPR, the
827 LCOE always matches the sum of the market value and capacity shadow prices for each technology, and for each year (Eq.
828 (12)). The difference between the dashed and solid lines are largely the generation capacity shadow prices. It is worth noting
829 that at the end of convergence, the sizes of the shadow prices are in general small for the main generator types, e.g. solar, wind
830 onshore, CCGT and OCGT. This indicates the fact that for these technologies for most periods, the optimal DIETER generation
831 mix is close to that of a green-field model. That is, DIETER hardly faces any exogenous constraints (except resource constraints
832 that are aligned with those of REMIND) and can make fully endogenous investment and dispatch decisions based on cost
833 information alone. On the whole, DIETER at the coupled convergence experiences only a small amount of distortion from the
834 brown-field model REMIND, especially concerning the “model suboptimal” real-world standing capacities from biomass, hydro
835 and coal.

836 In Fig. 8(a), we show the REMIND LCOE and market values for the same generation technologies. Due to the intertemporal
837 nature of REMIND, the sum of market value and capacity shadow price for each technology, and for each year matches the
838 LCOE generally slightly less well than DIETER. This means for REMIND the ZPR (Eq. (10)) for each generator type is also
839 satisfied to a good degree for main generator types, e.g. solar, wind onshore, coal, CCGT and OCGT. The mismatch in biomass
840 and hydro might come from the shadow price from historical capacities.

841 Since the differences between market values and costs are accounted for by capacity shadow price to a large degree, it is worth
842 interpreting physically the sources of these “hidden” costs/revenues. For REMIND, the capacity shadow prices consist of those
843 in (c2), (c5), (c6), as well as the “peak residual demand constraint” from DIETER (c7). Constraint (c7) is created to circumvent
844 high markups especially from peaker gas plants (Appendix H.1). Because peaker gas plants generate power mostly only at hours
845 with high prices (especially scarcity hour price), and therefore have very high market values compared to annual average
846 electricity price. The high market values of OCGT – usually more than 5 times the average annual electricity prices – acts as a
847 large incentive in the next iteration REMIND, and leads to overinvestment in capacities. Over iterations, this causes oscillations
848 in the quantities and prices in the coupled model and prevents model convergence. To circumvent the issue of high markup, we
849 implement (c7) as an equivalent peak residual demand constraint. As can be shown mathematically (Appendix H), (c7)
850 generates essentially the scarcity hour price, and it is very easy to validate this for OCGT in Fig. 8(a). The capacity shadow
851 price derived from this peak residual demand constraint, when translated to energy terms and added to the market value,
852 correctly recovers the LCOE for OCGT, recovering the original ZPR (Appendix H.1.2). This indicates that under multiscale
853 model coupling, an extra constraint is an effective way to circumvent potential issues of numerical divergence due to the large
854 impact from short-term dynamics, such as the large market value of peaker gas plants.

855 For DIETER, the two sources of capacity shadow price are the total renewable potential limit (constraint (c2) in Sect. 3.1), and
856 the standing capacity constraint from REMIND (constraint (c8) in Sect. 3.2.3). For the first type, the resulting capacity shadow
857 price is a hidden “positive cost” from the perspective of the power user. Since endogenously DIETER would like to invest more,
858 but is limited by the natural resources available. An example for this first type is hydroelectric power between 2020 and 2035,
859 due to the limited resource (run-of-the-river) in Germany. It is worth noting that from the generator’s perspective, the capacity
860 shadow price from resource constraint can be interpreted as an extra resource rent. The second type of capacity constraint
861 originates from the standing capacity, the latter is received by DIETER from REMIND as a lower bound. This constraint usually
862 results in a hidden “negative cost” from the perspective of a power user, i.e. a part of the cost (LCOE) does not get passed on to
863 the electricity price, so the users get part of the capacity “for free”. (This can also be interpreted as subsidies for generators to
864 sustain these unprofitable capacities.) This is because based on greenfield cost optimization, DIETER endogenously would
865 invest less in certain technologies. However, since the standing capacities account for the existing generation assets in the real



866 world, which can be model suboptimal, the overall costs are above a greenfield equilibrium and above the prices the user pays.
867 We find examples of such a capacity shadow price manifested in biomass, coal and hydroelectric, all of which are part of the
868 existing German power capacity mix, but evidently not all of them for any given period are “green-field optimal” based on pure
869 cost consideration in DIETER. Interestingly, after 2035, the sign of the capacity shadow price for hydroelectric generators
870 reverses. This is likely due to the continuous decline of the VRE costs after 2035 tips the power sector into a regime where
871 hydroelectric becomes less economically competitive in DIETER, at least compared to REMIND. As a result, the standing
872 constraint from REMIND starts to be binding on the capacity from below, relieving the resource constraint binding from above.
873 For DIETER, the capacity shadow price from standing capacities also indicates the degree of disagreement between DIETER
874 and REMIND. For most future years, REMIND standing capacity constraints are not binding in DIETER for solar, wind
875 onshore, CCGT and OCGT, indicating good agreement between the models. The small amount of shadow prices near 2060 for
876 OCGT and solar in Fig. 8(b) are likely due to the time step size change in REMIND which causes a small jump in the interest
877 rates near these years.
878 Lastly, in Fig. 4 before we observe a slightly higher average electricity price in REMIND than in DIETER, especially in the
879 intermediate years. This could be due to fixed offshore wind capacities, which are never economical to be invested
880 endogenously in the parameterization used here. This generates a high capacity shadow price until around 2045-2060, visible in
881 both DIETER and REMIND.

882 **5 Scenario results under baseline and policy scenarios**

883 In this section, we present baseline and policy scenario results for Germany, using a more realistic configuration of the coupled
884 model with electricity storage and flexible electrolyzer demand for green hydrogen production which is then used outside the
885 power sector (e.g. in industry or heavy trucks). We show results for a baseline scenario and a net-zero by 2045 climate policy
886 scenario. Note that due to REMIND’s global scope, under the net-zero scenario we also assume a larger climate policy
887 background of 1.5C goal for end-of-century temperature rise globally (corresponding to a 500Gt of CO₂ emission budget until
888 2100), and a larger regional goal of EU-wide net-zero emission. Both scenarios consider nuclear phaseout law in Germany.
889 In Sect. 5.1, we present long-term power sector development. In Sect. 5.2, we present short-term power sector hourly dispatch
890 and price results. In the following, we broadly describe how these additional features are implemented:

891 1. Storage: We use a simple storage implementation where DIETER makes endogenous investment into two kinds of storage
892 technologies:

- 893 1) lithium-ion utility-scale batteries;
- 894 2) onsite green hydrogen production via flexible electrolyzers, storage and combustion for power production.

895 The principle of the coupling remains mostly unchanged. REMIND receives the price markups from generation technologies
896 as in the case before without storage. However, for simplicity, the capacities of storage are not part of endogenous
897 investment in REMIND. In REMIND, the energy loss due to storage conversion efficiency is taken as a fraction of total
898 demand from DIETER as a parameter, and stabilized with a prefactor for each type of renewable generation (similar to the
899 case of curtailment rate in Sect. 3.3.2, 4). Our battery cost development is given in Supplemental Material S1-2.

900 The reason we only allow DIETER to endogenously invest in storage technologies, is that the additional intertemporal
901 optimization offered in REMIND is relatively less important than that for the investment of generation technologies. In
902 REMIND, intertemporality mainly accounts for two aspects in the real-world: 1) implementing adjustment cost and 2)
903 tracking of standing capacity. The adjustment costs simulate system inertia to rapid capacity addition or removal. In the case
904 of battery and other storage technologies, the ramp up of deployment faces relatively fewer inertia compared to wind and



905 solar. Compared to generation technologies such as wind and solar, the storage technologies tend to have lower total
 906 capacities, meaning their ramp up rate is usually lower. Also, their deployment is mostly constrained by their higher cost.
 907 For utility storage technologies, they are mostly not yet deployed at scale, which means there is very little existing capacity,
 908 the investment for storage in REMIND is mostly green-field, rendering it unnecessary to give DIETER a standing capacity
 909 of them.

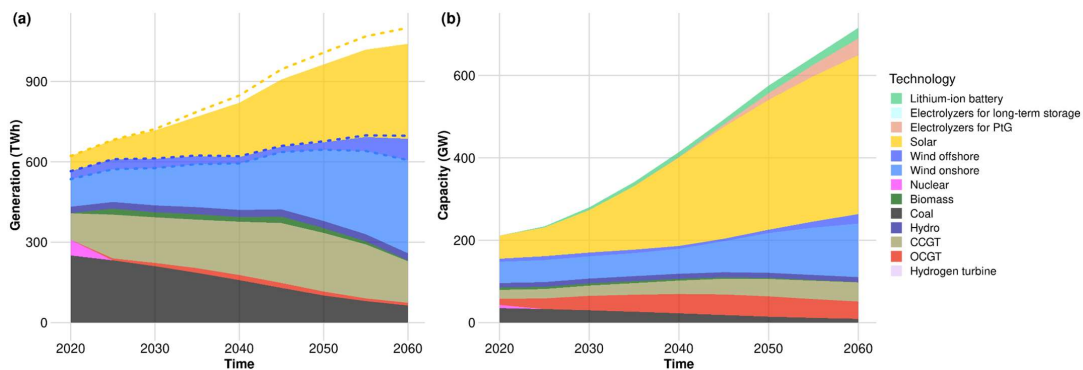
910 2. Flexible demand: As a simple representation of flexible demand, we choose to implement a common Power-to-Gas (PtG)
 911 technology, namely the so-called “green hydrogen” electrolysis. We split the total power demand required to produce green
 912 hydrogen from REMIND from the total power demand $d_y(i - 1)$ (Sect. 3.3.1, 3) – both demands are endogenous in
 913 REMIND. We implement the electrolysis demand as completely flexible in DIETER, i.e. there is no ramping cost or
 914 constraint. Thereby flexibilizing part of endogenous total power demand $d_y(i - 1)$ in REMIND. As a result, the cost
 915 minimization in DIETER automatically allocates the flexible demand to hours where electricity costs are low due to the
 916 existence of low-cost VRE. The economic value of flexible demand can be quantified by the capture price. The annual
 917 capture price of demand-side technology s_d is the annual average price of the hours when the flexible demand consumes
 918 electricity, weighted by the hourly flexible power demand by electrolyzers: $CP_{s_d} = \frac{\sum_{h,s_d} d_{h,s_d} \lambda_h}{\sum_{h,s_d} d_{h,s_d}}$.

919 **This concept is equivalent to the market value for a variable or dispatchable generator, but here for a flexible or**
 920 **inflexible demand source. Similar to before, we implement a stabilization measure using a prefactor (Appendix H.2, 5).**

921 **5.1. Long-term development**

922 This section presents scenario results of the coupled model with a long-term view on capacity and generation, using either the
 923 proof-of-concept scenario or more realistic configurations.

924 **5.1.1 Baseline scenario**



925
 926 **Figure 9: DIETER-REMIND converged results of the long-term (a) generation and (b) capacity expansion for**
 927 **Germany’s power sector in the baseline scenario, assuming a constant 37\$/tCO2 CO2 price. Dashed lines represent**
 928 **generation before storage loss and curtailment. Storage generation is not visualized in (a).**
 929

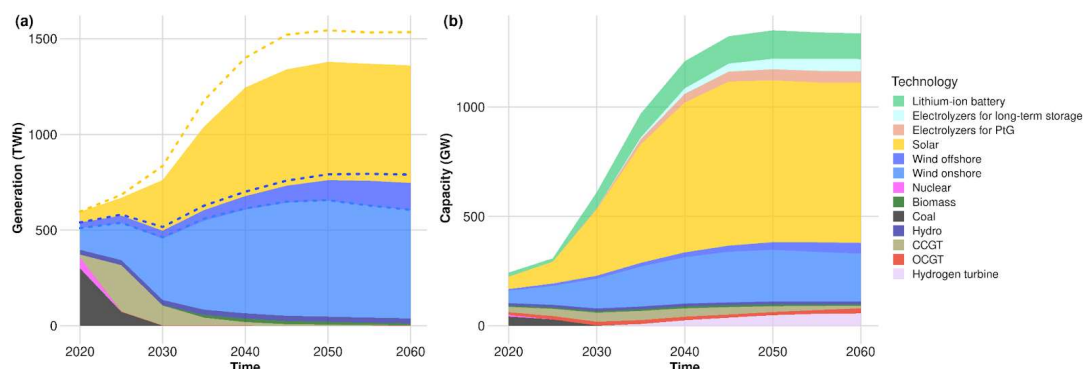
930 In Fig. 9(a), under baseline scenario, and with available storage and flexible demand, we observe a more than 35% increase of
 931 the total power demand from 2020 to 2045, and more than 65% by 2080. This is due to an increase in end-use electrification.



932 The increased electrification comes from a moderate growth in electricity use in the building sector and a more significant
 933 growth in EV fleet. In the building sector, the final energy share of electricity is projected to increase from 28% in 2020 to 39%
 934 in 2045. The final energy share of electricity in the transport sector is 22% by 2045, up from 2% in 2020. Note that even under
 935 no additional climate policies, based on only the increase in EVs shares in new-cars sales in many world markets today, we
 936 expect higher power usage from EVs in the future. Within the energy mix, we see a slow decline in coal generation over time,
 937 which is replaced by CCGT generation and a significant increase of VRE. VRE share reaches above 50% by 2045, but slightly
 938 less than half of the energy mix still contains coal and gas power. In terms of capacity expansion (Fig. 9(b)), due to both lower
 939 generation cost and higher power demand, solar capacity expands by almost 5 times from today until 2045. However, the
 940 moderate VRE shares mean that the requirement on battery capacity is not high, namely only 12GW of batteries by 2045. Due
 941 to the low CO₂ price, long-term electricity storage through hydrogen does not appear to be economically competitive and is not
 942 invested under the baseline.

943 By comparing the above baseline scenario (with storage and flexible demand) (Fig. 9) with the “proof-of-concept” baseline
 944 scenario (without storage or flexible demand) before (Fig. 5 and 6), it is clear that while battery storage and partial demand
 945 flexibility play a role after 2040 in increasing the VRE share in Fig. 9, in the near term, the scenarios with and without available
 946 storage and demand flexibility look very similar under no additional climate policies. However, due to technological learning
 947 effect, even absent additional CO₂ price policy, the energy mix here has a relatively high VRE share (>60%) after 2050
 948 compared to the basic case without storage and demand-side flexibilization. However, due to the low CO₂ price there is still a
 949 significant share of dispatchable technologies such as CCGT and OCGT, which is more economical than the implementation of
 950 long-term power storage via electrolysis and hydrogen turbines.

951 5.1.2 Net-zero policy scenario



952
 953 **Figure 10: DIETER-REMIND results of the long-term generation and capacity expansion for Germany’s power sector**
 954 **in the “net-zero 2045” scenario. CO₂ price is endogenously determined based on the climate goal. It is 115\$/tCO₂ for**
 955 **2030, 292\$/tCO₂ for 2035, 464\$/tCO₂ for 2040, and 636\$/tCO₂ for 2045. Dashed lines represent pre-curtailment**
 956 **generation. Storage generation is not visualized in (a).**

957
 958 In Fig. 10, under stringent climate policy (economic-wide carbon neutrality in 2045), with available storage and partially
 959 flexibilized demand (for hydrogen production used in other sectors), the total power demand more than doubles, and the power
 960 mix is dramatically transformed. Compared to both the baseline case without storage and demand-side flexibilization (Fig. 5 and



961 6) and the baseline scenario with storage and flexible demand (Fig. 9), a very high VRE share in the generation mix is reached
962 already by 2040 (>94%). This is mostly due to an earlier investment in VRE to drive down the cost, combined with the
963 increased deployment of both short- and long-term storage and flexibilization of part of the demand. Capacities for storage
964 increase significantly: lithium-ion batteries from 18GW in 2020 to 125GW in 2045, and 37 GW of hydrogen electrolysis and
965 hydrogen turbine capacity (with ~40TWh of H₂ storage capacity). Despite high storage capacities, due to high VRE share,
966 curtailment and storage loss still increases quite significantly with time, especially for solar PV. But note that in a coupled run
967 where interregional transmission expansion is possible connecting Germany and the rest of Europe, this loss can be reduced (see
968 Sec. 6.3). In terms of capacity expansion (Fig. 10(b)), gas power plants are mostly replaced, as hydrogen turbines fill the role of
969 peaking dispatchable plants that guarantee supply for peak demand hours. The CCGT gas turbines are equipped with CCS.
970 Under the stringent climate policy scenario, dramatic changes in the end-use sectors will be underway in the form of direct
971 electrification and substitution of fossil gas with hydrogen. In the building sector, the final energy share of electricity is
972 projected to increase from 28% in 2020 to 66% in 2045. In transport, the final energy share of electricity is 56% by 2045. In the
973 industry sector, the share of electricity increases from 25% to 63%. By 2045 there is also a notable increase in the use of green
974 hydrogen produced from 45GW flexible electrolyzers (at about 42% average annual capacity factor), amounting to 0.5EJ (3.5
975 million tons) per year in the final energy, which is primarily used in industry.

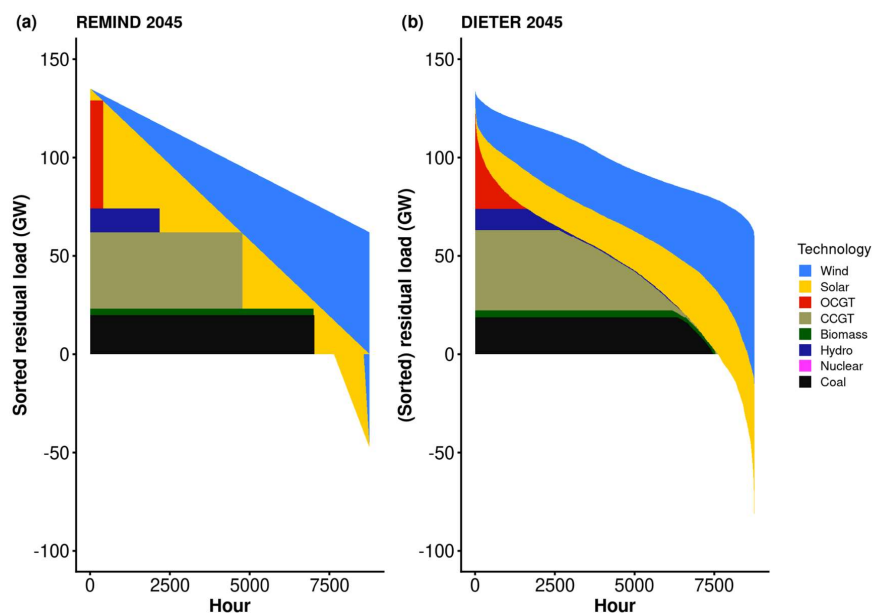
976 **5.2. Short-term dispatch**

977 In this section, results of hourly resolution are shown and discussed for a selected model year. We use established methods such
978 as residual load duration curves (RLDCs) to visualize the hourly dispatch result, as well as show the hourly generation and
979 dispatch time series for some typical days in summer and winter.

980 **5.2.1 Residual load duration curve model comparison**

981 RLDCs can be used to visualize the dispatch of energy system models. Each subsequent curve is calculated by subtracting the
982 generation of a technology from the hourly residual demand curve, and then sorting the remaining demand in descending order.
983 On the left-side of RLDC graphs one can easily check the amount of residual demand not met by variable wind and solar
984 production. The top-most line in RLDC graph is the load duration curve for inflexible demand (excluding the demand from
985 flexible electrolysis for hydrogen production used in other sectors).

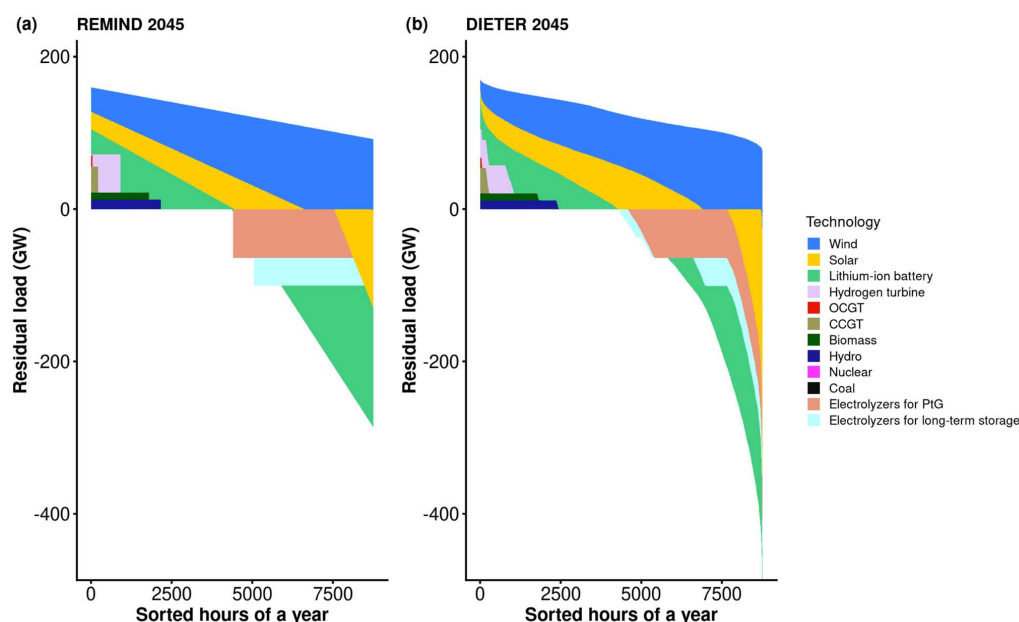
986 In a baseline configuration without flexibilized demand or storage, despite lacking the explicit hourly dispatch, via bidirectional
987 soft-linkage, REMIND could achieve a final dispatch result that replicates DIETER to a satisfactory degree (Fig. 11). This is a
988 combined effect of a convergence of capacities (Sect. 4.2) and full-load hours at the end of the coupled run. In the peak residual
989 demand hour (the leftmost point in the RLDC), the DIETER-coupled REMIND accounts for the requirement of dispatchable
990 capacities via the constraint (c7), and the composition of the mix is replicated from DIETER and correctly guarantees that the
991 peak hourly demand is met.



992

993 **Figure 11: Side-by-side RLDC comparison between (a) REMIND and (b) DIETER for the simple configuration under**
994 **the baseline scenario without storage or flexible demand. The DIETER RLDC (panel (b)) is constructed by subtracting**
995 **hourly generation from hourly load and sorting, with dispatchable generation technologies plotted in order of their**
996 **annual average capacity factors. VREs are arranged such that the generation with higher curtailment rate (i.e., solar, in**
997 **this case) is on the inside of the graph. To construct the REMIND RLDC (panel (a)), the dispatchable generations are**
998 **sorted by their capacity factors and stacked from the bottom. The rectangles depicting dispatchable generation are made**
999 **up by the width equal to the full-load-hour and the height equal to the capacity. The top-most lines on either side are**
1000 **load-duration curves (sorted hourly demand, which is entirely inflexible under this setup). For the purpose of better**
1001 **visualizations, solar and wind RLDCs are tilted at an angle for REMIND and plotted in the same order as the DIETER**
1002 **RLDC. For simplicity, in REMIND wind and solar RLDC share the same top pivot point in peak residual demand hour.**
1003

1004 In net-zero policy with storage and flexible electrolysis demand, comparing dispatch results under both scenarios (Fig. 11 and
1005 12) for model year 2045, it can be observed that under a stringent emission constraint, the system allocates a significant amount
1006 of short-term storage to replace the dispatchable generation such as coal and CCGT. Long-term storage such as hydrogen
1007 electrolysis combined with hydrogen turbines further reduce the capacity factor of remaining OCGT and CCGT. Besides
1008 storage, there is also a significant amount of deployment of flexible electrolysis demand for producing hydrogen (PtG), which is
1009 not used in the power sector, but in industry or heavy-duty transport. The use of PtG technologies leverages cheap variable wind
1010 and solar energy to achieve the goal of sector coupling. By way of storage and PtG, a significant share of the curtailment can be
1011 utilized (more than 70%), either by shifting the supply to times of low VRE production via storage, or by producing hydrogen
1012 using surpluses which can be used in other sectors.
1013



1014

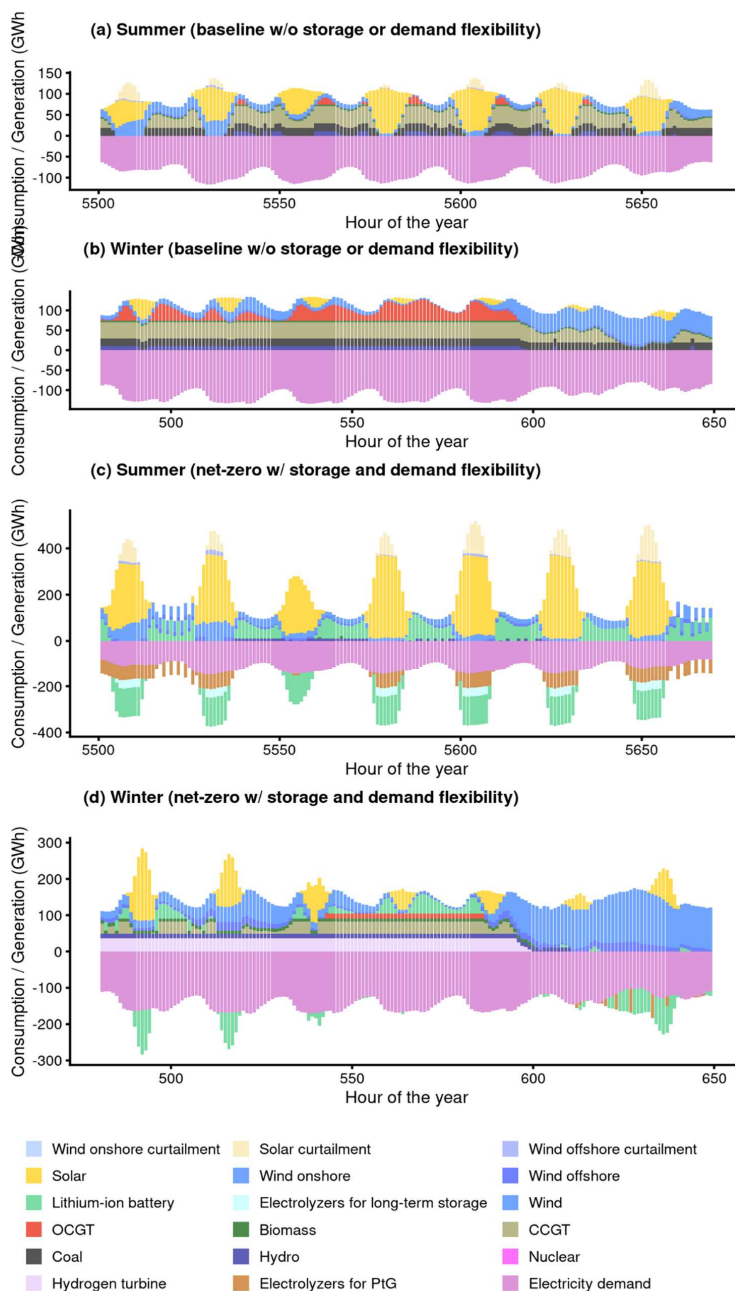
1015 **Figure 12: Side-by-side comparison between (a) REMIND and (b) DIETER RLDCs for net-zero by 2045 scenario with**
1016 **storage and flexibilized demand for Germany. The storage loading and discharging in DIETER RLDC (panel (b)) is**
1017 **constructed by subtracting hourly loading or discharging from hourly inflexible load and sorting. The REMIND RLDC**
1018 **(panel (a)) is constructed similar to Fig. 11. The top-most lines on either side are load-duration curves for inflexible**
1019 **demand. For better visual comparison, in REMIND solar RLDC starts at 80% of the peak residual demand.**

1020 5.2.2 Hourly dispatch and power consumptions for typical days in summer and winter

1021 To more directly inspect the results of the hourly dispatch under various scenarios, we visualize the hourly generation and
1022 demand for typical days. Due to the climate in Germany, solar potential is particularly low during winter months. Therefore it is
1023 important to observe the periods in both summer and winter.

1024 From the optimal hourly dispatch results of typical days from the coupled model, we observe that compared to baseline (Fig.
1025 13a-b), in 2045 for a net-zero year (Fig. 13c-d), there is a significant amount of surplus solar generation in the summer during
1026 the day, and some amount of surplus wind generation in the winter during nights and days. Under a net-zero scenario, the
1027 generation from fossil fuel plants in the baseline is replaced by battery dispatch (especially in summer) and hydrogen turbines
1028 (especially in winter), and the peaker plants, which under baseline are turned on in the summer evening, are partially replaced by
1029 solar over-capacity and batteries. A significant share of renewable surplus energy is used for the production of green hydrogen –
1030 hydrogen made from zero-carbon electricity. Due to the complete flexibility of electrolyzers, the capture price of hydrogen
1031 production is only around $\frac{1}{3}$ of the average price of electricity (Supplemental Material S2 and Fig. S1 in Supplemental
1032 Material).

1033 In winter, hydrogen turbines serve as a baseload for the few days when wind generation is insufficient to meet the demand. To
1034 ensure supply during longer winter periods of “renewable droughts” with little wind and solar output, e.g., over a 2-3-day period
1035 (hour 540-600 in Fig. 13d), long-term duration storage with hydrogen electrolysis and hydrogen turbines, as well as some
1036 dispatchable generation (such as CCGT with CCS and integrated biomass gasification combined cycle) play a major role.



1037

1038 **Figure 13: Comparison of hourly generation (positive) and consumption/storage loading (negative) for a few consecutive**
 1039 **typical days in two seasons in Germany in 2045. (a) Summer, under “proof-of-concept” baseline scenario, no storage or**
 1040 **flexible demand; (b) Winter, under “proof-of-concept” baseline scenario, no storage or flexible demand; (c) Summer,**
 1041 **net-zero scenario, with storage and flexible demand; (d) Winter, net-zero scenario, with storage and flexible demand.**



1042 **6 Discussion**

1043 In this section, we discuss the reasons for remaining differences between the coupled models, as well as the assumptions and
1044 limitations of the soft-coupling.

1045 **6.1 Remaining discrepancies**

1046 In all our test runs, at the end of the coupling, it is always the case that the two models cannot be perfectly harmonized, and
1047 there is a slight residual difference in the convergence results (Section 4). The reason is two-fold.

1048 The first reason is “legacy mismatch”, i.e. a mismatch in brown-field standing capacity constraints in the two models. The
1049 coupling method we develop here is mostly based on price information for achieving convergence. Therefore, capacity
1050 constraints that are present in the standalone long-term model but not in the standalone hourly dispatch model need to be
1051 transferred. These standing capacities are hard to evaluate purely based on economic terms, as they are ultimately a result of
1052 real-world actions and policies, which might not align with the simplified economic incentives in techno-economic energy
1053 models. Therefore, the only way this information can be transferred from the “brown-field” model to the “green-field” model is
1054 by implementing a lower capacity bound in the latter. However, this bound nevertheless might not capture all the shadow prices
1055 caused by the standing capacities in REMIND. This is ultimately due to the specific generic form of the constraint we
1056 implemented, i.e. we pass on the pre-investment capacities as a lower bound regardless of technology types. In general, hidden
1057 “legacy revenues”, which are manifested as the shadow prices of economically less competitive generators in DIETER, such as
1058 biomass, coal, hydroelectric (solid line lower than bars in Fig. 8), provide incentives for brown-field models to deploy them over
1059 long-term, but does not provide enough economic case for the green-field model. This results in an observed phenomenon in the
1060 coupled run, that if these “legacy” capacities and their impact on the costs have not been fully transferred to the green-field
1061 model, the prices of the green-field model tend to be lower than the coupled brown-field models, causing distortion to the
1062 convergence of quantities. The effect of legacy mismatch and illustrative test run results are discussed in more detail in
1063 Supplemental Material S3.

1064 The second reason for the discrepancies at the end of the coupling is that there are actual mismatches in the Lagrangian
1065 harmonization itself, which can originate from multiple sources. It could be due to intertemporal constraints and dynamics (such as
1066 adjustment costs and brown-field constraints) not linearly reducible to single-year dynamics, resulting in misalignment between
1067 multi-period REMIND and single-year DIETER. It could be also due to slight numerical inaccuracies of the interest rate
1068 estimate, which is not explicit in REMIND, but are derived from endogenous and intertemporal consumption. Lastly, there
1069 could be a mismatch due to a linear fitting of REMIND endogenous time series of fuel costs (biomass, oil, coal, uranium) before
1070 passing this information to DIETER which might a small amount of mismatch for fuel costs between REMIND and DIETER.

1071 **6.2 Limitation of the coupling methodology**

1072 There are limitations to our proposed methodology, both in terms of converging two multiscale power sector models, as well as
1073 other potential applications of model convergence. Firstly, in terms of the problem presented here – a multiscale power sector
1074 model coupling, the method derived here is only necessary for a full convergence, but may not be sufficient, i.e. a full
1075 convergence is not guaranteed. A number of additional factors could prevent a full convergence. One is the “legacy mismatch”
1076 and misalignment in Lagrangian mappings mentioned above in Sect. 6.1. Another factor is the role prefactors play (Sect. 3.3.2,
1077 Appendix H.2). The prefactors help stabilize the coupling by turning exogenous values obtained from last-iteration DIETER to
1078 endogenous values in REMIND, such that they can be adjusted to be in line with the optimal mix of current iteration. However,



1079 they usually contain some small positive or negative parameters that are determined heuristically (e.g. $b_{y,s}$ in Eq. (H13)). These
1080 heuristic parameters usually come from rough estimates based on relations between variables in the system and generation
1081 shares, e.g. how much market value of solar generation will decrease when solar generation share increases by a certain
1082 percentage. In practice, while the prefactors help stabilize the run and improve convergence speed, choosing the wrong prefactor
1083 parameters can lead to divergence or instability. Second, another limitation when it comes to modeling power market multiscale
1084 coupling, is the number of products in the market. In the formulation here, both models describe the general equilibrium of a
1085 competitive market with one type of homogenous goods, i.e. electricity. However, if we introduce heat as a by-product, such as
1086 from a combined heat and power plant, then there are two types of goods: heat and electricity. The feasibility of coupling
1087 models with more than one type of goods/market is not yet explored. Thirdly, there are multiple iterative processes that are
1088 internal to REMIND, which happen concurrent with the DIETER-REMIND coupled convergence. Among these processes,
1089 DIETER and the REMIND “Nash” algorithms (for inter-regional trading) both run between the internal REMIND “Nash”
1090 iterations, which means they are external to the REMIND single-region optimization problems and therefore are soft-linked.
1091 Nevertheless, in our runs, we observe the power sector convergence to be rather swift and smooth, and happen in parallel to
1092 other iterative processes, such as the “Nash” algorithm and the CO2 price path algorithm (for climate policy runs). However, a
1093 systematic monitoring of the multiple internal convergence processes in REMIND during the REMIND-DIETER convergence
1094 processes under other model setups and configurations is still to be more thoroughly researched.
1095 More generally, the approach developed here – the Lagrangian mapping method for converging two multiscale optimization
1096 problems – could be useful for a general modeling of market equilibrium of multiple time resolutions. In this study, the
1097 resolution in the coupled problems is specifically only meant for temporal resolution. However, mathematically speaking,
1098 coupling models of different spatial resolutions (or both temporal and spatial resolutions) should be very similar. At least in
1099 theory, the soft-coupling approach developed here should be applicable to increasing the resolution in any arbitrary
1100 independent/orthogonal dimension of the problem of finding equilibrium market dynamics. In theory, it is also possible to build
1101 a multi-layer coupled problem architecture, where at each level the low-resolution variables can be disaggregated into finer
1102 resolution along some dimensions. However, further research is needed to explore the feasibility and convergence performance
1103 of such schemes.

1104 **6.3 Limitation of coupled results**

1105 Since the nature of this study is a proof-of-concept, the scenario results presented should be primarily interpreted as such.

1106 Nevertheless, it may be useful to enumerate a list of limitation for a more accurate interpretation of the results:

- 1107 1) The power-sector is only coupled for one single global region, i.e. information exchange only occurs for the variables
1108 of one region – Germany, while all other regions contain the low-resolution version of the power sector of uncoupled
1109 REMIND. The former coupled one-region result is based on a time series of VRE production today in a world of low to
1110 medium VRE share and very limited power grid expansion (in 2019). The latter results of the uncoupled regions
1111 however are parametrized based on results from detailed PSM under a more optimistic assumption of transmission
1112 build-out, which allows VRE pooling from an expanded EU-wide power grid to smooth out regional weather variations
1113 (Ueckerdt et al., 2017). Note that in standalone REMIND, while by default there are no annual electricity import and
1114 export imbalances between countries and regions, transmission during the year is implicitly assumed, especially for the
1115 EU region. Comparing the capacity and generation mixes of the coupled and uncoupled runs (Appendix J), we find that
1116 in the uncoupled case, there are slightly more solar and wind capacities and generations, and much less gas generation



- 1117 in the long term. EU-wide transmission expansion would pool both supply and demand variability, thus reducing the
1118 need for dispatchable capacity for meeting the peak demand.
- 1119 2) Due to the scope of this study, we implemented a limited set of options on storage and sector coupling technologies in
1120 this study, and neglected the additional supply-side details for the German power market (such as the reserve market).
1121 Many potentially significant technological options consisting of pumped hydro storage, compressed-air energy storage,
1122 vehicle-to-grid, and flexible heat-pumps are not explicitly modeled.
- 1123 3) Ramping costs for dispatchable generators are not considered, although the effect should be small (Schill et al., 2017).
- 1124 4) In terms of power transmission and trading inside Germany, we assume a very simple “copperplate” spatial resolution,
1125 not explicitly modeling transmission bottlenecks inside the region.
- 1126 5) Near-term events: we have not modeled the current gas and energy crisis in Europe, which is likely to imply an
1127 overestimation of near-term gas availability in the power sector. Relatedly, we are likely to have overestimated the
1128 early retirement of coal power plants, which are capped at maximum 9% per year of current capacity early retirement
1129 rate in REMIND if it is uneconomical relative to cheaper sources of generation. We have included the COVID shock to
1130 the GDP projection.
- 1131 6) Only one weather year (2019) is used for the DIETER input data. From the perspective of sufficient power supply
1132 under all weather conditions with few blackout events, this could introduce an underestimation of the need for reserve
1133 capacity, storage and demand-side flexibility.

1134 **7 Conclusion and Outlook**

1135 In this study, we develop a new method of soft-coupling an IAM with a coarse temporal resolution and a PSM with an hourly
1136 temporal resolution. Our coupling method can be shown both mathematically and in practice to produce a convergence of the
1137 two systems to a sufficient degree. This method allows the incorporation of the temporal details of variable renewable
1138 generation explicitly in large-scope IAM modeling frameworks, and increases the accuracy of power sector dynamics in long
1139 term models. Furthermore, it allows a more explicit modeling of the power sector and sector-coupling, a vision of the energy
1140 transition where end-use demand sectors such as building, industry and transport make economic use of the generation from
1141 variable sources by

- 1142 1) directly using the power at the time of production for inflexible form of demand,
1143 2) shifting time of power supply via battery and other power storage technology,
1144 3) transforming it to another energy carrier or product ahead of time of consumption and at times of surplus wind and
1145 solar production (e.g. PtG), without conversion back to electricity.

1146 The fully coupled framework allows a more explicit modeling of economic competition of these options under high shares of
1147 variable renewables, finding more accurate optimal paths under long-term climate scenarios towards a net-zero power sector and
1148 the wider economy globally. In future research we plan to expand the study in the direction of demand-side management and
1149 flexibilization, and later possibly in the direction of heat storage.

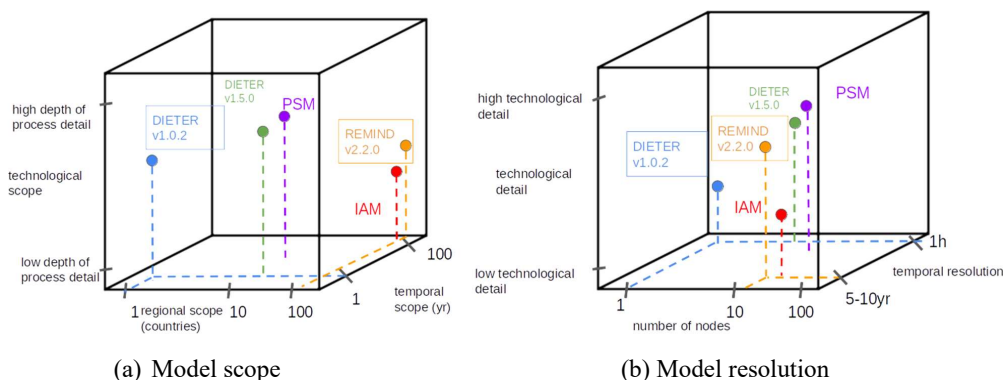
1150 Coupling DIETER to the global model REMIND for the single region Germany, this study serves as a proof-of-concept. Our
1151 main innovation is two-fold: we derive convergence theoretically, and show almost full convergence numerically. Theoretically,
1152 we derive the coupling methodology by mapping the KKT Lagrangians of the simplified versions of the two models. One key
1153 aspect of the mapping consists of iterative adjustment of the market value (i.e. the annual average revenue of one energy unit of
1154 generation) or the capture price (i.e. the annual average price of one energy unit of consumption) in the low-resolution IAM
1155 such that they take on the values as those in the high-resolution PSM. By finding the set of mathematical coupling conditions



1156 necessary for an iterative convergence as defined by the convergence of both quantities and prices, we could then design the
 1157 coupling interface accordingly, such that at the end of the coupling a joint optimal result can be found.
 1158 Numerically, we compare the converged results of the two models by examining the long-term power mix (both capacity and
 1159 generation quantities), prices of electricity, as well as generation dispatch (via RLDC), and find good agreement between the
 1160 two models at the end of coupled convergence despite some slight mismatches. For a “proof-of-concept” baseline scenario
 1161 under simple configuration without storage or flexible demand, we could achieve an energy mix with 4.4% tolerance for any
 1162 technology’s absolute share difference in each time step. For a climate policy scenario under a more realistic configuration with
 1163 storage and flexible demand, we could achieve 6-7% tolerance. The cost breakdown and prices of power generations for both
 1164 models are found to be very similar at the end of the iterative process, providing additional evidence that the quantity
 1165 harmonization follows the underlying principle of the price and cost harmonization. The remaining differences can be partially
 1166 explained by the lack of full harmonization of the brown-field and near-term capacity constraints, as well as potential
 1167 mismatches due to numerical techniques aimed at enhancing performance and stability. Using the coupling methodology, we
 1168 provide scenarios for power sector transition under a stringent German climate goal. Under this scenario, we observe a least-cost
 1169 pathway consisting of an almost complete transformation to a wind- and solar-based power system. The results indicate an
 1170 increasing role of storage and dispatchable capacity in a deep decarb scenario, consistent with the findings of previous PSM
 1171 studies, but which is now transferred to the long-term models via soft-coupling.
 1172 For future works, besides expanding the research program on sector coupling into a direction containing a broader technological
 1173 portfolio, we also aim to apply this framework to other world regions of interest in the REMIND model. Another important
 1174 aspect would be to represent the variability-smoothing effect of transmission grids by using the same coupling framework to
 1175 couple REMIND to other power sector models with more explicit modeling of transmission bottlenecks and expansion for two
 1176 or more regions.

1177 **Appendices**

1178 **Appendix A: Comparison of model scope and specification**



1179

1180

1181 **Figure A1: Comparison of resolution and scope for REMIND and a typical IAM, as well as two versions of DIETER**
 1182 **(v1.0.2 is used in this study) and a typical PSM.**



	Model name and version	REMIND v3.0.0 (dev)	DIETER v1.0.2
	model type	IAM	PSM
Scope and resolution	spatial scope	entire globe	single region (Germany)
	intertemporal scope of “perfect foresight”	2005-2100 (in actual model it is 2005-2150)	any year-long period
	temporal resolution	5- or 10-year time-step	hourly
	regional resolution	single EU region	single EU region
	sectoral scope	all energy sectors (transport, building, industry), industrial processes, air pollution, land-use sector, etc	power sector
	available climate policy options	CO2 price, early-phase nuclear and coal phase out (for Germany), EU-ETS	CO2 price
Power sector dynamics	endogenous hourly dispatch	no	yes
	differentiated market value for various technologies	no	yes
	price-demand elasticity	yes	no
	capital cost of technology	endogenous via learning curve (Leimbach et al., 2010)	exogenous
	vintage tracking of existing capital stock	yes	no
	transmission assumption	copper plate within region	copper plate within region
Model code and data specification	programming language	GAMS	GAMS
	input data openness	partially open data	fully open data (for Germany)
	source code openness	open	open
	solver	CONOPT	CPLEX

1183 **Table A1: Comparison between the coupled models REMIND and DIETER.**

1184

1185 Because IAMs usually start out with certain assumptions for the development of macroeconomic metrics such as for GDP and
 1186 population, which in turn determine the corresponding energy service levels to a larger degree prior to optimizing the energy
 1187 system mix to meet demand, they are also frequently referred to as “top-down” energy system models. PSMs usually start out



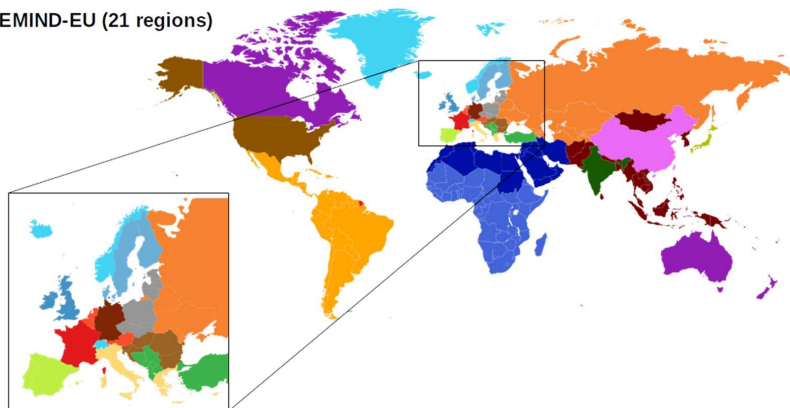
1188 modeling the fine spatiotemporal detail of the real-world power systems, expanding the capacity installation of power
1189 generating plants, grid transmission and storage at minimum cost. Such models are also known as “unit commitment models”
1190 for electrical power production (Padhy, 2004). Later in model development PSMs usually expand to include other energy
1191 services such as heating and transportation which are electrified. In this way PSMs are also often referred to as “bottom-up”
1192 models. Reviews and intercomparison of IAMs have been carried out recently where various IAMs are analyzed and
1193 harmonized (Weyant, 2017; Butnar et al., 2019; Keppo et al., 2021; Wilson et al., 2021; Giarola et al., 2021).
1194 For methodological reasons, we have to set the length of the model time horizon to be until 2150, which is longer than the valid
1195 model time horizon until 2100. This is because without the extra years after 2100, the model has much less time to utilize the
1196 capacities installed in the few decades before 2100, making it more difficult to justify the installation of new capacity
1197 economically. This is manifested in a model artifact, where in the last few model periods investment in capacities decrease in
1198 general. By extending the time horizon, this “boundary” effect is pushed further to the future, so the artifact only appears after
1199 2100. Therefore the meaningful model results for REMIND are only between 2005-2100, even though years until 2150 are also
1200 modeled and coupled.

1201 Both models have open published source code. Partially thanks to the PSM community’s advocacy of “open models”, which
1202 encompasses all steps from input data, model source code to numerical solvers (openmod - Open Energy Modelling Initiative,
1203 2022), many research institutions also responded to their calls to openly publish their models. For example, the IAM used in this
1204 study – REMIND, has for two years opened its source code on popular hosting site GitHub.

1205 **Appendix B: Model coupling scope**

1206 While REMIND and DIETER can both model a European-wide system with spatial subdivision (see Fig. B1 for REMIND
1207 regional division), the soft-coupling currently is only applied to Germany. The coupling is from 2020 to 2150 for every defined
1208 REMIND period. All common and available REMIND generating technologies are enabled for the coupling, as shown in Fig.
1209 B2. The information for the species of technologies in REMIND are upscaled and coupled to DIETER, whereas information
1210 from DIETER is then downscaled during the feedback loop that completes the coupled iteration.

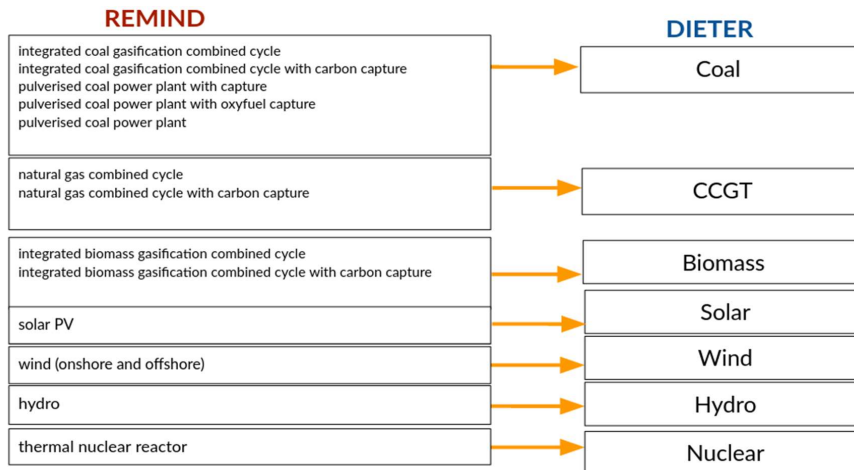
1211 **REMIND-EU (21 regions)**



1212 **Figure B1: REMIND regional resolution used in this study (21 global regions, including detailed differentiations of EU**
1213 **regions). The spatial resolution of REMIND is flexible and depends on the resolution of the input data. Regional**
1214 **mapping is from the REMIND-EU model (Rodrigues et al., 2022).**



1215



1216

1217 **Figure B2: Mapping of coupled technologies between REMIND and DIETER.**

1218 **Appendix C: REMIND’s interannual intertemporal objective function for single-region**

1219 Single-region interannual intertemporal welfare is an aggregated utility, which in turn is a logarithm function of consumption. In
 1220 REMIND, the total welfare of a region is maximized and is equal to

1221
$$W_{reg} = \sum_{y=2005}^{2150} \frac{1}{(1 + \rho_{reg})^{y-2005}} * \Delta y * V_{y,reg} * \ln \left(\frac{\chi_{y,reg}}{\Gamma_{y,reg}} \right),$$

1222 where regional consumption is $\chi_{y,reg}$ at model time y , and the weight of the consumption determined by the pure rate of time
 1223 preference ρ_{reg} and population $V_{y,reg}$. The consumption $\chi_{y,reg}$ at time y is in turn equal to the difference between regional
 1224 income (gross domestic product) minus export (which is not available for consumption) and saving (i.e. investments), subtracted
 1225 by the cost of the energy system (including the power sector) and other costs in the economy. For simplicity we do not discuss
 1226 several other expenditures such as capital investment for energy service, other energy related expenditures such as R&D and
 1227 innovation, taxes, cost of pollution and land-use change.

1228 **Appendix D: Deriving the soft-coupling convergence conditions**

1229 In Sect. 3.2.1, we sketch the derivation procedure and offer a short summary of the analytical results. Here we describe the
 1230 derivation procedure of the coupled convergence framework in detail.

1231 Using the Lagrangian multiplier method, based on the objective functions (Eqs. (1-2)) and constraints (c1-c6) in Sect. 3.1 we
 1232 can construct the KKT Lagrangians (Karush, 1939; Kuhn and Tucker, 1951; Gan et al., 2013):

1233 REMIND:



$$\begin{aligned}
 1235 \quad \mathcal{L} = & \underbrace{\sum_{y,s} (c_{y,s} P_{y,s} + o_{y,s} G_{y,s})}_{\text{REMIND objective function}} + \underbrace{\sum_y \lambda_y \left[d_y - \sum_s G_{y,s} (1 - \alpha_{y,s}) \right]}_{\text{annual electricity balance equation constraint}} + \underbrace{\sum_{y,s} \omega_{y,s} (P_{y,s} - \psi_s)}_{\text{resource constraint}} + \underbrace{\sum_{y,s} \xi_{y,s} (-G_{y,s})}_{\text{positive generation constraint}} \\
 1236 \quad & + \underbrace{\sum_{y,s} \mu_{y,s} (G_{y,s} - 8760 * \phi_{y,s} P_{y,s})}_{\text{maximum generation from capacity constraint}} + \underbrace{\sum_{y \leq 2} \sigma_{y,s} (P_{y,s} - P_{y-1,s})}_{\text{standing capacity constraint}} + \underbrace{\sum_{y=202} \gamma_{y,s} (P_{y,s} - P_{y-1,s} - q_{y,s})}_{\text{near-term ramp-up capacity constraint}}, \quad (D1)
 \end{aligned}$$

1234 DIETER:

$$\begin{aligned}
 1237 \quad \underline{\mathcal{L}} = & \underbrace{\sum_s \left[c_s P_s + o_s \sum_h (G_{h,s} + \Gamma_{h,vre}) \right]}_{\text{DIETER objective function}} + \underbrace{\sum_h \lambda_h \left(d_h - \sum_s G_{h,s} \right)}_{\text{hourly electricity balance equation constraint}} + \underbrace{\sum_s \omega_s (P_s - \psi_s)}_{\text{resource constraint}} + \underbrace{\sum_{h,s} \xi_{h,s} (-G_{h,s})}_{\text{positive generation constraint}} \\
 1238 \quad & + \underbrace{\sum_{h,dis} \mu_{h,dis} (G_{h,dis} - P_{dis})}_{\text{maximum dispatchable generation from capacity constraint}} + \underbrace{\sum_{h,vre} \mu_{h,vre} (G_{h,vre} + \Gamma_{h,vre} - \phi_{h,vre} P_{vre})}_{\text{maximum renewable generation from capacity and weather constraint}}. \quad (D2)
 \end{aligned}$$

1239 Comparing Lagrangians \mathcal{L} and $\underline{\mathcal{L}}$, there are notable similarities between the terms. But first, we can reduce the complexity by
 1240 noticing that there are terms containing capacity shadow prices that are either trivial or already harmonized: resource constraint
 1241 shadow prices ω are already identical for both models by design (constraint (c2) in Sect. 3.1); positive generation constraint
 1242 shadow price ξ is 0 due to KKT conditions for both models (constraint (c3)). These constraint terms can be safely excluded from
 1243 the subsequent mapping. We then note the important fact that REMIND Lagrangian is a sum over multiple years, whereas
 1244 DIETER Lagrangian is for each year. To make a direct comparison and therefore mapping possible, we assume that the brown-
 1245 field and near-term constraints are not binding. After this simplifying assumption, we realize that REMIND becomes linearly
 1246 independent in terms of the temporal slices, because by now the only yet-to-be-harmonized constraints left in the standalone
 1247 models are (c1) and (c4), which are both constraints for each year and do not result in temporal correlations. Note that this
 1248 simplifying assumption is assumed to be valid only for the derivation in this section. Later in actual simulations, we see that
 1249 these bounds generate shadow prices which are not necessarily small, impacting the degree of convergence especially in earlier
 1250 years. These constraints are also temporally localized in early periods, exerting little impact on later, more “green-field” years.
 1251 In fact, when including brown-field constraint into DIETER (c8), the model convergence is improved (Sec. 6.1).

1252 After the aforementioned simplifications, we can construct a single-year REMIND Lagrangian \mathcal{L}_y :

$$1254 \quad \mathcal{L}_y = \underbrace{\sum_s (c_{y,s} P_{y,s} + o_{y,s} G_{y,s})}_{\text{REMIND objective function}} + \underbrace{\lambda_y \left[d_y - \sum_s G_{y,s} (1 - \alpha_{y,s}) \right]}_{\text{annual electricity balance equation constraint}} + \underbrace{\sum_s \mu_{y,s} (G_{y,s} - 8760 * \phi_{y,s} P_{y,s})}_{\text{maximum generation from capacity constraint}}, \quad (D3)$$

1253 and map it to the single-year DIETER Lagrangian $\underline{\mathcal{L}}$:

$$\begin{aligned}
 1255 \quad \underline{\mathcal{L}} = & \underbrace{\sum_s \left[c_s P_s + o_s \sum_h (G_{h,s} + \Gamma_{h,vre}) \right]}_{\text{DIETER objective function}} + \underbrace{\sum_h \lambda_h \left(d_h - \sum_s G_{h,s} \right)}_{\text{hourly electricity balance equation constraint}} + \underbrace{\sum_{h,dis} \mu_{h,dis} (G_{h,dis} - P_{dis})}_{\text{maximum dispatchable generation from capacity constraint}} \\
 1256 \quad & + \underbrace{\sum_{h,vre} \mu_{h,vre} (G_{h,vre} + \Gamma_{h,vre} - \phi_{h,vre} P_{vre})}_{\text{maximum renewable generation from capacity and weather constraint}}. \quad (D4)
 \end{aligned}$$

1257 These are the same as Eqs. (3)-(4).

1258 Comparing \mathcal{L}_y and $\underline{\mathcal{L}}$, we can map them by matching the following four terms in the Lagrangians individually:

- 1259 A) annual total power sector costs: $Z_y = \sum_s (c_{y,s} P_{y,s} + o_{y,s} G_{y,s})$ and $\underline{Z} = \sum_s [c_{y,s} P_{y,s} + o_{y,s} \sum_h (G_{y,h,s} + \Gamma_{y,h,vre})]$,
- 1260 B) annual revenue of usable (post-curtailment) generation for each generator s : $\lambda_y G_{y,s} (1 - \alpha_{y,s})$ and $\sum_h \lambda_{y,h} G_{y,h,s}$,
- 1261 C) annual payment made by the consumers: $\lambda_y d_y$ and $\sum_h \lambda_{y,h} d_{y,h}$,



1262 D) maximum generation from capacity constraint term for each generator $s: \mu_{y,s}(G_{y,s} - 8760 * \phi_{y,s} P_{y,s})$ and
 1263 $\sum_h \mu_{y,h,s} (\underline{G}_{y,h,s} + \underline{L}_{y,h,s} - \underline{\phi}_{y,h,s} \underline{P}_{y,s})$ (we write the two terms for VRE and dispatchable into one term for DIETER here
 1264 for simplicity, i.e. $\underline{L}_{y,h,dis} = 0$ and $\underline{\phi}_{y,h,dis} = 1$ for dispatchables).

1265 The following conditions (h1-h7) can be derived from the harmonization of terms (A)-(D). Each term is harmonized by
 1266 matching the values in front of decision variables at the aggregated levels, namely capacities and annual generations.

1267 Term A) can be mapped if:

1268 **h1)** annual fixed costs are harmonized for each generator species $s: c_{y,s} = \underline{c}_{y,s}$,

1269 **h2)** annual variable costs are harmonized for each generator species $s: o_{y,s} = \underline{o}_{y,s}$.

1270 Term B) can be mapped if:

1271 **h3)** for each generator species s , the annual average revenue per unit generation, i.e. the market value, is harmonized by
 1272 exogenously manipulating the market value in REMIND to be the same as the last-iteration annual average market value in
 1273 DIETER. We achieve this by adding a correction term, thereby modifying REMIND original objective function Z to Z' :

$$1274 Z' = Z - \sum_{y,s} \eta_{y,s}(i-1) G_{y,s}(1 - \alpha_{y,s}),$$

1275 where $\eta_{y,s}(i-1)$ is the markup for technology s in DIETER in the last iteration $i-1$, i is the index of the iteration of the
 1276 iterative soft-coupling. Z' is the modified REMIND objective function in the coupled version.

1277 The detailed derivation is as follows.

1278 Lagrangian term B for the models have the physical meanings of total annual revenue of usable (post-curtailment)
 1279 generation. (Annual revenue is equal to the product of usable generation and annual market value.) We denote total annual
 1280 revenue from technology s as $\theta_{y,s}$ for REMIND and $\underline{\theta}_{y,s}$ for DIETER. Then for REMIND the revenue (term B) is

$$1281 \theta_{y,s} = \lambda_y G_{y,s}(1 - \alpha_{y,s}), \quad (D5)$$

1282 and for DIETER

$$1283 \underline{\theta}_{y,s} = \sum_h \lambda_{y,h} \underline{G}_{y,h,s}. \quad (D6)$$

1284 To harmonize terms $\theta_{y,s}$ and $\underline{\theta}_{y,s}$, our goal is to create a one-to-one mapping of the values in front of the decision variable
 1285 annual aggregated post-curtailment generation of technology s , which is $G_{y,s}(1 - \alpha_{y,s})$ for REMIND and $\sum_h \underline{G}_{y,h,s}$ for
 1286 DIETER, the latter is namely a direct sum of the hourly generations. However, we notice for DIETER revenue $\underline{\theta}_{y,s}$ is a
 1287 weighted sum of the hourly generation, and the direct sum cannot be separated in a straight-forward way. So first we have
 1288 to rewrite $\underline{\theta}_{y,s}$ (Eq. (D6)) by first dividing then multiplying by the aggregated annual generation:

$$1291 \underline{\theta}_{y,s} = \frac{\sum_h \lambda_{y,h} \underline{G}_{y,h,s}}{\sum_h \underline{G}_{y,h,s}} \sum_h \underline{G}_{y,h,s}. \quad (D7)$$

1289 We notice that the multiplicative term in front of the DIETER annual aggregated generation $\sum_h \underline{G}_{y,h,s}$ is $\frac{\sum_h \lambda_{y,h} \underline{G}_{y,h,s}}{\sum_h \underline{G}_{y,h,s}}$, which
 1290 is nothing other than the market value of generation technology s (see also Eq. (F24)).

1292 We now take a look at revenue $\theta_{y,s}$ on the REMIND side, which is equal to $\lambda_y G_{y,s}(1 - \alpha_{y,s})$ (Eq. (D5)). To map (D5) to
 1293 the DIETER revenue term $\underline{\theta}_{y,s}$ (Eq. (D7)) in terms of the aggregated decision variable $G_{y,s}(1 - \alpha_{y,s})$ and $\sum_h \underline{G}_{y,h,s}$, we

1294 essentially would like the multiplicative term in front of the generation variable in $\theta_{y,s}$, which is λ_y , to be also $\frac{\sum_h \lambda_{y,h} \underline{G}_{y,h,s}}{\sum_h \underline{G}_{y,h,s}}$

1295 like in DIETER. This means the DIETER-corrected revenue in REMIND *should* be

$$1296 \theta'_{y,s} = \frac{\sum_h \lambda_{y,h} \underline{G}_{y,h,s}}{\sum_h \underline{G}_{y,h,s}} G_{y,s}(1 - \alpha_{y,s}). \quad (D8)$$



1297 To harmonize $\theta_{y,s}$ and $\underline{\theta}_{y,s}$, we can simply add a linear correction term to compensate for the difference between them.

1298 Noticing in Eq. (D5), the multiplicative term in front of the REMIND generation variable $G_{y,s}(1 - \alpha_{y,s})$ is λ_y , which can
 1299 be interpreted as the REMIND market value, we realize essentially for a linear correction term, we should add the market
 1300 value difference $\Delta MV_{y,s}$ between the two models

$$1301 \quad \Delta MV_{y,s} = \underline{MV}_s - MV_s = \frac{\sum_h \lambda_{y,h} \underline{G}_{y,h,s}}{\sum_h \underline{G}_{y,h,s}} - \lambda_y, \quad (D9)$$

1302 to the multiplicative term λ_y in $\theta_{y,s}$, so λ_y is canceled. Note that in Eq. (D9), as discussed before, the DIETER market
 1303 value is dependent on technology index s , whereas the REMIND one does not.

1304 After adding the linear correction term, the modified revenue in REMIND $\theta'_{y,s}$ after harmonization is:

$$1305 \quad \theta'_{y,s} = \theta_{y,s} + \Delta MV_{y,s} G_{y,s} (1 - \alpha_{y,s}) = (\Delta MV_{y,s} + \lambda_y) G_{y,s} (1 - \alpha_{y,s}), \quad (D10)$$

1306 plugging in (D9),

$$1307 \quad \theta'_{y,s} = \left(\frac{\sum_h \lambda_{y,h} \underline{G}_{y,h,s}}{\sum_h \underline{G}_{y,h,s}} - \lambda_y + \lambda_y \right) G_{y,s} (1 - \alpha_{y,s}) = \frac{\sum_h \lambda_{y,h} \underline{G}_{y,h,s}}{\sum_h \underline{G}_{y,h,s}} G_{y,s} (1 - \alpha_{y,s}), \quad (D11)$$

1308 which is as desired in (D8).

1309 In practice, in the case of annual shadow price λ_y in REMIND, we find that the coupling behaves more stable numerically,
 1310 if we use the annual average electricity price of DIETER instead of the last-iteration electricity price of REMIND λ_y in
 1311 (D9). The equivalence between the two prices is expressed later in (h5). We can use this substitution, since as we show
 1312 later that (h5) can be derived from market value harmonization (h3) and demand harmonization (h4). With this
 1313 substitution, the correction term which we call $\eta_{y,s}$ is in fact:

$$1314 \quad \eta_{y,s} = \underline{MV}_s - J = \frac{\sum_h \lambda_{y,h} \underline{G}_{y,h,s}}{\sum_h \underline{G}_{y,h,s}} - \frac{\sum_h \lambda_{y,h} \underline{d}_{y,h}}{\sum_h \underline{d}_{y,h}}, \quad (D12)$$

1315 where $J = \frac{\sum_h \lambda_{y,h} \underline{d}_{y,h}}{\sum_h \underline{d}_{y,h}}$ is the annual average electricity price in DIETER. We calculate (D12) using the last iteration

1316 DIETER solutions. Note that compared to the earlier (D9), we have simply replaced the second term REMIND annual
 1317 price with DIETER annual price.

1318 It is not hard to recognize $\eta_{y,s}$ as the “markup” for technology s in DIETER, where markup as defined before is the
 1319 difference between the market value of a technology \underline{MV}_s and the load-weighted annual average electricity price J (see
 1320 Sect. 3.1 introduction).

1321 Now we have concluded the derivation for the markup term $\eta_{y,s}$ in (h3).

1322 Although the multiplicative terms in front of decision variables in the two models can be harmonized via the correction
 1323 term (D12), we notice that it contains endogenous values, i.e. hourly generation $\underline{G}_{y,h,s}$ and hourly shadow price $\lambda_{y,h}$ in
 1324 DIETER. Since any endogenous value can only be known ex post, this means the Lagrangian mapping relies on
 1325 endogenous values from the last iteration, i.e.

$$1326 \quad \eta_{y,s}(i-1) = \underline{MV}_s(i-1) - J(i-1) = \frac{\sum_h \lambda_{y,h}(i-1) \underline{G}_{y,h,s}(i-1)}{\sum_h \underline{G}_{y,h,s}(i-1)} - \frac{\sum_h \lambda_{y,h}(i-1) \underline{d}_{y,h}(i-1)}{\sum_h \underline{d}_{y,h}(i-1)}.$$

1327 Now, using the markup term $\eta_{y,s}$, we define the linear correction term for the revenue in REMIND $\theta_{y,s}$ as

$$1328 \quad \Delta \theta_{y,s} = \eta_{y,s}(i-1) G_{y,s} (1 - \alpha_{y,s}).$$

1329 The physical meaning of $\Delta \theta_{y,s}$ is the revenue difference in the two models for technology s , given that the post-
 1330 curtailment generations are expressed in terms of REMIND variables.



1331 The coupled REMIND has a modified objective function Z' based on a linear correction. The correction term $\Delta\theta_{y,s}$ need to
 1332 be summed over s and y and subtracted – due to the negative sign in front of term B, from the REMIND objective function
 1333 Z , since the objective term as a part of the Lagrangian can be directly manipulated:

$$1334 \quad Z' = Z - M = Z - \sum_{y,s} \Delta\theta_{y,s} = Z - \sum_{y,s} \eta_{y,s}(i-1)G_{y,s}(1-\alpha_{y,s}),$$

1335 where we call the total system revenue differences M , again, these are revenues where the post-curtailment generations are
 1336 expressed in terms of REMIND variables (and not DIETER variables).

1337 Now we have concluded the derivation for the convergence condition (h3).

1338 Depending on the starting point of the REMIND power system, and due to the internal iterative changes of REMIND
 1339 results due to the adjustments in trade between regions during the “Nash” algorithm, coupled convergence usually can only
 1340 be achieved over multiple iterations. Therefore the derived markup equation (Eq. (D12)) in general can be only expected to
 1341 reflect the actual market value differences approximately in the two models. This is the reason that in the iterative
 1342 algorithm after the first iteration, we add $M(i) - M(i-1)$ to the objective function Z , as the quantities and prices
 1343 gradually converge between the two models. As convergence is approached, the total revenue difference between iteration
 1344 $M(i) - M(i-1)$ should go to zero. This is confirmed by the numerical experiments (not shown).

1345 Term C) can be mapped if:

1346 **h4)** annual power demand in the two models are harmonized: $d_y = \sum_h d_{y,h}$,

1347 **h5)** annual average price of electricity is mapped to each other $\lambda_y = \frac{\sum_h \lambda_{y,h} d_{y,h}}{\sum_h d_{y,h}}$ (dividing term (C) by (h4)). Because

1348 electricity price is by definition equal to total annual system revenue divided by total annual demand, (h5) can be shown to
 1349 hold true, given technology-specific revenues are harmonized in (h3) and demand are harmonized in (h4). (If technology-
 1350 specific revenues are harmonized in (h3), then the system revenues which are technology-specific revenues summed over
 1351 technologies are also harmonized.) (h5) therefore can be seen as a derived condition from (h3) and (h4).

1352 Term D) can be mapped if:

1353 **h6)** annual average capacity factors are harmonized, i.e. $\phi_{y,s}$ in REMIND is set to equal to the endogenous last-iteration
 1354 DIETER result for each generation type s :

$$1355 \quad \phi_{y,s} = \sum_h \phi_{y,h,s} / 8760 ,$$

1356 where $\phi_{y,h,s} = \frac{G_{y,h,s}}{P_{y,s}}$ is the hourly capacity factor in DIETER. Without explicit manipulation of the shadow prices $\mu_{y,s}$ and
 1357 $\mu_{y,h,s}$, we show the following claim is true, i.e. by above capacity factor harmonization, the terms containing endogenous
 1358 shadow prices will be automatically mapped. Showing this requires careful mathematical argument, which we make in
 1359 detail in the case of dispatchable, and later argue the case is similar for renewable.

1360 For dispatchable generators the argument is as follows. (For simplicity we use the generic index s .)

1361 We first rewrite REMIND term D by plugging in the harmonization condition $\phi_{y,s} = \sum_h \phi_{y,h,s} / 8760$:

$$1362 \quad \mu_{y,s}(G_{y,s} - 8760 * \phi_{y,s} P_{y,s}) = \sum_y \mu_{y,s} \left(G_{y,s} - \sum_h \phi_{y,h,s} P_{y,s} \right),$$

1363 and it should be mapped to the term $\sum_{y,h} \mu_{y,h,s} (G_{y,h,s} - P_{y,s})$ in DIETER.

1364 Splitting the two terms, these four terms need to be harmonized:

$$1365 \quad \mu_{y,s} G_{y,s} \quad \text{and} \quad \sum_h \mu_{y,h,s} G_{y,h,s} \tag{D13}$$



$$\mu_{y,s} \sum_h \phi_{y,h,s} P_{y,s} \quad \text{and} \quad \sum_h \mu_{y,h,s} P_{y,s} \quad (D14)$$

for all y, s .

To show the mappings (D13)-(D14) are automatically satisfied given (h6), we first consider two simplified power sector toy problems, Q1 and Q2, with only dispatchable technologies. Both problems have identical objective functions $\tilde{Z} = \sum_s (\tilde{c}_s \tilde{P}_s + \tilde{o}_s \tilde{G}_s)$, and the fixed and variable cost parameters \tilde{c}_s and \tilde{o}_s are identical. Both problems have identical hourly balance equation constraint, but with two different kinds of maximum generation constraint, Q1 has an inequality constraint for each hour, Q2 has an aggregated annual equality constraint:

$$Q1: \min Z, \text{ s.t. } \tilde{G}_{h,s} \leq \tilde{P}_s \quad \perp \quad \tilde{\mu}_{h,s}, \quad \tilde{d}_h = \sum_s \tilde{G}_{h,s} \quad \perp \quad \tilde{\lambda}_h$$

$$Q2: \min Z, \text{ s.t. } \sum_h \tilde{G}_{h,s} = 8760 * \tilde{\phi}_s \tilde{P}_s \quad \perp \quad \tilde{\mu}'_s, \quad \tilde{d}_h = \sum_s \tilde{G}_{h,s} \quad \perp \quad \tilde{\lambda}'_h$$

Then the Lagrangians are:

$$\tilde{L}_1 = \underbrace{\sum_s \left(\tilde{c}_s \tilde{P}_s + \tilde{o}_s \sum_h \tilde{G}_{h,s} \right)}_{\text{objective function}} + \underbrace{\sum_h \tilde{\lambda}_h \left(\tilde{d}_h - \sum_s \tilde{G}_{h,s} \right)}_{\text{hourly electricity balance equation constraint}} + \underbrace{\sum_{h,s} \tilde{\mu}_{h,s} \left(\tilde{G}_{h,s} - \tilde{P}_s \right)}_{\text{maximum generation from capacity constraint}}$$

$$\tilde{L}_2 = \underbrace{\sum_s \left(\tilde{c}_s \tilde{P}_s + \tilde{o}_s \sum_h \tilde{G}_{h,s} \right)}_{\text{objective function}} + \underbrace{\sum_h \tilde{\lambda}'_h \left(\tilde{d}_h - \sum_s \tilde{G}_{h,s} \right)}_{\text{hourly electricity balance equation constraint}} + \underbrace{\sum_s \tilde{\mu}'_s \left(\sum_h \tilde{G}_{h,s} - 8760 \tilde{\phi}_s \tilde{P}_s \right)}_{\text{maximum generation from capacity constraint}}.$$

The relevant KKT conditions:

Stationarity condition for Q1:

$$\frac{\partial \tilde{L}_1}{\partial \tilde{P}_s} = \tilde{c}_s - \sum_h \tilde{\mu}_{h,s} = 0 \quad (D15)$$

Stationarity condition for Q2:

$$\frac{\partial \tilde{L}_2}{\partial \tilde{P}_s} = \tilde{c}_s - 8760 \tilde{\phi}_s \tilde{\mu}'_s = 0 \quad (D16)$$

Since the fixed cost \tilde{c}_s are equal for the two models, from Eqs. (D15)-(D16) we can derive the relation between the two shadow prices:

$$8760 * \tilde{\phi}_s \tilde{\mu}'_s = \sum_h \tilde{\mu}_{h,s}. \quad (D17)$$

Note that for the toy models, the identical balance equation constraints do not contain capacity P , which is why the balance equation constraints do not influence the stationary conditions for P (Eqs. (D15)-(D16)).

We now show (D14) is automatically mapped given capacity factor harmonization (h6). We first write the equality condition for the REMIND-DIETER case, analogous to the toy model result (D17),

$$8760 * \phi_{y,s} \mu_{y,s} = \sum_h \mu_{y,h,s}. \quad (D18)$$

Note that we can apply the toy model case to the REMIND-DIETER coupling case in rather straight-forward way, because in the case of REMIND-DIETER, the objective function terms have been already harmonized by (h1)-(h2), and the balance equation constraint terms do not contain P , so they have no bearing on the generation-capacity constraint term, just like in the case of the toy models.

Plugging (h6) $\phi_{y,s} = \sum_h \phi_{y,h,s} (i-1) / 8760$ into (D18), we have derived the equality for the parameter mapping required in (D14), i.e.,

$$\mu_{y,s} \sum_h \phi_{y,h,s} (i-1) = \sum_h \mu_{y,h,s}.$$

To show (D13), we first use hourly capacity factor from DIETER,

$$\underline{G}_{y,h,s} = \underline{\phi}_{y,h,s} P_{y,s}, \quad (D19)$$



1400 as well as the primal feasibility condition from REMIND $G_{y,s} = 8760 * \phi_{y,s} P_{y,s}$ (Eq. (F9)), to rewrite both sides of the
 1401 mapping in (D13) in capacity terms. For REMIND, plugging in (F9),

$$1402 \quad \mu_{y,s} G_{y,s} = \mu_{y,s} * 8760 * \phi_{y,s} P_{y,s} , \quad (D20)$$

1403 and for DIETER, plugging in (D19),

$$1404 \quad \sum_h \mu_{y,h,s} \underline{G}_{y,h,s} = \sum_h \mu_{y,h,s} \phi_{y,h,s} \underline{P}_{y,s} . \quad (D21)$$

1405 Take the complementary slackness condition of DIETER $\mu_{h,s} (\underline{G}_{h,s} - \underline{P}_s) = 0$ (Eq. (F16)), insert (D19) on the left-hand-
 1406 side, we obtain

$$1407 \quad \mu_{h,s} (\underline{G}_{h,s} - \underline{P}_s) = \mu_{h,s} (\phi_{y,h,s} \underline{P}_{y,s} - \underline{P}_s) = 0 .$$

1408 Rearranging, we get

$$1409 \quad \mu_{y,h,s} \phi_{y,h,s} \underline{P}_s = \mu_{y,h,s} \underline{P}_s , \quad (D22)$$

1410 for each hour h .

1411 Plug (D22) and then (D18) into the right-hand-side of (D21), to obtain

$$1412 \quad \sum_h \mu_{y,h,s} \underline{G}_{y,h,s} = \sum_h \mu_{y,h,s} \underline{P}_{y,s} = 8760 * \phi_{y,s} \mu_{y,s} \underline{P}_{y,s} . \quad (D23)$$

1413 Compare (D20) with (D23), they now have identical parameters in front of the capacity variable $P_{y,s}$ and $\underline{P}_{y,s}$, as desired.

1414 We concluded the proof that by exogenously setting the annual capacity factor of REMIND to that of the last iteration
 1415 DIETER, we automatically harmonize the generation-capacity constraint term of the Lagrangian, in the case of
 1416 dispatchable generators.

1417 **h7)** for VRE, annual curtailment rates are harmonized $G_{y,vre} \alpha_{y,vre} = \sum_h \underline{L}_{y,h,vre}$, i.e. by exogenously setting curtailment rate
 1418 in REMIND $\alpha_{y,vre} = \sum_h \underline{L}_{y,h,vre} (i - 1) / G_{y,vre}$, taking the endogenously determined curtailed power $\underline{L}_{y,h,vre}$ from the last
 1419 iteration DIETER. This in general also harmonizes terms other than term D, as it harmonizes the definition for generation
 1420 variable in DIETER which is post-curtailment and REMIND definition for generation variable which is pre-curtailment.

1421 For VREs the derivation is conceptually similar to the above case for dispatchable in (h6), since we can define a real
 1422 capacity factor (post-curtailment) similar to the capacity factor for the dispatchable generators above,

$$1423 \quad \phi_{y,h,vre} = \underline{G}_{h,vre} / \underline{P}_{vre} .$$

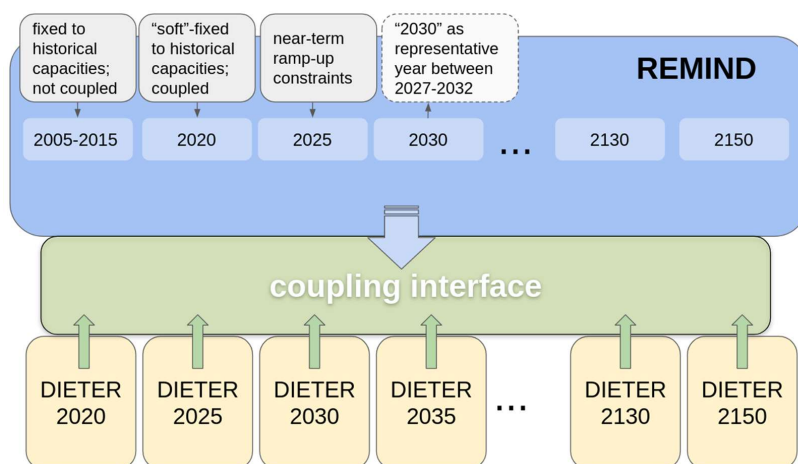
1424 Due to the limitations of this paper, we will not present the derivation here. A detailed derivation is available upon request.

1425 Appendix E: Coupling iteration schematics

1426 Coupled region: Germany

1427 Coupled REMIND time horizon: 2020-2150 (2010-2015 are not coupled since they are historical years and have mostly hard-

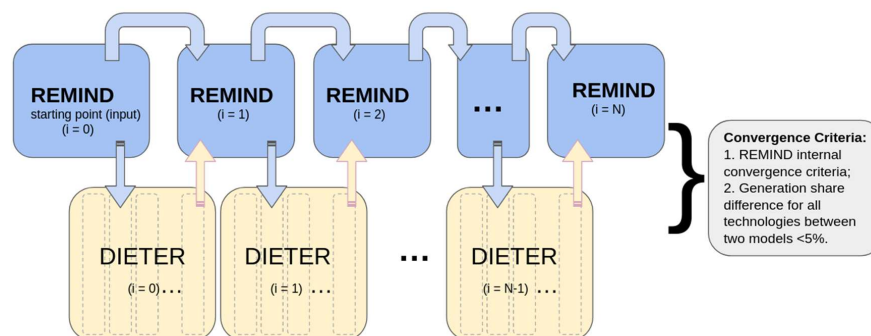
1428 fixed quantities)



1429

1430

(a) Graphic illustration of the bi-directional coupling in the temporal dimension.



1431

1432

(b) Graphic illustration of the bi-directional coupling in the iteration dimension.

1433

1434

1435

1436

1437

1438

1439

1440

1441

1442

1443

1444

1445

Figure E1: A graphic description of the model iterative coupling. (a) The temporal slices of REMIND which are mapped to multiple parallel year-long DIETER problems are illustrated here. The convergence conditions are iteratively mapped at the interface. (b) Every i -th iteration of REMIND takes the $(i-1)$ -th iteration of REMIND as a starting point for optimization, and the endogenous output of the $(i-1)$ -th DIETER as exogenous input parameters. When the convergence conditions are met, i.e. REMIND satisfies its internal convergence condition, and the coupled models differ in their generation share of each technology at most by a certain percentage (e.g. 5% for baseline run without storage), the coupled run halts.

Under simple configuration (no storage, no flexible demand), every REMIND run takes around 3 minutes and DIETER run takes a few seconds to solve. Under more detailed configurations (with storage and flexible demand) and climate policies, every REMIND run takes around 4 minutes and a DIETER run takes a few minutes to solve. The entire REMIND-DIETER coupled run for a single region Germany under simple configuration is around 3~4 hours. It is around 6~10 hours for the more detailed configurations under climate policies.



1446 **Appendix F: Derivation of the equilibrium conditions for uncoupled REMIND and DIETER**

1447 In this appendix, we discuss the equilibrium conditions of the uncoupled models, resulting in a rigorous formulation of the so-
 1448 called “zero-profit rules” (ZPRs). We first construct the Lagrangians and compute KKT conditions, then derive the ZPRs for the
 1449 standalone versions of REMIND reduced power-sector model and DIETER model.

1450 Using the objective functions and constraints in Sect. 3.1, we can construct Lagrangians for the two standalone models. Using
 1451 the KKT conditions derived from the Lagrangians, we can show that if the historical and resource constraint are non-binding,
 1452 i.e. shadow prices ω , σ and γ are zero, then each generator would have recovered their fixed, variable cost and curtailment cost
 1453 through their total market revenue, i.e. each producer of electricity gets “zero profit”, given that the profits are defined as the
 1454 difference between revenue and cost. When the capacity constraints exist and are binding, we arrive at a modified version of the
 1455 original ZPR, which describes the relation between cost, revenue and the capacity shadow prices.

1456 Here we first construct the Lagrangians and derive the KKT conditions from them (Sect. F.1) for both models. Then both
 1457 models’ ZPRs are derived, two for each model, namely, the technology-specific ZPR and the system ZPR (Sect. F.2).

1458 **F.1 Lagrangians and KKT conditions**

1459 The Lagrangians of the uncoupled model have been constructed in Appendix D (Eqs. (D1)-(D2)). From the KKT conditions for
 1460 minimization, we can ascertain the following first-order conditions at stationarity for each model.

1461 For REMIND,

1462 1) Stationary conditions:

$$1463 \quad \frac{\partial \mathcal{L}}{\partial P_{y,s}} = 0 \Rightarrow c_{y,s} + \omega_{y,s} - 8760 * \mu_{y,s} \phi_{y,s} - \sigma_{y,s} + \gamma_{y,s} = 0, \quad (F1)$$

$$1464 \quad \frac{\partial \mathcal{L}}{\partial G_{y,s}} = 0 \Rightarrow o_{y,s} - \lambda_y (1 - \alpha_{y,s}) - \xi_{y,s} + \mu_{y,s} = 0. \quad (F2)$$

1465 2) Complementary slackness:

$$1466 \quad \omega_{y,s} (P_{y,s} - \psi_s) = 0, \quad (F3)$$

$$1467 \quad \xi_{y,s} G_{y,s} = 0, \quad (F4)$$

$$1468 \quad \mu_{y,s} (G_{y,s} - 8760 * \phi_{y,s} P_{y,s}) = 0, \quad (F5)$$

$$1469 \quad \sigma_{y,s} (p_{y,s} - P_{y,s}) = 0, \quad (y \leq 2020), \quad (F6)$$

$$1470 \quad \gamma_{y,s} (P_{y,s} - P_{y-2y,s} - q_{y,s}) = 0, \quad (y = 2025). \quad (F7)$$

1471 3) Primal feasibility:

$$1472 \quad d_y - \sum_s G_{y,s} (1 - \alpha_{y,s}) = 0, \quad (F8)$$

$$1473 \quad G_{y,s} - 8760 * \phi_{y,s} P_{y,s} = 0, \quad (F9)$$

1474 4) Dual feasibility:

$$1475 \quad \xi_{y,s} \geq 0, \omega_{y,s} \geq 0, \sigma_{y,s} \geq 0, \gamma_{y,s} \geq 0. \quad (F10)$$

1476 For DIETER,

1477 1) Stationary conditions:

$$1478 \quad \frac{\partial \mathcal{L}}{\partial P_s} = 0 \Rightarrow \underline{c}_s + \underline{\omega}_s - \sum_h \underline{\phi}_{h,s} \underline{\mu}_{h,s} = 0, \quad \underline{\phi}_{h,s} = 1 \text{ for dispatchables, } 0 < \underline{\phi}_{h,s} < 1 \text{ for renewables} \quad (F11)$$

$$1479 \quad \frac{\partial \mathcal{L}}{\partial G_{h,s}} = 0 \Rightarrow \underline{o}_s - \underline{\lambda}_h - \underline{\xi}_{h,s} + \underline{\mu}_{h,s} = 0, \quad (F12)$$

$$1480 \quad \frac{\partial \mathcal{L}}{\partial \underline{h}_{h,vre}} = 0 \Rightarrow \underline{o}_{vre} + \underline{\mu}_{h,vre} = 0. \quad (F13)$$



1481 2) Complementary slackness:

$$1482 \quad \omega_s (P_s - \psi_s) = 0, \tag{F14}$$

$$1483 \quad \xi_{h,s} \underline{G}_{h,s} = 0, \tag{F15}$$

$$1484 \quad \mu_{h,dis} (\underline{G}_{h,dis} - P_{dis}) = 0, \tag{F16}$$

1485 3) Primal feasibility:

$$1486 \quad \underline{d}_h = \sum_s \underline{G}_{h,s}, \tag{F17}$$

$$1487 \quad \underline{G}_{h,vre} + \underline{L}_{h,vre} = \underline{\phi}_{h,vre} \underline{P}_{vre}, \tag{F18}$$

1488 4) Dual feasibility:

$$1489 \quad \omega_s \geq 0, \xi_{h,s} \geq 0, \mu_{h,dis} \geq 0. \tag{F19}$$

1490 F.2 Derivation of the zero-profit rules

1491 F.2.1 REMIND

1492 The derivation of ZPRs is very similar to the one in Brown and Reichenberg, 2021. Starting with the total costs for technology s
1493 for all years, and applying various KKT conditions (after “|”),

$$1494 \quad \sum_y (c_{y,s} P_{y,s} + o_{y,s} G_{y,s})$$

$$1495 \quad = \sum_y \{ (-\omega_{y,s} + 8760 * \mu_{y,s} \phi_{y,s} + \sigma_{y,s} - \gamma_{y,s}) P_{y,s} + [\lambda_y (1 - \alpha_{y,s}) + \xi_{y,s} - \mu_{y,s}] G_{y,s} \} \tag{F1}, (F2)$$

$$1496 \quad = \sum_y \{ (-\omega_{y,s} + 8760 * \mu_{y,s} \phi_{y,s} + \sigma_{y,s} - \gamma_{y,s}) P_{y,s} + [\lambda_y (1 - \alpha_{y,s}) - \mu_{y,s}] G_{y,s} \} \tag{F4}$$

$$1497 \quad = \sum_y \{ (-\omega_{y,s} + \sigma_{y,s} - \gamma_{y,s}) P_{y,s} + \lambda_y G_{y,s} (1 - \alpha_{y,s}) \} \tag{F5}$$

1498 Rearranging, we arrive at the ZPR of multi-year uncoupled REMIND for technology cost-revenue balance:

$$1499 \quad \frac{\sum_y (c_{y,s} P_{y,s} + o_{y,s} G_{y,s})}{\text{Generation costs}_s} = - \frac{\sum_y (\omega_{y,s} - \sigma_{y,s} + \gamma_{y,s}) P_{y,s}}{\text{Capacity shadow revenues}_s} + \frac{\sum_y \lambda_y G_{y,s} (1 - \alpha_{y,s})}{\text{Generation revenues}_s} \tag{F20}$$

1500 Normally, when there are no capacity shadow prices, or when the capacity constraints are not binding, the cost exactly equals
1501 revenue. However, when capacity shadow prices are non-zero, i.e. the constraints (c2) and (c5-c6) are binding, the capacity
1502 shadow prices act as a distortion to the equality relation between costs and revenues. As an example, the shadow price $\omega_{y,s}$ from
1503 limited generation resources (e.g. hydroelectric power in Germany) would be positive $\omega_{y,s} > 0$, when the constraint is binding,
1504 and would appear as a “positive cost”, or a “negative revenue” in the modeled power market. We can therefore put it either on
1505 the left (cost) or right (revenue) side of the equation. Here we group it together with revenues.

1506 One observes that from the right-hand-side of Eq. (F20), there is no differentiation between the annual market values of variable
1507 and dispatchable generations such as gas and solar – they are both equal to the annual electricity price λ_y .

1508 From Eq. (F20), we can derive a ZPR between levelized cost of electricity (LCOE), capacity shadow price and market value
1509 (MV), for each generator type. Taking Eq. (F20), we separate the pre-curtailment LCOE from the LCOE due to curtailment,
1510 then divide by total post-curtailment generation $\sum_y G_{y,s} (1 - \alpha_{y,s})$ for the generator type s , to obtain the technology-specific
1511 ZPR:

$$1512 \quad \frac{\sum_y (c_{y,s} P_{y,s} + o_{y,s} G_{y,s})}{\sum_y G_{y,s}} + \frac{\sum_y (c_{y,s} P_{y,s} + o_{y,s} G_{y,s}) \alpha_{y,s}}{\sum_y G_{y,s} (1 - \alpha_{y,s})} = - \frac{\sum_y (\omega_{y,s} - \sigma_{y,s} + \gamma_{y,s}) P_{y,s}}{\sum_y G_{y,s} (1 - \alpha_{y,s})} + \frac{\sum_y \lambda_y G_{y,s} (1 - \alpha_{y,s})}{\sum_y G_{y,s} (1 - \alpha_{y,s})} \tag{F21}$$

Pre-curtailment LCOE_s
Curtailment LCOE_s
Capacity shadow price_s
Market Value_s



1513 The pre-curtailment LCOE is the cost of one unit of generated electricity – regardless whether it is curtailed or being used to
 1514 meet demand, whereas the curtailment LCOE is the cost of one unit of curtailed electricity. Together they add up to post-
 1515 curtailment LCOE, i.e. the cost of one unit of usable electricity.

1516 To obtain the ZPR for the whole power system in REMIND, we first sum Eq. (F20) over all generator types s , and obtain the
 1517 ZPR for system cost and revenue. Then dividing by total post-curtailment system generation, and split the LCOE into pre-
 1518 curtailment and curtailment components, we get

$$1519 \frac{\sum_{y,s} (c_{y,s} P_{y,s} + o_{y,s} G_{y,s})}{\sum_{y,s} G_{y,s}} + \frac{\sum_{y,s} (c_{y,s} P_{y,s} + o_{y,s} G_{y,s}) \alpha_{y,s}}{\sum_{y,s} G_{y,s} (1 - \alpha_{y,s})} = - \frac{\sum_{y,s} (\omega_{y,s} - \sigma_{y,s} + \gamma_{y,s}) P_{y,s}}{\sum_{y,s} G_{y,s} (1 - \alpha_{y,s})} + \frac{\sum_{y,s} \lambda_y G_{y,s} (1 - \alpha_{y,s})}{\sum_{y,s} G_{y,s} (1 - \alpha_{y,s})}, \quad (F22)$$

1520 i.e. the LCOE of the system for usable (pre-curtailment) power, which is equal to the sum of the system LCOE for total power
 1521 generated and the curtailment cost, can be recovered by the average electricity price of the system minus system-wide capacity
 1522 constraint shadow price per energy unit.

1523 The ZPRs of REMIND hold for the aggregate over multiple years.

1524 From Eqs. (F21)-(F22), we learn that when a market equilibrium can be found, i.e. when the optimization problem can be
 1525 successfully solved, there is an equality relation between the generation cost and market value for each generator type, and
 1526 similarly between generation cost and price of electricity for the entire system. Capacity shadow prices due to various extra
 1527 capacity constraints imposed on the models, distort the equality relation between costs and prices by a linear term, making the
 1528 prices be either higher or lower than the costs at the market equilibrium.

1529 F.2.2 DIETER

1530 Similar to uncoupled REMIND, from KKT conditions, at stationarity, we can obtain the cost-revenue ZPR for a single
 1531 technology s for standalone DIETER. We take the total costs for technology s for all years, and applying various KKT
 1532 conditions (after “|”),

$$1533 \underline{c}_s P_s + \sum_h [\underline{q}_s (\underline{G}_{h,s} + \underline{I}_{b,vre})]$$

$$1534 = \left(-\underline{\omega}_s + \sum_h \underline{\phi}_{h,s} \underline{\mu}_{h,s} \right) P_s + \sum_h \left(\underline{\lambda}_h - \underline{\mu}_{h,s} + \underline{\xi}_{h,s} \right) (\underline{G}_{h,s} + \underline{I}_{b,vre}) \quad | \quad (F11),(F12)$$

$$1535 = -\underline{\omega}_s P_s + \sum_h \underline{\phi}_{h,vre} \underline{\mu}_{h,vre} P_{vre} + \sum_h \left(\underline{\lambda}_h - \underline{\mu}_{h,vre} + \underline{\xi}_{h,vre} \right) (\underline{G}_{h,vre} + \underline{I}_{b,vre}) + \sum_h \underline{\mu}_{h,dis} P_{dis} + \sum_h \left(\underline{\lambda}_h - \underline{\mu}_{h,dis} \right) \underline{G}_{h,dis}$$

1536 | split $\sum_h \underline{\phi}_{h,s} \underline{\mu}_{h,s}$ into vre and dis , apply (F15) for dispatchable, i.e. $\underline{\xi}_{h,dis} \underline{G}_{h,dis} = 0$

$$1537 = -\underline{\omega}_s P_s + \sum_h \underline{\phi}_{h,vre} \underline{\mu}_{h,vre} P_{vre} + \sum_h \left(\underline{\lambda}_h - \underline{\mu}_{h,vre} + \underline{\xi}_{h,vre} \right) (\underline{G}_{h,vre} + \underline{I}_{b,vre}) + \sum_h \underline{\lambda}_h \underline{G}_{h,dis} \quad | \quad (F16)$$

$$1538 = -\underline{\omega}_s P_s + \sum_h \underline{\lambda}_h \underline{G}_{h,vre} + \sum_h \left(\underline{\lambda}_h + \underline{\xi}_{h,vre} \right) \underline{I}_{h,vre} + \sum_h \underline{\lambda}_h \underline{G}_{h,dis} \quad | \quad (F18), \text{ apply (F15) for VRE, i.e. } \underline{\xi}_{h,vre} \underline{G}_{h,vre} = 0$$

$$1539 = -\underline{\omega}_s P_s + \sum_h \underline{\lambda}_h \underline{G}_{h,vre} + \sum_h \underline{\lambda}_h \underline{G}_{h,dis} \quad | \quad (F12) \ \& \ (F13) \Rightarrow \underline{\lambda}_h + \underline{\xi}_{h,vre} = 0$$

1540 Rearranging, we arrive at the ZPR of single-year uncoupled DIETER for technology-specific cost-revenue balance:

$$1541 \frac{\underline{c}_s P_s + \underline{q}_s \sum_h (\underline{G}_{h,s} + \underline{I}_{h,vre})}{\text{Annual generation costs}_s} = - \frac{\underline{\omega}_s P_s}{\text{Annual capacity shadow revenue}_s} + \frac{\sum_h \underline{\lambda}_h \underline{G}_{h,s}}{\text{Annual generation revenue}_s}. \quad (F23)$$

1542 Dividing Eq. (F23) by annual aggregated generation of technology s , we obtain the technology-specific ZPR for DIETER,

$$1543 \frac{\underline{c}_s P_s + \underline{q}_s \sum_h (\underline{G}_{h,s} + \underline{I}_{h,vre})}{\sum_h \underline{G}_{h,s}} = - \frac{\underline{\omega}_s P_s}{\sum_h \underline{G}_{h,s}} + \frac{\sum_h \underline{\lambda}_h \underline{G}_{h,s}}{\sum_h \underline{G}_{h,s}}. \quad (F24)$$



1544 One observes that from the term of *Market Value*, compared to the REMIND case (right-hand-side of Eq. (F21)), DIETER
1545 has differentiated annual market values of gas and solar generators.

1546 Summing Eq. (F24) over s , dividing both sides by total annual generation $\sum_{h,s} \underline{G}_{h,s}$, using identity $\underline{d}_h = \sum_s \underline{G}_{h,s}$ for
1547 simplification, we obtain the ZPR for the whole power system in DIETER,

$$1548 \frac{\sum_s [\underline{c}_s P_s + o_s \sum_h (\underline{G}_{h,s} + \Gamma_{h,vre})]}{\sum_{h,s} \underline{G}_{h,s}} = - \frac{\sum_s \omega_s P_s}{\sum_{h,s} \underline{G}_{h,s}} + \frac{\sum_h \lambda_h \underline{d}_h}{\sum_h \underline{d}_h} \quad (F25)$$

LCOE_{system}
Annual capacity shadow price_{system}
Annual average electricity price_{system}

1549 Similar to the case of REMIND, Eqs. (F24)-(F25) show us the equality relations between cost and value (or price) for each
1550 generator type and for the system hold also for DIETER at its market equilibrium. Compared to REMIND, there are no brown-
1551 field or near-term capacity shadow price contributions in DIETER in the standalone versions. The DIETER ZPRs hold for one
1552 year instead of the aggregate of multiple years like in REMIND. For simplicity, even though it is possible to write the LCOE in
1553 pre-curtailment and curtailment terms, but because for DIETER it is relatively cumbersome to do, we do not do it here.

1554 In summary, at REMIND and DIETER power market equilibriums, each generator exactly recovers its cost of one unit of
1555 generation through market value, and obtains “zero profit” under a completely competitive market over its modeling time. In the
1556 aggregate, the entire power sector obtains its cost of one unit of generation through the price of electricity that the consumer
1557 pays. Both types of relations can be distorted by the existence of capacity shadow prices.

1558 **Appendix G: Derivation of the equilibrium conditions for the coupled models**

1559 Here in this Appendix, we gradually build up the derivation for the ZPRs of the coupled REMIND and DIETER, which will be
1560 used later for validating numerical results. The derivation consists of three steps:

- 1561 1) ZPRs for the uncoupled model REMIND and DIETER;
- 1562 2) ZPRs for coupled model REMIND and DIETER (simplified version, only considering convergence condition (h1-h7));
- 1563 3) ZPRs for coupled model REMIND and DIETER (full version, also considering (c7 and c8)).

1564 Step (1) is entirely derived in Appendix F.

1565 For step (2), based on the uncoupled ZPRs, we recognize that from convergence condition (h1-h7), the only condition which
1566 impacts the form of the ZPR is (h3), because the markup terms modify the objective function of the (simplified) coupled version
1567 of REMIND (Eq. (6)). Following similar procedure as in Appendix F, we can derive the technology-specific ZPR for the
1568 coupled REMIND (simplified version) as follows:

$$1569 \frac{\sum_y (c_{y,s} P_{y,s} + o_{y,s} G_{y,s})}{\sum_y G_{y,s}} + \frac{\sum_y (c_{y,s} P_{y,s} + o_{y,s} G_{y,s}) \alpha_{y,s}}{\sum_y G_{y,s} (1 - \alpha_{y,s})} = - \frac{\sum_y (\omega_{y,s} - \sigma_{y,s} + \gamma_{y,s}) P_{y,s}}{\sum_y G_{y,s} (1 - \alpha_{y,s})} + \frac{\sum_y (\lambda_y + \eta_{y,s}) G_{y,s} (1 - \alpha_{y,s})}{\sum_y G_{y,s} (1 - \alpha_{y,s})} \quad (G1)$$

Pre-curtailment LCOE_s
Curtailment cost_s
Capacity shadow price_s
Market Value_s

1570 Compared with the ZPR of the uncoupled version (F24), the only difference is that we replace the market value in the uncoupled
1571 REMIND λ_y with the DIETER-markup corrected market value $\lambda_y + \eta_{y,s}$. DIETER’s ZPR is unchanged at this step.

1572 Step (3) involves two extra capacity constraints, one in each model, the first of which, (c7), is discussed in detail in Appendix H.
1573 The implementation of (c7) further modifies Eq. (G1) and results in the ZPRs of the coupled REMIND. The other constraint
1574 (c8) will be the focus of discussion here. It only modifies the ZPRs for the coupled DIETER and not for the coupled REMIND.
1575 Constraint (c8) is a brown-field capacity constraint implemented in DIETER to address the fact that DIETER is a green-field
1576 model, which is otherwise ignorant about standing-capacities in the real world. There are many ways we can implement this
1577 standing capacity constraint in DIETER. The most straight-forward way is to implement the “standing capacity” at the
1578 beginning of each REMIND period, which REMIND sees before it invests additional capacities, as a lower bound on



1579 endogenous capacities in DIETER. This helps put DIETER and REMIND on equal footing before the 5- or 10-year investment
 1580 period starts, allowing us to compare their investment intentions.

1581 c8) “standing capacity constraint” in DIETER, i.e. DIETER capacities at time y need to be larger or equal to the REMIND
 1582 standing capacities at the beginning of the time period:

$$1583 \quad P_s \geq P_{y-\Delta y/2,s} / (1 - ER) \quad \perp \zeta_s,$$

1584 where the time-step Δy is divided by 2 because the representative year in REMIND is in the middle of the time step, ER is
 1585 the endogenous early retirement rate in REMIND.

1586 The reason we implement the standing capacity in this way, is in part because as a proof-of-concept, we want to give DIETER
 1587 endogenous freedom to invest in all model years, so we use only the pre-investment capacities as “soft” corridors to bound the
 1588 DIETER capacities from below. If we were to transfer precisely the brown-field and near-term constraints from REMIND to
 1589 DIETER, it requires a complete list of constraints for each technology, and an identical implementation of all of them in
 1590 DIETER. This may raise the precision of convergence in some years for some technologies, but in practice it can be more
 1591 complicated to implement than a generic lower bound for all technologies.

1592 To obtain the ZPRs of coupled DIETER, we simply modify the capacity shadow price term of the uncoupled DIETER ZPRs
 1593 (Eqs. (F24)-(F25)) by the additional capacity shadow price ζ_s from (c8):

$$1594 \quad \text{Capacity shadowprice}'_s = \frac{(\omega_s + \zeta_s) P_s}{\sum_n \underline{a}_{h,s}}, \quad (G2)$$

$$1595 \quad \text{Capacity shadowprice}'_{system} = \frac{\sum_s (\omega_s + \zeta_s) P_s}{\sum_{h,s} \underline{a}_{h,s}}. \quad (G3)$$

1596 **Appendix H: Additional methods for numerical stability in coupled runs**

1597 Here, we introduce the two methods we employed to improve numerical stability of the coupled runs: 1) the dispatchable
 1598 capacity constraint by peak demand to avoid high markups being exchanged (Sect. H.1); 2), endogenous prefactors for all
 1599 quantities from last-iteration DIETER to current-iteration REMIND (Sect. H.2).

1600 **H.1 Dispatchable capacity constraints by peak demand**

1601 **H.1.1 Description of the capacity constraint and price manipulation in DIETER post-processing**

1602 Scarcity hour price can occur in a PSM run, which is the highest hourly price in a year, and it is usually equal to the annuitized
 1603 fixed cost of Open Cycle Gas Turbine (OCGT) (capital investment cost and fixed O&M costs) (Hirth and Ueckerdt, 2013). In
 1604 our simulations, the scarcity prices are usually above 50\$/KWh. If we include the scarcity price into the markups, OCGT will
 1605 receive an annual markup usually more than 5 times higher than the annual average electricity price. The high markup results in
 1606 OCGT plants receiving too high an incentive in the next iteration REMIND, and the model overshoots (overinvests) in
 1607 capacities. Over iterations, this causes oscillations in the quantity and prices in the coupled model. For better numerical stability,
 1608 instead of passing on the full markups from DIETER, we only pass on the portion of the annual markups unrelated to scarcity
 1609 hour prices, and replace the exchange of the part of the markup due to scarcity hours from DIETER to REMIND with
 1610 implementing an additional capacity constraint in REMIND for coupled runs. The two actions can be later shown to be
 1611 mathematically equivalent. Generators other than OCGT which produce at the scarcity hours also get paid in the hour at this
 1612 high price. However, because they also produce at other hours with lower prices, their average market values are only
 1613 moderately impacted by the scarcity hour price, and do not in general lead to instability issues.



1614 Below, we first introduce the aforementioned capacity constraint implemented on the side of REMIND, then discuss the
 1615 corresponding manipulation of the markups in DIETER. Lastly, we show their mathematical equivalence, and state the modified
 1616 ZPR of coupled REMIND due to these actions.

1617 The extra capacity constraint states that the sum of all dispatchable capacities needs to be at least as large as the peak residual
 1618 demand:

$$1619 \quad (c7) \sum_{dis} P_{y,dis} > d_{y,residual} \perp v_{y,dis},$$

1620 where $d_{y,residual}$ is peak residual demand in REMIND and is semi-endogenous. $d_{y,residual}$ is a function of the peak hourly
 1621 residual demand in the last iteration of DIETER $\underline{d}_{residual}(y, i - 1)$. The peak hourly residual demand in DIETER is in turn
 1622 defined as the maximum hourly amount of inflexible demand not met by wind, solar or hydro generations, and hence must
 1623 be met by dispatchable generations (under no storage conditions):

$$1624 \quad \underline{d}_{residual} = \max_h (\underline{d}_h - \underline{G}_{h,Solar} - \underline{G}_{h,Wind} - \underline{G}_{h,Hydro}). \quad (H1)$$

1625 $v_{y,dis}$ is the shadow price of the capacity constraint for dispatchable technology dis .

1626 For the exact implementation of (c7) in coupled run, see Sect. 3.3.2, 2. Under storage implementation, in addition to the
 1627 variable renewable contribution, the hourly storage discharge is also subtracted from the residual demand.

1628 Simultaneous to implementing this capacity constraint, we remove the surplus scarcity prices in post-processing of DIETER
 1629 before passing it onto REMIND. In DIETER, we define the scarcity price as the maximum hourly price in a year:

$$1630 \quad \underline{\lambda}_{y,h_{scar}} = \max_h (\underline{\lambda}_{y,h}), \quad (H2)$$

1631 and the surplus scarcity hour price is the difference between the scarcity price and the second highest price:

$$1632 \quad \underline{\lambda}_{y,surplus} = \underline{\lambda}_{y,h_{scar}} - \max (\underline{\lambda}_{y,h|h \neq h_{scar}}) = \max_h (\underline{\lambda}_{y,h}) - \max (\underline{\lambda}_{y,h|h \neq h_{scar}}), \quad (H3)$$

1633 where h_{scar} is the scarcity hour when scarcity price occurs, corresponding to the peak residual demand hour.

1634 Using this, we manipulate the market value and annual average electricity price in DIETER ex post, excluding the surplus
 1635 scarcity hour price:

$$1636 \quad \underline{MV}'_s = \frac{\sum_{h|h \neq h_{scar}} \underline{G}_{h,s} \underline{\lambda}_h + \sum_{h|h_{scar}} \underline{G}_{h,s} * \max (\underline{\lambda}_{h|h \neq h_{scar}})}{\sum_{h=1}^{8760} \underline{G}_{h,s}}, \quad (H4)$$

$$1637 \quad \underline{J}' = \frac{\sum_{h|h \neq h_{scar}} \underline{d}_h \underline{\lambda}_h + \sum_{h|h_{scar}} \underline{d}_h * \max (\underline{\lambda}_{h|h \neq h_{scar}})}{\sum_{h=1}^{8760} \underline{d}_h}, \quad (H5)$$

1638 where \underline{MV}'_s is the annual average market value without the surplus scarcity hour price, and \underline{J}' is the annual average electricity
 1639 price without the surplus scarcity hour price. Thus, the corresponding modified markup term without the surplus scarcity hour
 1640 price is:

$$1641 \quad \underline{\eta}'_s = \underline{MV}'_s - \underline{J}'. \quad (H6)$$

1642 Note that since the above manipulation is done in a post-processing step, the LCOE in DIETER is still fully covered by MV, as
 1643 the KKT conditions and ZPRs still hold by default in an optimized DIETER model.

1644 With the implementation of (c7), the coupled ZPR (Eq. (G1)) is then further modified to include the new shadow price $v_{y,s}$ as
 1645 well as the modified markup $\underline{\eta}'_{y,s}$ (without surplus scarcity price). (We write from now on $v_{y,dis}$ simply as $v_{y,s}$.) Then,

1646 technology-specific ZPR of coupled REMIND is:

$$1647 \quad \frac{\sum_y (G_{y,s} P_{y,s} + o_{y,s} G_{y,s})}{\sum_y G_{y,s}} + \frac{\sum_y (G_{y,s} P_{y,s} + o_{y,s} G_{y,s}) \alpha_{y,s}}{\sum_y G_{y,s} (1 - \alpha_{y,s})} = - \frac{\sum_y (\omega_{y,s} - \sigma_{y,s} + \gamma_{y,s} + v_{y,s}) P_{y,s}}{\sum_y G_{y,s} (1 - \alpha_{y,s})} + \frac{\sum_y (\lambda_y + \underline{\eta}'_{y,s}) G_{y,s} (1 - \alpha_{y,s})}{\sum_y G_{y,s} (1 - \alpha_{y,s})} \quad (H7)$$

Pre-curtailment LCOE_s Curtailment LCOE_s Capacity shadow price_s Market Value_s

1648 System ZPR of coupled REMIND is:



$$1649 \quad \frac{\sum_{y,s}(c_{y,s}P_{y,s}+o_{y,s}G_{y,s})}{\sum_{y,s}G_{y,s}} + \frac{\sum_{y,s}(c_{y,s}P_{y,s}+o_{y,s}G_{y,s})\alpha_{y,s}}{\sum_{y,s}G_{y,s}(1-\alpha_{y,s})} = - \frac{\sum_{y,s}(\omega_{y,s}-\sigma_{y,s}+\gamma_{y,s}+\nu_{y,s})P_{y,s}}{\sum_{y,s}G_{y,s}(1-\alpha_{y,s})} + \frac{\sum_{y,s}(\lambda_y+\eta'_{y,s})G_{y,s}(1-\alpha_{y,s})}{\sum_{y,s}G_{y,s}(1-\alpha_{y,s})} \quad (H8)$$

Pre-curtailment LCOE_{system}
Curtailment cost_{system}
Capacity shadow price_{system}
Electricity Price_{system}

1650 These are the ZPRs of the coupled REMIND for the full version.

1651 H.1.2 Equivalence between surplus scarcity price in DIETER and capacity shadow price due to peak residual demand in 1652 REMIND

1653 Because of the intuitive relation between the scarcity price and the peak residual demand – i.e., that scarcity price occurs in the
1654 hour with peak hourly residual demand due to the pricing power of the peaker gas turbines in the hour where VRE is most
1655 scarce, we can draw a quantitative equivalence between the scarcity price contribution to the markup and the capacity constraint
1656 shadow price v_y . This means that the revenue the plant receives in scarcity hour in capacity terms (i.e. capacity credit), can be
1657 transformed directly to a revenue in energy terms (i.e. a part of the annual market value). At convergence, for any given year y ,
1658 the negative shadow price, $-v_{y,dis}$, when translated into annual generation terms via capacity factor $\phi_{y,s}$ of dispatchable
1659 technology s , should be equal to the scarcity hour surplus revenue divided by annual generation by s in DIETER:

$$1660 \quad \frac{-v_{y,dis}}{\phi_{y,dis} * 8760} = \frac{\lambda_{y,surplus} \underline{G}_{h,scar,dis}}{\sum_h \underline{G}_{y,h,dis}} \quad (H9)$$

1661 In practice, this equivalence is confirmed by numerical results (e.g. Fig. 8 subplot for OCGT).

1662 Using this equivalence, we can show as follows, that at convergence, λ_y should be equal to DIETER power price without
1663 surplus scarcity price J' (Eq. (H5)), and $\lambda_y + \eta'_{y,s}$ should be equal to DIETER market value without scarcity price MV' (Eq.
1664 (H4)).

1665 At convergence, the annual generations have identical solutions in the two models, i.e. $\sum_h \underline{G}_{y,h,s} = G_{y,s}(1 - \alpha_{y,s})$. We plug this
1666 and REMIND capacity factor $\phi_{y,s} = \frac{G_{y,s}(1-\alpha_{y,s})}{P_{y,s} * 8760}$ into Eq. (H9) to obtain

$$1667 \quad v_{y,s} P_{y,s} = \lambda_{y,surplus} \underline{G}_{y,h,scar,s} \quad (H10)$$

1668 Take Eq. (H7), and only consider REMIND annual revenue by multiplying generation $\sum_y G_{y,s}(1 - \alpha_{y,s})$ then on the right-
1669 hand-side, take both revenue and the capacity shadow revenue contribution from $v_{y,s}$ for a single year, which is equal to the total
1670 single-year REMIND revenue:

$$1671 \quad \Theta_{y,s} = - \frac{v_{y,s} P_{y,s}}{\text{Capacity shadow revenue from } c(7)_s} + \frac{(\lambda_y + \eta'_{y,s}) G_{y,s}(1 - \alpha_{y,s})}{\text{Generation revenue}'_s}$$

1672 and plug in (H10), (H6),

$$1673 \quad \Theta_{y,s} = \frac{\lambda_{y,surplus} \underline{G}_{y,h,scar,s}}{\text{surplus scarcity revenue in scarcity hours}_s} + \frac{(MV'_{y,s} - J'_y + \lambda_y) G_{y,s}(1 - \alpha_{y,s})}{\text{Generation revenue}'_s}$$

1674 Plugging in (H4),

$$1675 \quad \Theta_{y,s} = \lambda_{y,surplus} \underline{G}_{y,h,scar,s} + \sum_{h \neq h_{scar}} \underline{G}_{y,h,s} \lambda_{y,h} + \underline{G}_{y,h,scar,s} * \max(\lambda_{y,h} | h \neq h_{scar}) - J'_y G_{y,s}(1 - \alpha_{y,s}) + \lambda_y G_{y,s}(1 - \alpha_{y,s})$$

1676 Lastly, plug in the definition for $\lambda_{y,surplus}$ (Eq. (H3)),

$$1677 \quad \Theta_{y,s} = \sum_h \lambda_{y,h} \underline{G}_{y,h,s} - J'_y G_{y,s}(1 - \alpha_{y,s}) + \lambda_y G_{y,s}(1 - \alpha_{y,s}) \quad (H11)$$

1678 Since the single-year revenue $\Theta_{y,s}$ in REMIND should be aligned with DIETER due to harmonization condition (h3), and the

1679 DIETER revenue is $\Theta_{y,s} = \sum_h \lambda_{y,h} \underline{G}_{y,h,s}$, that means the last two terms in (H11) should sum to 0. Therefore REMIND

1680 electricity price λ_y should be equal to J'_y .



1681 H.2 Stabilization techniques using prefactors

1682 In this Appendix, we describe the detailed implementations of prefactors for information exchanged from DIETER to REMIND.

1683 1. Markup prefactor:

1684 In order to facilitate convergence in REMIND, we implement an endogenous prefactor $f_{y,s}^\eta$ for MV in the REMIND
 1685 markup equation Eq. (5):

$$1686 \eta_{y,s}(i) = f_{y,s}^\eta(i) * \underline{MV}'_{y,s}(i-1) - \underline{J}'_y(i-1). \quad (H12)$$

1687 The endogenous prefactor $f_{y,s}^\eta$ is dependent on the difference between in-iteration endogenous generation share and last-
 1688 iteration DIETER generation share:

$$1689 f_{y,s}^\eta(i) = 1 - \underline{b}_{y,s}(i-1)\Delta S_{y,s}, \quad (H13)$$

1690 where $\underline{b}_{y,s}$ is a positive parameter, equal to the ratio between market values and average price depending on their
 1691 relationship in the last iteration DIETER,

$$1692 \underline{b}_{y,s} = \frac{\underline{MV}'_{y,s}}{\underline{J}'_y} \text{ if } \underline{MV}'_{y,s} > \underline{J}'_y,$$

$$1693 \underline{b}_{y,s} = \frac{\underline{J}'_y}{\underline{MV}'_{y,s}} \text{ if } \underline{MV}'_{y,s} < \underline{J}'_y,$$

1694 and where the generation share difference across models and consecutive iteration $\Delta S_{y,s}$ is,

$$1695 \Delta S_{y,s} = \frac{G_{y,s}(i)(1-\alpha_{y,s}(i))}{\sum_s G_{y,s}(i)(1-\alpha_{y,s}(i))} - \frac{\sum_h G_{y,s}(i-1)}{\sum_h G_{y,s}(i-1)}.$$

1696 The values of $\underline{b}_{y,s}$ are heuristically determined (see Sect. 6.2).

1697 When in-iteration REMIND solar generation share increases due to the price signal from the last-iteration DIETER market
 1698 value, such that the REMIND share is larger than in the last DIETER iteration, the formula Eq. (H13) results in a prefactor
 1699 smaller than one, decreasing in-iteration markup $\eta_{y,s}(i)$.

1700 2. Peak demand prefactor:

1701 The peak demand in REMIND $d_{residual,y}$ depends on the last iteration DIETER peak hourly residual demand

1702 $\underline{d}_{residual}(y, i-1)$. Implementing it in constraint (c7),

$$1703 \sum_{dis} P_{y,dis} < d_{residual,y} * f_y^{d_{residual}}(i),$$

1704 for iteration i , we use $f_y^{d_{residual}}(i)$ as a prefactor for stabilization,

$$1705 f_y^{d_{residual}}(i) = 1 - b_{y,peak} * \Delta S_{y,wind}.$$

1706 $b_{y,peak}$ is a heuristic constant dependent on y , $\Delta S_{y,wind}$ is the wind generation share. We use the wind generation share in
 1707 the current iteration of REMIND for stabilization, because in the peak residual demand hour, there usually is some wind
 1708 production for the historical year we chose (but no solar). In general, $b_{y,peak}$ is 0.5 for earlier years, and increasing to 1 for
 1709 later years, under a baseline scenario. For climate scenarios, $b_{y,peak}$ is around 1.5 for less stringent scenarios, and for more
 1710 stringent scenarios, it is 0.5 for earlier years, and increasing to 3 for later years.

1711 3. Capacity factor prefactor:

1712 We set REMIND capacity factor $\phi_{y,dis}$ to be equal to the DIETER annual average capacity factor from the last iteration
 1713 multiplied by a prefactor:

$$1714 \phi_{y,dis}(i) = \underline{\phi}_{dis}(y, i-1) * f_{y,s}^{\phi_{dis}}(i),$$



1715 where DIETER annual average capacity factor is $\phi_{dis} = \frac{\sum_h G_{h,dis}}{P_{dis} * 8760}$ for each year y . In order to facilitate convergence, a

1716 similar prefactor $f_{y,s}^{\phi_{dis}}$ as in Eq. (H13) is implemented:

1717 $f_{y,s}^{\phi_{dis}}(i) = 1 - 0.5\Delta S_{y,s}$ if $\phi_{dis}(y, i - 1) < 0.5$ (i.e. the plant is “peaker” or “mid-load” type in the last iteration),

1718 $f_{y,s}^{\phi_{dis}}(i) = 1 + 0.5\Delta S_{y,s}$ if $\phi_{dis}(y, i - 1) \geq 0.5$ (i.e. the plant is “base-load” type in the last iteration),

1719 where 0.5 is a heuristic factor.

1720 The sign in the prefactor formula is determined based on the observation that under a system with variable renewable
 1721 generations, for generator plants that have relatively high running cost and low investment cost, i.e. they are most
 1722 economically operated as “peaker” plants or as “mid-load” plants of lower capacity factor, so when their generation share
 1723 incrementally increases, their capacity factor decreases. Conversely, for generators with relatively low running cost and
 1724 high investment cost, i.e. they are most economically operated as “base-load” plants, when their generation share
 1725 incrementally increases, their capacity factor increases.

1726 4. Curtailment prefactor:

1727 The curtailment ratio in REMIND $\alpha_{y,vre}$ is equal to last iteration DIETER curtailment ratio, multiplied by prefactor $f_{y,vre}^{\alpha}$:

$$1728 \alpha_{y,vre}(i) = \frac{\sum_h \underline{y}_{h,vre}(y,i-1)}{\sum_{h,s} \underline{G}_{h,vre}(y,i-1)} * f_{y,vre}^{\alpha}(i),$$

1729 where the prefactor is $f_{y,vre}^{\alpha}(i) = 1 + \Delta S_{y,vre}$.

1730 5. Capture price prefactor:

1731 Similar to the case of markup from the demand side, the markup for any demand-side technology given to REMIND is:

$$1732 \eta_{y,s_d}(i) = f_{y,s_d}^{\eta}(i) * \underline{C}_{P_{y,s_d}}(i - 1) - J_y(i - 1),$$

1733 where J_y is the annual average electricity price of all demand types s_d for period y ,

$$1734 \underline{J} = \frac{\sum_h (\sum_{s_d} \underline{d}_{h,s_d}) * \underline{\Delta}h}{\sum_{h,s_d} \underline{d}_{h,s_d}},$$

1735 and $f_{y,s_d}^{\eta}(i)$ is an endogenous stabilization prefactor for the flexible-demand markup based on shares of demand by s_d in
 1736 total demand for each year.

1737 Appendix I: Derivation for equilibrium condition for REMIND in the case of additional adjustment cost

1738 Adjustment cost – an additional linear term in the objective function, acts as an inertia against fast or slow capacity additions or
 1739 retirement. The implementation of positive adjustment costs mimics the challenges of scaling up the supply chains and of
 1740 training new workers to do installation and construction. Adjustment costs are applied to all model time periods, so it is by
 1741 nature intertemporal. The objective function for power sector including the adjustment cost $\Xi_{y,s}$ is

$$1742 Z = \sum_{y,s} (c_{y,s} P_{y,s} + o_{y,s} G_{y,s} + \Xi_{y,s}),$$

1743 where $\Xi_{y,s}$ is a quadratic function of the difference between capacity additions of subsequent time periods $y - \Delta y$ and y :

$$1744 \Xi_{y,s} = c_{y,s} k_s \left(\frac{\Delta P_{y,s} - \Delta P_{y-\Delta y,s}}{\Delta y} \right)^2 / \left(\frac{\Delta P_{y-\Delta y,s}}{\Delta y} + \beta_{y,s} \right),$$

1745 where $\Delta P_{y,s}$ is as before the capacity addition during time period y of technology s , $\beta_{y,s}$ is an offset parameter to offset additions
 1746 in initial time periods, k_s is a regional technological coefficient, $c_{y,s}$ is the capital expenditure cost per capacity unit as before.

1747 Because the adjustment cost is a quadratic function of the endogenous variable $P_{y,s}$, it turns the power sector cost minimization
 1748 in REMIND into a nonlinear problem.



1749 Similar to the case without adjustment costs in Sect. 3.2.3, the first stationary condition becomes:

$$1750 \frac{\partial \mathcal{L}}{\partial P_{y,s}} = 0, \Rightarrow c_{y,s} + \omega_{y,s} - \mu_{y,s} \phi_{y,s} - \sigma_{y,s} + \gamma_{y,s} + 2c_{y,s} k_s \frac{\Delta P_{y,s} - \Delta P_{y-\Delta y,s}}{(\Delta P_{y-\Delta y,s} + \beta_{y,s}) \Delta y^2} = 0,$$

1751 simplifying,

$$1752 c_{y,s} = -\omega_{y,s} + \mu_{y,s} \phi_{y,s} + \sigma_{y,s} - \gamma_{y,s} - a_{y,s} c_{y,s},$$

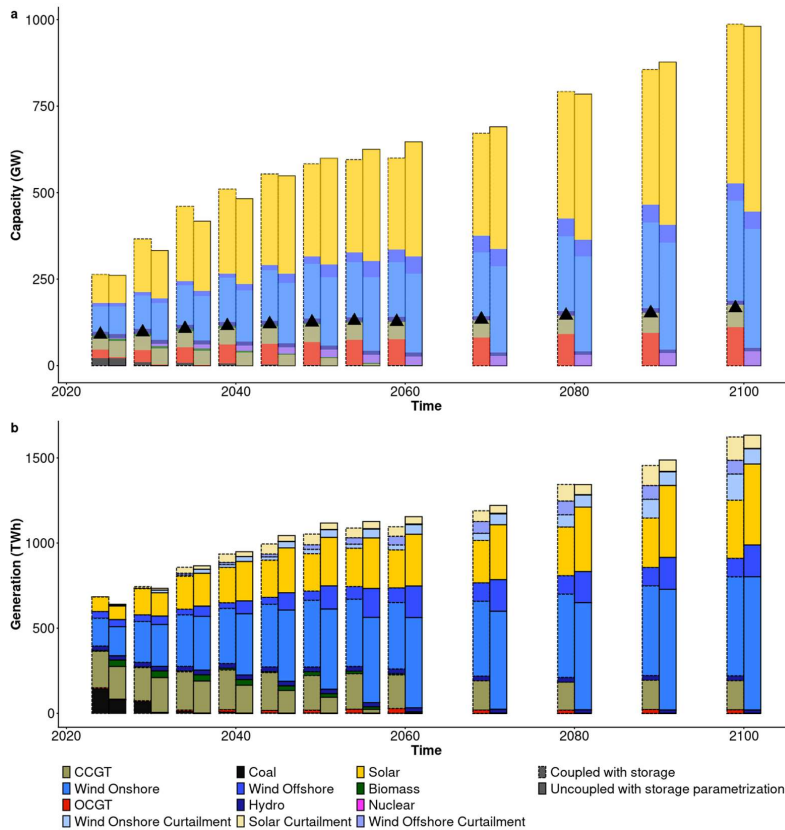
1753 where $a_{y,s} = 2k_s \frac{\Delta P_{y,s} - \Delta P_{y-\Delta y,s}}{(\Delta P_{y-\Delta y,s} + \beta_{y,s}) \Delta y^2}$ is the endogenous adjustment factor of investment, and is a function of capacity.

1754 The new ZPR including the adjustment cost in terms of cost and revenue for technology s , can be derived

$$1755 \sum_y [(c_{y,s} + a_{y,s} c_{y,s}) P_{y,s} + o_{y,s} G_{y,s} + \lambda_y \alpha_{y,s} G_{y,s} + (\omega_{y,s} - \sigma_{y,s} + \gamma_{y,s}) P_{y,s}] = \sum_y (\lambda_y G_{y,s}).$$

1756 The adjustment cost $a_{y,s} c_{y,s}$ can act as a disincentive or an incentive to capacity additions. If capacity addition in the current
 1757 period is higher than in the last period $\Delta P_{y,s} > \Delta P_{y-\Delta y,s}$, i.e. a ramp-up case of capacity addition, the adjustment cost is positive
 1758 and acts as a disincentive, so the ramp-up speed is slower. When added capacities are decreasing with time, i.e. a ramp-down
 1759 case of capacity addition, adjustment cost is negative and acts as an incentive, and as a result, the ramp-down speed is slower.
 1760 In the coupled run we see only a moderate adjustment cost which drops down fast as a function of time (see e.g. Fig.6).

1761 **Appendix J: Comparing the coupled and uncoupled run**



1762



1763 **Figure J1: Under the 2C global scenario (no German net-zero goal), we compare (a) the capacity mix and (b) the**
 1764 **generation mix of Germany for the DIETER-coupled version of REMIND with endogenous storage (dashed bar) and for**
 1765 **the uncoupled version of REMIND with parametrized storage (solid bar). In (a), triangle dots indicate the peak residual**
 1766 **demand of the year as determined in DIETER.**

1767 **Appendix K: Complete list of mathematical symbols**

1768 The units used in the two models are usually different. Here we uniformly use MWh for energy units, and MW for capacity
 1769 units. In the main text, underscore $_$ is used to denote DIETER parameters and variables. An apostrophe is used to indicate a
 1770 modified version of the variable. An asterisk is used to indicate the values of variables at the optimum of objective functions.

Symbol	Description	Unit	Symbol	Description	Unit
$y, \Delta y$	REMIND time period, REMIND time step	-	h	Hour	-
s	Supply-side technology type	-	dis, vre	Dispatchable generators, Variable Renewable	-
s_d	Demand-side technology type	-	i	Iteration	-
reg	Region	-	\mathcal{L}	Lagrangian	\$
Z	Objective function	\$	G	Generation	MWh
c	Fixed cost	\$/MW	ψ	Total annual renewable potential	MWh
o	Variable cost	\$/MWh	ϕ	Capacity factor	1
α	Annual curtailment to pre-curtailment generation ratio in REMIND model	1	d	Exogenous demand	MWh
P	Capacity	MW	p	Standing capacity in REMIND	MW
Γ	Curtailment	MWh	η	Markup	\$/MWh
λ	Shadow price of power supply-demand balance equation / power price	\$/MWh	MV	Market value	\$/MWh
q	Near-term ramp up constraint for capacities in REMIND	MW	θ	revenue	\$
M	Difference in total revenues in the two models	\$	ξ	Shadow price due to positive generation	\$/MWh



ω	Shadow price due to limited renewable potential	\$/MW	γ	Shadow price due to near-term ramp up constraint	\$/MW
μ	Shadow price due to limit on generation from capacity	\$/MWh	ζ	DIETER shadow price due to standing capacity constraint from REMIND	\$/MW
σ	Shadow price due to standing capacities in REMIND	\$/MW	CP	Capture price of demand-side technologies	\$/MWh
ν	Shadow price due to peak residual demand constraint	\$/MWh	ΔS	Difference in generation shares between models	1
f	Prefactor for numeric stabilization	1	W	Economic welfare	-
b, b_{peak}	Multiplicative prefactors parameter	1	ρ	Pure rate of time preference	1
ε	Adjustment cost	\$	β	Offset parameters in adjustment cost	\$
χ	Consumption	\$	a	Adjustment factor of investment	1
V	Population	1	k	Regional technological coefficient for adjustment cost	1
ER	Early retirement rate in REMIND	1	J	Annual average DIETER electricity price	\$/MWh

1771 **Table K1: Complete list of mathematical symbols. For simplicity, in general, we only list the symbols, not their indices or**
 1772 **in which model they are used.**

1773 **Appendix L: Complete list of abbreviations**

Abbreviation	Description	Abbreviation	Description
IAM	Integrated assessment model	LCOE	Levelized cost of electricity
PSM	Power sector model	MV	Market value
VRE	Variable renewable	O&M	Operation and maintenance
GHG	Greenhouse gas	OMF	Operation and maintenance fixed cost
NLP	Nonlinear programming	OMV	Operation and maintenance variable cost
LP	Linear programming	OCGT	Open cycle gas turbine



CES	Constant elasticity of substitution	CCGT	Combined cycle gas turbine
IPCC	Intergovernmental Panel on Climate Change	CP	Capture price
RLDC	Residual load duration curve	PtG	Power-to-Gas
ZPR	Zero-profit rule	PDC	Price duration curves
KKT	Karush–Kuhn–Tucker	CCS	Carbon capture and storage
EV	Electric Vehicles	GAMS	General Algebraic Modeling System

1774 **Table L1: Complete list of abbreviations.**

1775

1776 **Code and data availability:** The coupled and uncoupled REMIND code are implemented in GAMS, and the code and data
 1777 management is done using R. The coupled and the uncoupled DIETER are entirely implemented in GAMS. The default
 1778 uncoupled REMIND v3.0.0 code is available from the GitHub website: <https://github.com/remindmodel/remind> (last access: 1
 1779 September 2022), and is archived on Zenodo under the GNU Affero General Public License, version 3 (AGPLv3) (Luderer et
 1780 al., 2022b). The technical model documentation is available under <https://rse.pik-potsdam.de/doc/remind/3.0.0/> (last access: 1
 1781 September 2022). The coupled version of REMIND is available from [https://github.com/cchrisgong/remind-coupling-
 1782 dieter/tree/couple](https://github.com/cchrisgong/remind-coupling-dieter/tree/couple) (last access: 2 September 2022); coupled DIETER is available from: [https://github.com/cchrisgong/dieter-
 1783 coupling-remind](https://github.com/cchrisgong/dieter-coupling-remind) (last access: 2 September 2022). The two sets of coupling codes are archived at Zenodo under Creative
 1784 Commons Attribution 4.0 International License (Luderer et al., 2022c). The GAMS code, results, and scripts to produce the
 1785 figures shown in this paper are archived at Zenodo (Gong, 2022).

1786 **Author contribution:** Methodology development was done by CG, FU, and RP. CG designed and carried out the numerical
 1787 implementation, and performed theoretical analysis of the methodology. The methodology was first conceptualized by GL.
 1788 Supervision and funding acquisition were carried out by FU and GL. OA participated in development of model post-processing
 1789 and the overall structuring of the manuscript. MK and WPS performed theoretical and conceptual validation of the manuscript.
 1790 CG prepared the manuscript with contributions from all co-authors.

1791 **Competing interests:** The authors declare that they have no conflict of interest.

1792 **Acknowledgement:** The authors thank Professor Dr. Tom Brown at The Technical University of Berlin, and Dr. Marian
 1793 Leimbach, Dr. Renato Rodrigues, Dr. Nico Bauer at the Potsdam Institute for Climate Impact Research for discussion. We
 1794 gratefully received financial support by the German Federal Ministry of Education and Research (BMBF) via the project
 1795 Kopernikus-Ariadne (FKZ 03SFK5N0, FKZ 03SFK5A) and via the INTEGRATE project (FKZ 01LP1928A). We also received
 1796 financial support from the German Federal Environmental Foundation (Deutsche Bundesstiftung Umwelt).

1797 **References**

1798 Alimou, Y., Maïzi, N., Bourmaud, J.-Y., and Li, M.: Assessing the security of electricity supply through multi-scale modeling:
 1799 The TIMES-ANTARES linking approach, *Appl. Energy*, 279, 115717, <https://doi.org/10.1016/j.apenergy.2020.115717>, 2020.
 1800 Data Platform – Open Power System Data: https://data.open-power-system-data.org/renewable_power_plants/2017-02-16, last
 1801 access: 22 January 2022.



- 1802 openmod - Open Energy Modelling Initiative: <https://openmod-initiative.org/>, last access: 21 January 2022.
- 1803 Release REMIND v3.0.0 · remindmodel/remind: <https://github.com/remindmodel/remind/releases/tag/v3.0.0>, last access: 11
- 1804 August 2022.
- 1805 Aryanpur, V., O’Gallachoir, B., Dai, H., Chen, W., and Glynn, J.: A review of spatial resolution and regionalisation in national-
- 1806 scale energy systems optimisation models, *Energy Strategy Rev.*, 37, 100702, <https://doi.org/10.1016/j.esr.2021.100702>, 2021.
- 1807 Azevedo, I., Bataille, C., Bistline, J., Clarke, L., and Davis, S.: Net-zero emissions energy systems: What we know and do not
- 1808 know, *Energy Clim. Change*, 2, 100049, <https://doi.org/10.1016/j.egycc.2021.100049>, 2021.
- 1809 Bauer, N., Calvin, K., Emmerling, J., Fricko, O., Fujimori, S., Hilaire, J., Eom, J., Krey, V., Kriegler, E., Mouratiadou, I., Sytze
- 1810 de Boer, H., van den Berg, M., Carrara, S., Daioglou, V., Drouet, L., Edmonds, J. E., Gernaat, D., Havlik, P., Johnson, N.,
- 1811 Klein, D., Kyle, P., Marangoni, G., Masui, T., Pietzcker, R. C., Strubegger, M., Wise, M., Riahi, K., and van Vuuren, D. P.:
- 1812 Shared Socio-Economic Pathways of the Energy Sector – Quantifying the Narratives, *Glob. Environ. Change*, 42, 316–330,
- 1813 <https://doi.org/10.1016/j.gloenvcha.2016.07.006>, 2017.
- 1814 Baumstark, L., Bauer, N., Benke, F., Bertram, C., Bi, S., Gong, C. C., Dietrich, J. P., Dirmaichner, A., Giannousakis, A., Hilaire,
- 1815 J., Klein, D., Koch, J., Leimbach, M., Levesque, A., Madeddu, S., Malik, A., Merfort, A., Merfort, L., Odenweller, A., Pehl, M.,
- 1816 Pietzcker, R. C., Piontek, F., Rauner, S., Rodrigues, R., Rottoli, M., Schreyer, F., Schultes, A., Soergel, B., Soergel, D., Streifer,
- 1817 J., Ueckerdt, F., Kriegler, E., and Luderer, G.: REMIND2.1: Transformation and innovation dynamics of the energy-economic
- 1818 system within climate and sustainability limits, *Geosci. Model Dev. Discuss.*, 1–50, <https://doi.org/10.5194/gmd-2021-85>, 2021.
- 1819 Bhaskar, A., Assadi, M., and Nikpey Somehsaraei, H.: Decarbonization of the Iron and Steel Industry with Direct Reduction of
- 1820 Iron Ore with Green Hydrogen, *Energies*, 13, 758, <https://doi.org/10.3390/en13030758>, 2020.
- 1821 Bistline, J. E. T.: The importance of temporal resolution in modeling deep decarbonization of the electric power sector, *Environ.*
- 1822 *Res. Lett.*, 16, 084005, <https://doi.org/10.1088/1748-9326/ac10df>, 2021.
- 1823 Blanford, G. J. and Weissbart, C.: A Framework for Modeling the Dynamics of Power Markets – The EU-REGEN Model, ifo
- 1824 Working Paper Series, ifo Institute - Leibniz Institute for Economic Research at the University of Munich, 2019.
- 1825 Böttger, D. and Härtel, P.: On wholesale electricity prices and market values in a carbon-neutral energy system, *Energy Econ.*,
- 1826 106, 105709, <https://doi.org/10.1016/j.eneco.2021.105709>, 2022.
- 1827 Brinkerink, M.: Assessing 1.5-2°C scenarios of integrated assessment models from a power system perspective - Linkage with a
- 1828 detailed hourly global electricity model, Monograph, IIASA, Laxenburg, Austria, 2020.
- 1829 Brown, T. and Reichenberg, L.: Decreasing market value of variable renewables can be avoided by policy action, *Energy Econ.*,
- 1830 100, 105354, <https://doi.org/10.1016/j.eneco.2021.105354>, 2021.
- 1831 Brown, T., Hörsch, J., and Schlachtberger, D.: PyPSA: Python for Power System Analysis, *J. Open Res. Softw.*, 6, 4,
- 1832 <https://doi.org/10.5334/jors.188>, 2018a.
- 1833 Brown, T., Schlachtberger, D., Kies, A., Schramm, S., and Greiner, M.: Synergies of sector coupling and transmission
- 1834 reinforcement in a cost-optimised, highly renewable European energy system, *Energy*, 160, 720–739,
- 1835 <https://doi.org/10.1016/j.energy.2018.06.222>, 2018b.
- 1836 Brunner, C., Deac, G., Braun, S., and Zöphel, C.: The future need for flexibility and the impact of fluctuating renewable power
- 1837 generation, *Renew. Energy*, 149, 1314–1324, <https://doi.org/10.1016/j.renene.2019.10.128>, 2020.
- 1838 Butnar, I., Li, P.-H., Strachan, N., Portugal Pereira, J., Gambhir, A., and Smith, P.: A deep dive into the modelling assumptions
- 1839 for biomass with carbon capture and storage (BECCS): A transparency exercise., *Environ. Res. Lett.*,
- 1840 <https://doi.org/10.1088/1748-9326/ab5c3e>, 2019.
- 1841 Calvin, K., Bond-Lamberty, B., Clarke, L., Edmonds, J., Eom, J., Hartin, C., Kim, S., Kyle, P., Link, R., Moss, R., McJeon, H.,



- 1842 Patel, P., Smith, S., Waldhoff, S., and Wise, M.: The SSP4: A world of deepening inequality, *Glob. Environ. Change*, 42, 284–
1843 296, <https://doi.org/10.1016/j.gloenvcha.2016.06.010>, 2017.
- 1844 Chang, M., Thellufsen, J. Z., Zakeri, B., Pickering, B., Pfenninger, S., Lund, H., and Østergaard, P. A.: Trends in tools and
1845 approaches for modelling the energy transition, *Appl. Energy*, 290, 116731, <https://doi.org/10.1016/j.apenergy.2021.116731>,
1846 2021.
- 1847 Cherp, A., Vinichenko, V., Tosun, J., Gordon, J. A., and Jewell, J.: National growth dynamics of wind and solar power
1848 compared to the growth required for global climate targets, *Nat. Energy*, 6, 742–754, [https://doi.org/10.1038/s41560-021-00863-](https://doi.org/10.1038/s41560-021-00863-0)
1849 0, 2021.
- 1850 Clarke, L., Wei, Y.-M., De La Vega Navarro, A., Garg, A., Hahmann, A. N., Khennas, S., Azevedo, I. M. L., Löschel, A.,
1851 Singh, A. K., Steg, L., Strbac, G., and Wada, K.: Energy Systems. In IPCC, 2022: Climate Change 2022: Mitigation of Climate
1852 Change. Contribution of Working Group III to the Sixth Assessment Report of the Intergovernmental Panel on Climate Change,
1853 219, <https://doi.org/doi:10.1017/9781009157926.008>, 2022.
- 1854 Creutzig, F., Agoston, P., Goldschmidt, J. C., Luderer, G., Nemet, G., and Pietzcker, R. C.: The underestimated potential of
1855 solar energy to mitigate climate change, *Nat. Energy*, 2, 17140, <https://doi.org/10.1038/nenergy.2017.140>, 2017.
- 1856 Deane, J. P., Chiodi, A., Gargiulo, M., and Ó Gallachóir, B. P.: Soft-linking of a power systems model to an energy systems
1857 model, *Energy*, 42, 303–312, <https://doi.org/10.1016/j.energy.2012.03.052>, 2012.
- 1858 DIW Berlin: Ampel-Monitor Energiewende Shows the Pace of the Energy Transition Must Be Accelerated Significantly:
1859 National long-term strategies: [https://ec.europa.eu/info/energy-climate-change-environment/implementation-eu-](https://ec.europa.eu/info/energy-climate-change-environment/implementation-eu-countries/energy-and-climate-governance-and-reporting/national-long-term-strategies_en)
1860 [countries/energy-and-climate-governance-and-reporting/national-long-term-strategies_en](https://ec.europa.eu/info/energy-climate-change-environment/implementation-eu-countries/energy-and-climate-governance-and-reporting/national-long-term-strategies_en), last access: 15 January 2022.
- 1861 Figueiredo, N. C. and Silva, P. P. da: The price of wind power generation in Iberia and the merit-order effect, *Int. J. Sustain.*
1862 *Energy Plan. Manag.*, 15, 21–30, <https://doi.org/10.5278/ijsepm.2018.15.4>, 2018.
- 1863 Frysztacki, M. M., Hörsch, J., Hagenmeyer, V., and Brown, T.: The strong effect of network resolution on electricity system
1864 models with high shares of wind and solar, *Appl. Energy*, 291, 116726, <https://doi.org/10.1016/j.apenergy.2021.116726>, 2021.
- 1865 Gaete-Morales, C., Kittel, M., Roth, A., and Schill, W.-P.: DIETERpy: A Python framework for the Dispatch and Investment
1866 Evaluation Tool with Endogenous Renewables, *SoftwareX*, 15, 100784, <https://doi.org/10.1016/j.softx.2021.100784>, 2021.
- 1867 Gan, D., Feng, D., and Xie, J.: *Electricity Markets and Power System Economics*, CRC Press, Boca Raton, 220 pp.,
1868 <https://doi.org/10.1201/b15550>, 2013.
- 1869 Giarola, S., Mittal, S., Vielle, M., Perdana, S., Campagnolo, L., Delpiazzi, E., Bui, H., Kraavi, A. A., Kolpakov, A., Sognnaes,
1870 I., Peters, G., Hawkes, A., Köberle, A. C., Grant, N., Gambhir, A., Nikas, A., Doukas, H., Moreno, J., and van de Ven, D.-J.:
1871 Challenges in the harmonisation of global integrated assessment models: A comprehensive methodology to reduce model
1872 response heterogeneity, *Sci. Total Environ.*, 783, 146861, <https://doi.org/10.1016/j.scitotenv.2021.146861>, 2021.
- 1873 Gils, H. C., Gardian, H., Kittel, M., Schill, W.-P., Zerrahn, A., Murmann, A., Launer, J., Fehler, A., Gaumnitz, F., van
1874 Ouwerkerk, J., Buřar, C., Mikurda, J., Torralba-Díaz, L., Janßen, T., and Krüger, C.: Modeling flexibility in energy systems —
1875 comparison of power sector models based on simplified test cases, *Renew. Sustain. Energy Rev.*, 158, 111995,
1876 <https://doi.org/10.1016/j.rser.2021.111995>, 2022a.
- 1877 Gils, H. C., Gardian, H., Kittel, M., Schill, W.-P., Murmann, A., Launer, J., Gaumnitz, F., van Ouwerkerk, J., Mikurda, J., and
1878 Torralba-Díaz, L.: Model-related outcome differences in power system models with sector coupling—Quantification and
1879 drivers, *Renew. Sustain. Energy Rev.*, 159, 112177, <https://doi.org/10.1016/j.rser.2022.112177>, 2022b.
- 1880 Gong, C. C.: REMIND-DIETER - code, reportings, scripts, <https://doi.org/10.5281/zenodo.7072625>, 2022.
- 1881 Griffiths, S., Sovacool, B. K., Kim, J., Bazilian, M., and Uratani, J. M.: Industrial decarbonization via hydrogen: A critical and



- 1882 systematic review of developments, socio-technical systems and policy options, *Energy Res. Soc. Sci.*, 80, 102208,
1883 <https://doi.org/10.1016/j.erss.2021.102208>, 2021.
- 1884 Guivarch, C., Kriegler, E., Portugal-Pereira, J., and Bosetti, V.: IPCC, 2022: Annex III: Scenarios and modelling methods, In
1885 IPCC, 2022., in: *Climate Change 2022: Mitigation of Climate Change. Contribution of Working Group III to the Sixth*
1886 *Assessment Report of the Intergovernmental Panel on Climate Change*, Cambridge University Press, Cambridge, United
1887 Kingdom and New York, NY, USA, <https://doi.org/10.1017/9781009157926.022>, 2022.
- 1888 Günther, C., Schill, W.-P., and Zerrahn, A.: Prosumage of solar electricity: Tariff design, capacity investments, and power
1889 sector effects, *Energy Policy*, 152, 112168, <https://doi.org/10.1016/j.enpol.2021.112168>, 2021.
- 1890 Haydt, G., Leal, V., Pina, A., and Silva, C. A.: The relevance of the energy resource dynamics in the mid/long-term energy
1891 planning models, *Renew. Energy*, 36, 3068–3074, 2011.
- 1892 Hildmann, M., Ulbig, A., and Andersson, G.: Empirical Analysis of the Merit-Order Effect and the Missing Money Problem in
1893 Power Markets With High RES Shares, *IEEE Trans. Power Syst.*, 30, 1560–1570,
1894 <https://doi.org/10.1109/TPWRS.2015.2412376>, 2015.
- 1895 Hirth, L.: The market value of variable renewables: The effect of solar wind power variability on their relative price, *Energy*
1896 *Econ.*, 38, 218–236, <https://doi.org/10.1016/j.eneco.2013.02.004>, 2013.
- 1897 Hirth, L.: What caused the drop in European electricity prices? A factor decomposition analysis, *Energy J.*, 39,
1898 <https://doi.org/10.5547/01956574.39.1.lhir>, 2018.
- 1899 Hirth, L. and Ueckerdt, F.: Redistribution effects of energy and climate policy: The electricity market, *Energy Policy*, 62, 934–
1900 947, <https://doi.org/10.1016/j.enpol.2013.07.055>, 2013.
- 1901 Huppmann, D., Gidden, M., Fricko, O., Kolp, P., Orthofer, C., Pimmer, M., Kushin, N., Vinca, A., Mastrucci, A., Riahi, K., and
1902 Krey, V.: The MESSAGEix Integrated Assessment Model and the ix modeling platform (ixmp): An open framework for
1903 integrated and cross-cutting analysis of energy, climate, the environment, and sustainable development, *Environ. Model. Softw.*,
1904 112, 143–156, <https://doi.org/10.1016/j.envsoft.2018.11.012>, 2019.
- 1905 ICCSD Tsinghua University: Power Sector, in: *China’s Long-Term Low-Carbon Development Strategies and Pathways:*
1906 *Comprehensive Report*, edited by: Institute of Climate Change and Sustainable Development of Tsinghua University et al.,
1907 Springer, Singapore, 109–130, https://doi.org/10.1007/978-981-16-2524-4_4, 2022.
- 1908 IEA: *World Energy Outlook 2021*, <https://www.iea.org/reports/world-energy-outlook-2021>, 2021.
- 1909 IPCC: *Climate change 2014: mitigation of climate change : Working Group III contribution to the Fifth assessment report of the*
1910 *Intergovernmental Panel on Climate Change*, edited by: Edenhofer, O., Pichs-Madruga, R., Sokona, Y., Farahani, E., Kadner, S.,
1911 Seyboth, K., Alder, A., Baum, I., Brunner, S., Eikemeier, P., Kriemann, B., Salolainen, J., Schlömer, S., Stechow, C. von,
1912 Zwickel, T., and Minx, J. C., Cambridge University Press, Cambridge, United Kingdom and New York, NY, USA, 2014.
- 1913 IRENA: *Renewable power generation costs in 2019*, International Renewable Energy Agency, 2020.
- 1914 Kannan, R. and Turton, H.: A Long-Term Electricity Dispatch Model with the TIMES Framework, *Environ. Model. Assess.*, 18,
1915 325–343, <https://doi.org/10.1007/s10666-012-9346-y>, 2013.
- 1916 Karush, W.: *Minima of functions of several variables with inequalities as side conditions.*, 1939.
- 1917 Keppo, I., Butnar, I., Bauer, N., Caspani, M., Edelenbosch, O., Emmerling, J., Fragkos, P., Guivarch, C., Harmsen, M., Lefèvre,
1918 J., Le Gallic, T., Leimbach, M., McDowall, W., Mercure, J.-F., Schaeffer, R., Trutnevyte, E., and Wagner, F.: Exploring the
1919 possibility space: taking stock of the diverse capabilities and gaps in integrated assessment models, *Environ. Res. Lett.*, 16,
1920 053006, <https://doi.org/10.1088/1748-9326/abe5d8>, 2021.
- 1921 Koch, J. and Leimbach, M.: Update of Ssp GDP Projections: Capturing Recent Changes in National Accounting, PPP



- 1922 Conversion and Covid 19 Impacts, <https://doi.org/10.2139/ssrn.4011838>, 2022.
- 1923 Koutstaal, P. R. and van Hout, M.: Integration costs and market value of variable renewables: A study for the Dutch power
1924 market, 2017.
- 1925 Kuhn, H. W. and Tucker, A. W.: Nonlinear Programming, Proc. Second Berkeley Symp. Math. Stat. Probab., 2, 481–493, 1951.
- 1926 Lazard: Lazard’s Levelized Cost of Energy Analysis - Version 15.0., 2021.
- 1927 Leimbach, M., Bauer, N., Baumstark, L., Luken, M., and Edenhofer, O.: Technological Change and International Trade -
1928 Insights from REMIND-R, *Energy J.*, 31, 109–136, <https://doi.org/10.5547/ISSN0195-6574-EJ-Vol31-NoSI-5>, 2010.
- 1929 Li, P.-H. and Pye, S.: Assessing the benefits of demand-side flexibility in residential and transport sectors from an integrated
1930 energy systems perspective, *Appl. Energy*, 228, 965–979, <https://doi.org/10.1016/j.apenergy.2018.06.153>, 2018.
- 1931 López Prol, J. and Schill, W.-P.: The Economics of Variable Renewable Energy and Electricity Storage, *Annu. Rev. Resour.*
1932 *Econ.*, 13, 443–467, <https://doi.org/10.1146/annurev-resource-101620-081246>, 2021.
- 1933 Luderer, G., Pietzcker, R. C., Carrara, S., de Boer, H. S., Fujimori, S., Johnson, N., Mima, S., and Arent, D.: Assessment of
1934 wind and solar power in global low-carbon energy scenarios: An introduction, *Energy Econ.*, 64, 542–551,
1935 <https://doi.org/10.1016/j.eneco.2017.03.027>, 2017.
- 1936 Luderer, G., Vrontisi, Z., Bertram, C., Edelenbosch, O., Pietzcker, R. C., Rogelj, J., De Boer, H. S., Drouet, L., Emmerling, J.,
1937 Fricko, O., Fujimori, S., Havlik, P., Iyer, G., Keramidas, K., Kitous, A., Pehl, M., Krey, V., Riahi, K., Saveyn, B., Tavoni, M.,
1938 Van Vuuren, D. P., and Kriegler, E.: Residual fossil CO₂ emissions in 1.5–2°C pathways, *Nat. Clim. Change*, 8, 626–633,
1939 <https://doi.org/10.1038/s41558-018-0198-6>, 2018.
- 1940 Luderer, G., Madeddu, S., Merfort, L., Ueckerdt, F., Pehl, M., Pietzcker, R., Rottoli, M., Schreyer, F., Bauer, N., Baumstark, L.,
1941 Bertram, C., Dirnaichner, A., Humpenöder, F., Levesque, A., Popp, A., Rodrigues, R., Strefler, J., and Kriegler, E.: Impact of
1942 declining renewable energy costs on electrification in low-emission scenarios, *Nat. Energy*, 7, 32–42,
1943 <https://doi.org/10.1038/s41560-021-00937-z>, 2022a.
- 1944 Luderer, G., Bauer, N., Baumstark, L., Bertram, C., Leimbach, M., Pietzcker, R., Strefler, J., Aboumahboub, T., Abrahão, G.,
1945 Auer, C., Benke, F., Bi, S., Dietrich, J., Dirnaichner, A., Giannousakis, A., Gong, C. C., Haller, M., Hasse, R., Hilaire, J.,
1946 Hoppe, J., Klein, D., Koch, J., Körner, A., Kowalczyk, K., Kriegler, E., Levesque, A., Lorenz, A., Ludig, S., Lüken, M., Malik,
1947 A., Manger, S., Merfort, A., Merfort, L., Moreno-Leiva, S., Mouratiadou, I., Odenweller, A., Pehl, M., Piontek, F., Popin, L.,
1948 Rauner, S., Richters, O., Rodrigues, R., Roming, N., Rottoli, M., Schmidt, E., Schötz, C., Schreyer, F., Schultes, A., Sörgel, B.,
1949 Ueckerdt, F., Verpoort, P., and Weigmann, P.: REMIND - REgional Model of INvestments and Development, Zenodo,
1950 <https://doi.org/10.5281/zenodo.6794920>, 2022b.
- 1951 Luderer, G., Bauer, N., Gong, C. C., Odenweller, A., Baumstark, L., Bertram, C., Leimbach, M., Pietzcker, R., Strefler, J.,
1952 Aboumahboub, T., Abrahão, G., Auer, C., Benke, F., Bi, S., Dietrich, J., Dirnaichner, A., Giannousakis, A., Haller, M., Hasse,
1953 R., Hilaire, J., Hoppe, J., Klein, D., Koch, J., Kowalczyk, K., Kriegler, E., Levesque, A., Ludig, S., Malik, A., Merfort, A.,
1954 Merfort, L., Moreno, S., Mouratiadou, I., Pehl, M., Piontek, F., Popin, L., Rauner, S., Richters, O., Schötz, C., Rodrigues, R.,
1955 Ueckerdt, F., Zerrahn, A., Schreyer, F., Sörgel, B., Weigmann, P., Schill, W.-P., Verpoort, P., and Rottoli, M.: REMIND -
1956 DIETER coupling, Zenodo, <https://doi.org/10.5281/zenodo.7053246>, 2022c.
- 1957 Ludig, S., Haller, M., Schmid, E., and Bauer, N.: Fluctuating renewables in a long-term climate change mitigation strategy,
1958 *Energy*, 36, 6674–6685, <https://doi.org/10.1016/j.energy.2011.08.021>, 2011.
- 1959 Martínez-Gordón, R., Morales-España, G., Sijm, J., and Faaij, A. P. C.: A review of the role of spatial resolution in energy
1960 systems modelling: Lessons learned and applicability to the North Sea region, *Renew. Sustain. Energy Rev.*, 141, 110857,
1961 <https://doi.org/10.1016/j.rser.2021.110857>, 2021.



- 1962 Mills, A. D. and Wiser, R. H.: Strategies to mitigate declines in the economic value of wind and solar at high penetration in
1963 California, *Appl. Energy*, 147, 269–278, <https://doi.org/10.1016/j.apenergy.2015.03.014>, 2015.
- 1964 NGFS: NGFS Climate Scenarios for central banks and supervisors, Network for Greening the Financial System, 2020.
- 1965 van Ouwkerk, J., Gils, H. C., Gardian, H., Kittel, M., Schill, W.-P., Zerrahn, A., Murmann, A., Launer, J., Torralba-Díaz, L.,
1966 and Buřar, C.: Impacts of power sector model features on optimal capacity expansion: A comparative study, *Renew. Sustain.*
1967 *Energy Rev.*, 157, 112004, <https://doi.org/10.1016/j.rser.2021.112004>, 2022.
- 1968 Padhy, N. P.: Unit commitment-a bibliographical survey, *IEEE Trans. Power Syst.*, 19, 1196–1205,
1969 <https://doi.org/10.1109/TPWRS.2003.821611>, 2004.
- 1970 Palzer, A. and Henning, H.-M.: A Future German Energy System with a Dominating Contribution from Renewable Energies: A
1971 Holistic Model Based on Hourly Simulation, *Energy Technol.*, 2, 13–28, <https://doi.org/10.1002/ente.201300083>, 2014.
- 1972 Parra, D., Valverde, L., Pino, F. J., and Patel, M. K.: A review on the role, cost and value of hydrogen energy systems for deep
1973 decarbonisation, *Renew. Sustain. Energy Rev.*, 101, 279–294, <https://doi.org/10.1016/j.rser.2018.11.010>, 2019.
- 1974 Pietzcker, R. C., Ueckerdt, F., Carrara, S., de Boer, H. S., Després, J., Fujimori, S., Johnson, N., Kitous, A., Scholz, Y.,
1975 Sullivan, P., and Luderer, G.: System integration of wind and solar power in integrated assessment models: A cross-model
1976 evaluation of new approaches, *Energy Econ.*, 64, 583–599, <https://doi.org/10.1016/j.eneco.2016.11.018>, 2017.
- 1977 Pina, A., Silva, C., and Ferrão, P.: Modeling hourly electricity dynamics for policy making in long-term scenarios, *Energy*
1978 *Policy*, 39, 4692–4702, <https://doi.org/10.1016/j.enpol.2011.06.062>, 2011.
- 1979 P.R. Shukla et al.: Climate Change 2022: Mitigation of Climate Change. Contribution of Working Group III to the Sixth
1980 Assessment Report of the Intergovernmental Panel on Climate Change, <https://doi.org/10.1017/9781009157926>, 2022.
- 1981 Prol, J. L. and Schill, W.-P.: The Economics of Variable Renewables and Electricity Storage, *ArXiv201215371 Econ Q-Fin*,
1982 2020.
- 1983 Ram, M., Bogdanov, D., Aghahosseini, A., Gulagi, A., Oyewo, S., Child, M., Caldera, U., Sadovskaia, K., Farfan Orozco, F.,
1984 Noel, L., Fasihi, M., Maybodi, S., and Fell, H.-J.: Global Energy System based on 100% Renewable Energy: Energy Transition
1985 in Europe Across Power, Heat, Transport and Desalination Sectors, <https://doi.org/10.13140/RG.2.2.10143.00160>, 2018.
- 1986 Ramsebner, J., Haas, R., Ajanovic, A., and Wietschel, M.: The sector coupling concept: A critical review, *WIREs Energy*
1987 *Environ.*, 10, e396, <https://doi.org/10.1002/wene.396>, 2021.
- 1988 Rechsteiner, R.: German energy transition (Energiewende) and what politicians can learn for environmental and climate policy,
1989 *Clean Technol. Environ. Policy*, 23, 305–342, <https://doi.org/10.1007/s10098-020-01939-3>, 2021.
- 1990 Rodrigues, R., Pietzcker, R., Fragkos, P., Price, J., McDowall, W., Siskos, P., Fotiou, T., Luderer, G., and Capros, P.: Narrative-
1991 driven alternative roads to achieve mid-century CO₂ net neutrality in Europe, *Energy*, 239, 121908,
1992 <https://doi.org/10.1016/j.energy.2021.121908>, 2022.
- 1993 Rogelj, J., Shindell, D., Jiang, K., Fifita, S., Forster, P., Ginzburg, V., Handa, C., Kheshgi, H., Kobayashi, S., Kriegler, E.,
1994 Mundaca, L., Séférian, R., and Vilariño, M. V.: Mitigation pathways compatible with 1.5°C in the context of sustainable
1995 development, in: *Special Report on the impacts of global warming of 1.5 °C*, Intergovernmental Panel on Climate Change,
1996 Geneva, 2018.
- 1997 Rotmans, J. and van Asselt, M. B. A.: Uncertainty in Integrated Assessment Modelling: A Labyrinthine Path, *Integr. Assess.*, 2,
1998 43–55, <https://doi.org/10.1023/A:1011588816469>, 2001.
- 1999 Ruhnau, O.: How flexible electricity demand stabilizes wind and solar market values: The case of hydrogen electrolyzers, *Appl.*
2000 *Energy*, 307, 118194, <https://doi.org/10.1016/j.apenergy.2021.118194>, 2022.
- 2001 Say, K., Schill, W.-P., and John, M.: Degrees of displacement: The impact of household PV battery prosumage on utility



- 2002 generation and storage, *Appl. Energy*, 276, 115466, <https://doi.org/10.1016/j.apenergy.2020.115466>, 2020.
- 2003 Schill, W.-P. and Zerrahn, A.: Long-run power storage requirements for high shares of renewables: Results and sensitivities,
- 2004 *Renew. Sustain. Energy Rev.*, 83, 156–171, <https://doi.org/10.1016/j.rser.2017.05.205>, 2018.
- 2005 Schill, W.-P. and Zerrahn, A.: Flexible electricity use for heating in markets with renewable energy, *Appl. Energy*, 266, 114571,
- 2006 <https://doi.org/10.1016/j.apenergy.2020.114571>, 2020.
- 2007 Schill, W.-P., Pahle, M., and Gambardella, C.: Start-up costs of thermal power plants in markets with increasing shares of
- 2008 variable renewable generation, *Nat. Energy*, 2, 1–6, <https://doi.org/10.1038/nenergy.2017.50>, 2017.
- 2009 Seljom, P., Rosenberg, E., Schäffer, L. E., and Fodstad, M.: Bidirectional linkage between a long-term energy system and a
- 2010 short-term power market model, *Energy*, 198, 117311, <https://doi.org/10.1016/j.energy.2020.117311>, 2020.
- 2011 Sensfuß, F.: Assessment of the impact of renewable electricity generation on the German electricity sector: An agent-based
- 2012 simulation approach, <https://doi.org/10.5445/IR/1000007777>, 2007.
- 2013 Sensfuß, F., Ragwitz, M., and Genoese, M.: The merit-order effect: A detailed analysis of the price effect of renewable
- 2014 electricity generation on spot market prices in Germany, *Energy Policy*, 36, 3076–3084, 2008.
- 2015 Sepulveda, N. A., Jenkins, J. D., de Sisternes, F. J., and Lester, R. K.: The Role of Firm Low-Carbon Electricity Resources in
- 2016 Deep Decarbonization of Power Generation, *Joule*, 2, 2403–2420, <https://doi.org/10.1016/j.joule.2018.08.006>, 2018.
- 2017 Stehfest, E., van Vuuren, D., Bouwman, L., and Kram, T.: Integrated assessment of global environmental change with IMAGE
- 2018 3.0: Model description and policy applications, Netherlands Environmental Assessment Agency (PBL), 2014.
- 2019 Stöckl, F., Schill, W.-P., and Zerrahn, A.: Optimal supply chains and power sector benefits of green hydrogen, *Sci. Rep.*, 11,
- 2020 14191, <https://doi.org/10.1038/s41598-021-92511-6>, 2021.
- 2021 Sullivan, P., Krey, V., and Riahi, K.: Impacts of considering electric sector variability and reliability in the MESSAGE model,
- 2022 *Energy Strategy Rev.*, 1, 157–163, <https://doi.org/10.1016/j.esr.2013.01.001>, 2013.
- 2023 The White House: The Long-Term Strategy of the United States: Pathways to Net-Zero Greenhouse Gas Emissions by 2050,
- 2024 United States Department of State and the United States Executive Office of the President, Washington DC., 2021.
- 2025 Ueckerdt, F., Brecha, R., Luderer, G., Sullivan, P., Schmid, E., Bauer, N., Böttger, D., and Pietzcker, R.: Representing power
- 2026 sector variability and the integration of variable renewables in long-term energy-economy models using residual load duration
- 2027 curves, *Energy*, 90, Part 2, 1799–1814, <https://doi.org/10.1016/j.energy.2015.07.006>, 2015.
- 2028 Ueckerdt, F., Pietzcker, R., Scholz, Y., Stetter, D., Giannousakis, A., and Luderer, G.: Decarbonizing global power supply under
- 2029 region-specific consideration of challenges and options of integrating variable renewables in the REMIND model, *Energy*
- 2030 *Econ.*, 64, 665–684, <https://doi.org/10.1016/j.eneco.2016.05.012>, 2017.
- 2031 UNEP: The Emissions Gap Report 2019, UNEP, Nairobi, Kenya, 2019.
- 2032 Welsch, M., Mentis, D., and Howells, M.: Chapter 17 - Long-Term Energy Systems Planning: Accounting for Short-Term
- 2033 Variability and Flexibility, in: *Renewable Energy Integration*, edited by: Jones, L. E., Academic Press, Boston, 215–225,
- 2034 <https://doi.org/10.1016/B978-0-12-407910-6.00017-X>, 2014.
- 2035 Weyant, J.: Some Contributions of Integrated Assessment Models of Global Climate Change, *Rev. Environ. Econ. Policy*, 11,
- 2036 115–137, <https://doi.org/10.1093/reep/rew018>, 2017.
- 2037 Wiese, F., Schlecht, I., Bunke, W.-D., Gerbaulet, C., Hirth, L., Jahn, M., Kunz, F., Lorenz, C., Mühlenpfordt, J., Reimann, J.,
- 2038 and Schill, W.-P.: Open Power System Data – Frictionless data for electricity system modelling, *Appl. Energy*, 236, 401–409,
- 2039 <https://doi.org/10.1016/j.apenergy.2018.11.097>, 2019.
- 2040 Wilson, C., Guivarch, C., Kriegler, E., van Ruijven, B., van Vuuren, D. P., Krey, V., Schwanitz, V. J., and Thompson, E. L.:
- 2041 Evaluating process-based integrated assessment models of climate change mitigation, *Clim. Change*, 166, 3,



- 2042 <https://doi.org/10.1007/s10584-021-03099-9>, 2021.
- 2043 Zerrahn, A. and Schill, W.-P.: Long-run power storage requirements for high shares of renewables: review and a new model, *Renew. Sustain. Energy Rev.*, 79, 1518–1534, <https://doi.org/10.1016/j.rser.2016.11.098>, 2017.
- 2044 Zerrahn, A., Schill, W.-P., and Kemfert, C.: On the economics of electrical storage for variable renewable energy sources, *Eur. Econ. Rev.*, 108, 259–279, <https://doi.org/10.1016/j.euroecorev.2018.07.004>, 2018.